

MODIFIED ANT COLONY ALGORITHM FOR COMBINATIONAL LOGIC CIRCUITS DESIGN

by

BAMBANG ALI BASYAH SARIF

A Thesis Presented to the
DEANSHIP OF GRADUATE STUDIES

In Partial Fulfillment of the Requirements
for the Degree of

MASTER OF SCIENCE

IN

COMPUTER ENGINEERING

KING FAHD UNIVERSITY OF PETROLEUM & MINERALS

Dhahran, Saudi Arabia

November 2003

KING FAHD UNIVERSITY OF PETROLEUM & MINERALS
DHAHRAN 31261, SAUDI ARABIA
DEANSHIP OF GRADUATE STUDIES

This thesis, written by

BAMBANG ALI BASYAH SARIF

under the direction of his Thesis Advisor and approved by his Thesis Committee,
has been presented to and accepted by the Dean of Graduate Studies, in partial
fulfillment of the requirements for the degree of

MASTER OF SCIENCE IN COMPUTER ENGINEERING

Thesis Committee

Prof. Mostafa Abd – El – Barr (Chairman)

Prof. Sadiq M. Sait (Co – Chairman)

Assoc. Prof. Alaaeldin A. M. Amin (Member)

Prof. Sadiq M. Sait
Department Chairman

Prof. Osama A. Jannadi
Dean of Graduate Studies

Date

*Dedicated as a humble tribute to
my beloved parents and to
the memory of my paternal grandfather.*

ACKNOWLEDGMENTS

First and foremost, all sincere praises and thanks are due to Allah, the most Beneficent and the most Merciful, who guided us to Islam and enabled me to complete my thesis work. I make a humble effort to thank Allah for His endless blessings on me, as His infinite blessings cannot be thanked for. I pray Allah to bestow peace on his last prophet Muhammad (*Sal-allah- 'Alaihe- Wa-Sallam*) and on all his righteous followers till the day of judgement. After that comes the following.

This thesis is never possible without the help, encouragement, motivation, and influence of a large number of people. Dr. Mostafa Abd-El-Barr, my advisor, taught me many things, but most importantly, how to do research and how to write well. He was an inexhaustible storehouse of knowledge, insight and help on just about any subject. His influence pervades this thesis and I am deeply indebted to him for being my advisor and for having a complete faith in me. Dr. Sadiq M. Sait, my co-advisor for his constant encouragement, unlimited support and guidance during the course of this thesis. Mr. Uthman Al-Saiari, my colleague, for providing me with any kind of help. Also Dr. Alaaeldin A. Amin, my thesis committee member, for his comments and critical review of the thesis.

I would like to pay a heartily tribute to all of my family members and especially to my parents, who guided me during all my life endeavors. Their love and support

motivated me to continue my education and achieve higher academic goals. Without their moral support and sincere prayers, I would have been unable to accomplish this task.

I acknowledge the academic and computing facilities provided by the Computer Engineering Department of King Fahd University of Petroleum & Minerals (KFUPM)

I would also to acknowledge the help of Dr. Carlos A. Coello for his valuable discussion during the course of this thesis.

Finally, I appreciate the friendly support from all my colleagues at KFUPM. In particular, I want to thank to Irman, Ya'u, Badawi, Sanaullah and Saqib, among others.

Contents

ACKNOWLEDGMENTS	iv
LIST OF TABLES	xi
LIST OF FIGURES	xiv
ABSTRACT (ENGLISH)	xix
ABSTRACT (ARABIC)	xx
1 INTRODUCTION	1
1.1 Conventional Logic Design	2
1.2 Evolutionary Logic Design	4
1.3 Motivation	7
1.4 Structure of the Thesis	9
2 BACKGROUND MATERIAL	10
2.1 Logic Synthesis Algorithms	12

2.2	Ant Colony Optimization Algorithm	15
2.3	The Multiobjective Optimization Problem	27
2.4	Fuzzy Logic	30
2.4.1	Fuzzy Set Theory	31
2.4.2	Multi-objective Optimization Using Fuzzy Logic	34
2.5	Concluding Remarks	36
3	LITERATURE REVIEW	37
3.1	Introduction	37
3.2	Classification of Evolutionary Logic Design	38
3.3	Existing ELD Techniques	39
3.3.1	EAs Based ELD	40
3.3.2	ACO Based ELD	46
3.3.3	Other Related Work	50
3.4	Discussion	51
3.5	Concluding Remarks	54
4	PROBLEM AND COST FUNCTION FORMULATION	56
4.1	Problem Formulation	56
4.2	Problem Statement	59
4.2.1	Assumptions	60
4.2.2	Input and Output	61

4.3	Cost Function Modeling	62
4.3.1	Gate Count Cost Function	62
4.3.2	Area Cost Function	63
4.3.3	Delay Cost Function	63
4.3.4	Power Consumption Cost Function	65
4.4	Weighted Sum Fitness Function Calculation	67
4.4.1	Functional Fitness	67
4.4.2	Objective Fitness	68
4.5	Fuzzy Fitness Function Calculation	70
4.5.1	Functional Fitness	70
4.5.2	Objective Fitness	70
4.6	Concluding Remarks	79
5	ACO ALGORITHM FOR COMBINATIONAL LOGIC DESIGN	80
5.1	Introduction	80
5.2	Modified-ACO (MACO) for Logic Design	82
5.2.1	Circuit Encoding	83
5.2.2	Modifications of the Ant Colony Algorithm	84
5.2.3	Filling the Matrix	88
5.2.4	Ant Activity	89
5.2.5	Removing the Unfit Cell	92

5.3	Improved-Modified ACO algorithm	99
5.3.1	Dynamic Search Space	99
5.3.2	Perturbation	101
5.3.3	Residual Function	106
5.4	Concluding Remarks	113
6	EXPERIMENTS AND RESULTS	114
6.1	Experimental Setup	114
6.2	Performance of Different Fitness Calculation	116
6.2.1	Effect of Different Weighting Scheme	116
6.2.2	Effect of Different FF Calculations	121
6.3	Dynamic Search Space	122
6.4	Residual Function	125
6.5	Different Optimization Objectives	126
6.6	Concluding Remarks	135
7	COMPARISON WITH EXISTING TECHNIQUES	136
7.1	Comparison with Existing ACO-based Technique	136
7.1.1	Comparison of Design Rate	137
7.1.2	Comparison of the Quality of Solutions	138
7.1.3	Comparison of Execution Time	141
7.2	Comparison with Existing Conventional Techniques	142

7.3	Comparison with other Techniques	149
7.3.1	Comparison with GAs	149
7.3.2	Comparison with SimE	152
7.4	Concluding Remarks	154
8	CONCLUSIONS AND FUTURE DIRECTIONS	155
8.1	Conclusion	156
8.2	Future Directions	157
	APPENDIX	159
A	File Format and Circuit Used as Test Cases	159
A.1	Library File Format	159
A.2	Input File Format	160
A.3	Randomly Generated Circuits	162
A.4	Benchmark Circuits	162
	BIBLIOGRAPHY	164
	VITA	177

List of Tables

2.1	Connectivity matrix of TSP example shown in Figure 2.3.	20
2.2	Heuristic value for each edge in Figure 2.3.	21
2.3	Solutions built by the ant in the first iteration.	23
2.4	Pheromone values for each edge after iteration 1.	24
2.5	Solutions built by the ant in the second iteration.	25
2.6	Pheromone values for each edge after iteration 2.	25
3.1	Possible cell functions in $[1, 2, 3, 4, 5]$	42
5.1	Gate ID, gate name and output of the gate, considering input a and b	83
5.2	AND decomposition table.	109
5.3	OR decomposition table.	109
5.4	XOR decomposition table.	110
6.1	Summary of circuits used for the experiments.	115
6.2	Experimental results for $WF = 0.5$	117

6.3	Experimental results for $WF = 0.75$	117
6.4	Experimental results for $WF = 0.875$	118
6.5	Experimental results for dynamic WF	120
6.6	Results obtained for different FF calculations.	122
6.7	Experimental result for static and dynamic matrix in terms of design rate and computation time.	124
6.8	Area result obtained using static and dynamic matrix size.	124
6.9	Results obtained using IMACO algorithm.	125
6.10	Results of different optimization objectives.	130
6.11	Results of DOAPC experiments normalized with respect to results of AODPC.	131
6.12	Results of POADC experiments normalized with respect to results of AODPC.	133
7.1	Comparison with Coello [6] in terms of <i>design rate</i>	137
7.2	Comparison with Coello [6] in terms of area, delay and power.	139
7.3	Comparison with Coello [6] in terms of execution time.	142
7.4	Comparison of IMACO and SIS in area optimization for single output circuits.	143
7.5	Comparison of MACO and SIS in area optimization for multiple out- put circuits.	145

7.6	Comparison of IMACO and SIS in delay optimization for single output circuits.	147
7.7	Comparison of MACO and SIS in delay optimization for multiple output circuits.	147
7.8	Comparison with GAs [7] technique in terms of area, delay and power.	150
7.9	Comparison with GA [7] technique in terms of execution time.	151
7.10	Comparison with SimE technique in terms of area, delay and power for area optimization.	152
7.11	Comparison with SimE technique in terms of area, delay and power for delay optimization.	153

List of Figures

1.1	Design space: area/delay trade-off for 64-bit adder [8].	3
1.2	Evolutionary design process [1].	5
1.3	Circuit design methodologies.	6
2.1	Double bridge experiment. (a) Ants start exploring the double bridge. (b) Eventually most of the ants choose the shortest path [9].	16
2.2	Ant Colony Algorithm.	18
2.3	Example of a TSP problem.	20
2.4	(a) Visualization of pheromone values and (b) Best solution built in the first iteration.	24
2.5	(a) Visualization of pheromone values and (b) Best solution built in the second iteration.	26
3.1	A mapping scheme used in [10].	40
3.2	Chromosome representation used by Miller et. al., [1, 2, 3, 4, 5]. . . .	41
3.3	Example of genotype-phenotype mapping used in [1, 2, 3, 4, 5]. . . .	43

3.4	Encoding of a cell used in [6, 7, 11].	44
3.5	Chromosome representation [12, 13].	45
3.6	Macro blocks and its genotype representation in [12, 13].	45
3.7	Mutation operators proposed in [12, 13].	46
3.8	The matrix's state after the filling of the first column.	48
3.9	The matrix's state after the filling of all cells	48
3.10	The cells used in the solution by an ant.	49
3.11	Problems that may appear in matrix representation: (a) fitness of F1 < 1 (b) fitness of F2 = 1.	51
3.12	An evolved two-bit odd parity circuit. (a) Fitness of F1 = 0 (b) Adding an inverter, fitness of F1 = 1 (c) Toggle the type of gate (XNOR \rightarrow XOR), fitness of F1 = 1	52
4.1	Membership function for area.	72
4.2	Membership function for delay.	74
4.3	Membership function for power.	76
4.4	Dynamic W_f calculation.	78
5.1	Figure Illustrating some of the possible paths in function f	81
5.2	Representation of a cell in the matrix.	83
5.3	Example of a circuit and its encoding.	84
5.4	Nest cell and matrix M for ant to be traversed.	85

5.5	Modified ACO algorithm for logic design.	86
5.6	Procedure Filling_the_Matrix.	89
5.7	Result of Filling the Matrix Procedure in the First Iteration for Ex- ample 1.	93
5.8	Removing of cells in the first iteration.	97
5.9	Filling the matrix in the second iteration	98
5.10	The Use of Row and Column Adjustment.	102
5.11	How the Neighboring Cells Affect the FF_n of Cell(i, j).	103
5.12	Perturbation Procedure.	104
5.13	Effect of perturbation on functional fitness value (a) $FF_n = 0.9375$ (b) $FF_n = 1$	105
5.14	Effect of perturbation on objective fitness (a) gate count = 10 (b) gate count = 8.	105
5.15	Example of using the residual function.	110
5.16	Decomposition procedure.	111
5.17	Improved-Modified ACO algorithm for logic design.	112
6.1	Behavior of functional fitness function for circuit1 in the first 2000 iterations using AODPC.	128
6.2	Behavior of functional fitness function for circuit1 in the first 50 iter- ations using AODPC.	128

6.3	Behavior of objective fitness function for circuit1 in the first 50 iterations using AODPC.	129
6.4	Behavior of objective fitness function for circuit1 in iteration 50 to iteration 200 using AODPC	129
6.5	Normalized results of DOAPC for single output circuits.	132
6.6	Normalized results of DOAPC for multiple output circuits.	132
6.7	Normalized results of POADC for single output circuits.	134
6.8	Normalized results of POADC for multiple output circuits.	134
7.1	Results of MACO normalized with respect to Coello [6].	138
7.2	2-bit Multiplier obtained by Coello [6].	140
7.3	2-bit Multiplier obtained by MACO.	140
7.4	Results of IMACO with AODPC for single output functions, normalized to SIS.	144
7.5	Results of MACO with AODPC for multiple outputs functions, normalized to SIS.	146
7.6	Results of IMACO with DOAPC for single outputs functions, normalized to SIS.	148
7.7	Results of MACO with DOAPC for multiple outputs functions, normalized to SIS.	148

7.8 Comparison with GA: normalized area, delay and power are always	
≤ 1	151

THESIS ABSTRACT

Name: BAMBANG ALI BASYAH SARIF
Title: MODIFIED ANT COLONY ALGORITHM
FOR COMBINATIONAL LOGIC CIRCUITS DESIGN
Major Field: COMPUTER ENGINEERING
Date of Degree: November 2003

Evolutionary computation presents a new paradigm shift in hardware design and synthesis. According to this paradigm, hardware design is pursued by deriving inspiration from biological organism. Instead of using human made models and techniques, the new methodology employs search heuristics to develop efficient designs. In this thesis, a multiobjective optimization for evolutionary logic design based on Ant Colony optimization algorithm is proposed. The result obtained using the proposed algorithms are compared to those obtained using existing evolutionary techniques as well as conventional techniques. Area, delay, and power consumption are used as performance measures based on which the proposed algorithms and the existing techniques are compared. It is shown that the designed circuits using the proposed algorithms outperform those of the existing techniques.

MASTER OF SCIENCE DEGREE

King Fahd University of Petroleum & Minerals, Dhahran, Saudi Arabia.

November 2003

ملخص الرسالة

الاسم : بامبج علي باشا شريف

عنوان الدراسة: خوارزم مملكة النمل المعدلة في تصميم الدوائر الرقمية

التخصص : هندسة الحاسب الآلي

تاريخ التخرج : نوفمبر ٢٠٠٣

يقدم الحساب الارتقائي تحول جذري جديدًا في تصميم الدوائر الرقمية. هذا التحول الجذري أدى إلى تقليد الكائنات الحية. بدلا من استخدام تصميم من صنع البشر, الطريقة الجديدة تستخدم البحث الاستدلالي لتطوير تصميم عمليه. في هذه الرسالة استخدمنا خوارزم مملكة النمل للحصول على تصاميم للدوائر الكهربائية باعتبار الأهداف المتعددة. النتائج التي حصلنا عليها من الخوارزم قارناها بمثيلاتها من الطرق الارتقائية و التقليدية. المساحة, الوقت والطاقة المستهلكة استخدمت كمقاييس للمقارنة.

درجة الماجستير في العلوم

الجامعة الملك فهد للبترول و معادن

ظهران - المملكة العربية السعودية

نوفمبر ٢٠٠٣

Chapter 1

INTRODUCTION

Design of digital circuits can be stated as a process of assembling a collection of logic components to perform a specified function optimized for a number of design objectives and subject to some design constraints, with respect to a specific target technology. Unfortunately, current design systems tend to depend on domain-specific knowledge, which is somewhat limited both by the training and experience of the designer. On the other hand, iterative and evolutionary heuristics, with little domain knowledge, may allow us to search in a design space, apply some assumptions and use domain-independent operators to generate candidate solutions. Therefore, heuristics have a tendency to search for solutions in a much larger, and often richer design space beyond the realms of the conventional design techniques.

Ant Colony Optimization (ACO) algorithm [14] is a new meta-heuristic that combines distributed computation, auto-catalysis (positive feedback) and construc-

tive greediness in finding optimal solutions to combinatorial optimization problems. Unlike Genetic Algorithms (GAs) [15], ACO involves cooperating agents. In ACO, interaction between components of the designed system can be easily analyzed. Some daemon actions or other heuristics can also be incorporated to further improve the quality of solutions. In this context, the central claim of this thesis is: ACO algorithm can provide a computational tool for the circuit design problem.

1.1 Conventional Logic Design

There are four stages in the production of integrated circuits. These are design, fabrication, testing and packaging [8]. The design stage itself is divided into three major tasks: modeling, synthesis and optimization, and validation. The modeling task consists of casting an idea into a model, that specifies the functionality of the circuit. Synthesis deals with refining an abstract model into a detailed one that has all the specifications required. Optimization is performed to maximize some figures of merits of the circuit that relate to its quality. Some of the important merits for optimization are: area, delay, power, testability, and fault tolerance.

Circuit models can be classified in terms of levels of abstraction: architectural, logical, and geometrical. Logic level model deals with all facets of combinational and sequential circuits. Logic synthesis can be defined as the manipulation of functional specifications to a model as an interconnection of primitives components. In other

words, logic synthesis determines the gate-level structure of circuits. The classical logic synthesis algorithms include the optimization of two quality measures, namely: area and performance [16, 17, 18, 19, 20, 21, 22]. The design objective can be either minimizing the area or maximizing the performance. Optimization can be subject to constraints, such as upper bound on area, as well as upper bounds on performance and lower bound on delay.

The possible configurations of a circuit are many. These different feasible structural implementations of a circuit define its design space. Figure 1.1 shows an example design space of a 64-bit adder circuit, considering delay and area of the circuit [8].

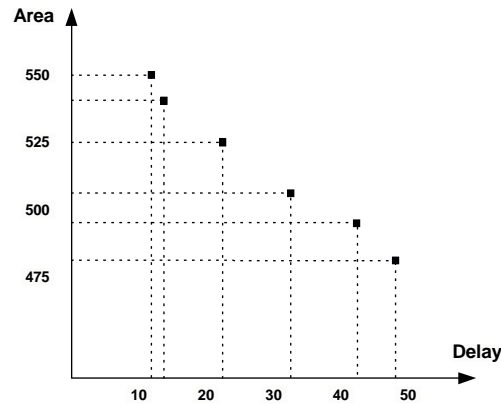


Figure 1.1: Design space: area/delay trade-off for 64-bit adder [8].

The design space consists of a finite set of design points. A point in the design space is called a *Pareto* point if there is no other point with at least an inferior objective, all others being inferior or equal [15]. This Pareto point can be easily observed in a small design space, i.e., small circuit with few design objectives. However, if the

size of the circuit as well as the design objectives and/or constraints are increased, the number of design points could be huge. Thus, it is more difficult to find the most optimal structure for the given circuit. Hence, current available techniques divide the circuit design problem into some sub-problems with lower dimensionality. However, this approach is somehow constrained both by the training and experience of the designer and by the amount of domain specific knowledge available. Thus, the most optimal representation is unlikely to be obtained from this approach.

1.2 Evolutionary Logic Design

In conventional logic design, circuit designers begin with a precise specification in the form of truth tables or Boolean expressions. These expressions are manipulated by applying logic synthesis algorithms, such as factorization and kernel extraction to minimize circuit representations. Therefore, the outcome of logic synthesis algorithms will be either in two-level, multi-level, or Reed Muller representations.

Iterative heuristic is a non-deterministic algorithm that has a hill climbing properties. It has a mechanism to bias the search so as to improve the quality of solution. Iterative heuristics work on a larger space that may not represent the desired function. Through the process of assemble and test, candidate solutions are built and evaluated. At the end, an optimal solution could evolve from this process. Figure 1.2 shows evolutionary algorithms work on space that may not represent the

desired function, but gradually pulls the specification of the circuit towards the target truth table.

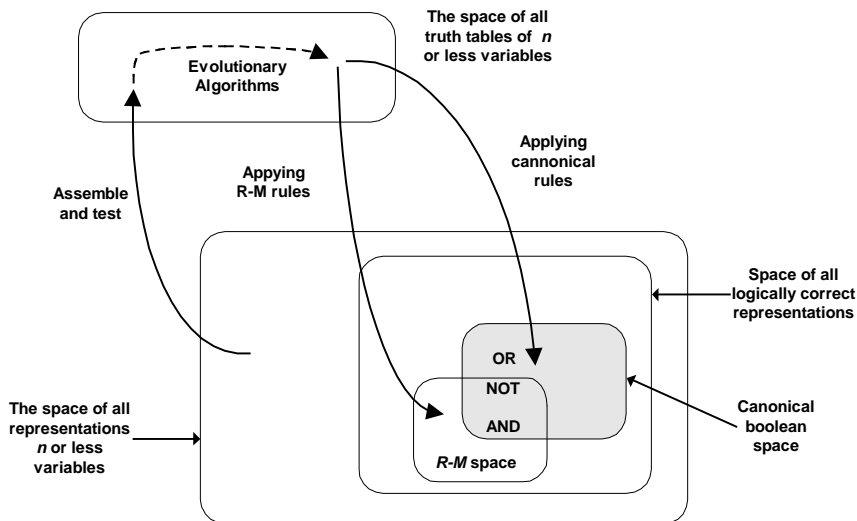


Figure 1.2: Evolutionary design process [1].

Furthermore, iterative heuristics may allow designers to define the search space of circuit design in a way that is natural to both the problem and the implementation. It may therefore be possible to use iterative heuristics to obtain novel designs that are difficult to obtain using conventional techniques. Figure 1.3 shows the difference between the conventional and the evolutionary methods for circuit design.

The first work in evolutionary design of digital circuits, Designer Genetic Algorithms (DGA), was proposed by Louis [10]. This work has led to the establishment of a new field of research called *Evolvable Hardware (EHW)* that was suggested by Hugo de Garris [23]. Later, Zebulum et al. [24, 25], used *Evolutionary Electronics* as the name for this field.

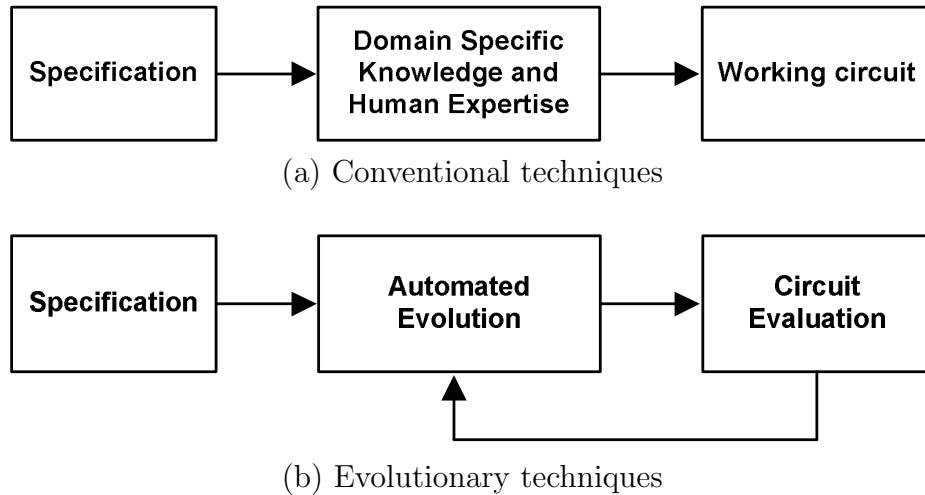


Figure 1.3: Circuit design methodologies.

Motivated by de Garris’s idea, Higuchi et al. [26] obtained an evolved circuit to solve the 6-multiplexer problem [27]. Later in 1995, Thompson managed to evolve a tone discriminator circuit in XC6200 FPGA [28]. He showed that Evolutionary Algorithms were able to produce a tone discriminator circuit without input clock, which is difficult to obtain by any conventional techniques. This work has hinted to the possibility of a new method of designing circuits.

Koza et al. employed Genetic Programming (GP) [29] and pioneered the evolution of analog circuits using a SPICE simulator. They were able to automatically generate circuits which are competitive with those obtained using conventional methods. They have shown further that it is possible to produce designs for quite complex analog circuits, namely: low-distortion op-amps, low-pass filters, and band-pass filters using GP [30]. A functional level evolution was proposed by Higuchi [31]. A complete review and taxonomy of the field is described in [32, 24, 33].

In a recent development [11, 34], much attention has been given to the evolutionary design of arithmetic circuits as they provide the essential building blocks needed for larger DSP applications. Such effort has resulted in the development of arithmetic circuits that range from a simple sequential adder to the more complex 3-bit multiplier. The work of Fogarty [35] and Miller [1] built some arithmetic circuits that cannot be produced by human designer's conventional methods. Coello et al. [11, 36] proposed a similar approach to evolve a circuit, which they showed was better than that of Miller's. Several other algorithms such as Ant Colony Optimization, Cartesian Genetic Programming and Particle Swarm Optimization have also been used for evolutionary logic design [6, 34, 37]. A complete review and taxonomy of the field could be found in [24, 25, 33].

1.3 Motivation

The advent of evolutionary computation has created a new paradigm shift in logic design and synthesis. It has radically changed the design procedure, and provided the potential for discovering novel designs and/or more efficient circuits that are beyond the scope of conventional methods.

Several approaches using evolutionary design of digital circuits were found in literature. The results shown in the literature were promising. However, the excessive runtimes and scalability characterize the use of iterative heuristics for any hard

combinatorial optimization problems. This provides incentive for investigating the effectiveness of using iterative heuristics in logic design. In addition to that, there are some other aspects that motivated this work. These aspects are listed below.

1. **Multiobjective Optimization**

Most of the existing techniques used the gate count as their optimization objective. With the increasing need for circuits that have better performance and lower power consumption, the objective of only minimizing the gate count is not anymore acceptable. In addition, the term ‘gate’ or basic module for the evolutionary logic design depends on the definition of the gate library that is used. Therefore, optimizing the circuits in terms of area (delay and/or power) is more appropriate compared to optimizing it in terms of gate count.

2. **Heuristics Used**

Most of the existing techniques in evolutionary logic design used Genetic Algorithms (GAs) or Genetic Programming (GP) [30]. However, there exists some other heuristics that are proved to be more efficient than GAs in solving combinatorial optimization problems. These heuristics include the Ant Colony Optimization (ACO) algorithm [14].

1.4 Structure of the Thesis

The rest of this thesis is organized as follows. Chapter 2 provides some background material. Some definitions in logic synthesis and a brief overview of conventional logic design are provided. The Ant Colony Optimization (ACO) algorithm is also described in this chapter.

Chapter 3 presents a literature survey on existing techniques in evolutionary design of combinational circuits. Observations, drawbacks, and possibility of improvements over the existing techniques are detailed in this chapter.

In Chapter 4, the multi-objective evolutionary logic design problem is formulated. The calculation of area, delay and power consumption and their contribution to the fitness function are designed.

The proposed algorithm for multi-objective evolutionary logic design problem is described in Chapter 5. Chapter 6 provides the experiments and results of the proposed techniques. Comparison with existing techniques is provided in Chapter 7. Finally, Chapter 8 provides some conclusions and possible future directions of this work.

Chapter 2

BACKGROUND MATERIAL

The dramatic increase in designer productivity over the past decade in the area of VLSI (Very Large Scale Integration) circuits can be attributed to the development of sophisticated Computer Aided Design (CAD) tools. The improvement in CAD tools has been made possible by the advances in the field of logic synthesis. Logic synthesis techniques speed up the design cycle and reduce the human effort. Logic Synthesis algorithms work on circuit model. Circuit representation is therefore important to understand [8]. In this chapter, we introduce some definitions and terminology.

- Definition 2.1. A *Boolean network* is a directed acyclic graph that represents a Boolean function f .
- Definition 2.2. A *cube* is a product of literals $(\bar{a}b, b\bar{e}, a\bar{c}d, \dots)$.

- Definition 2.3. An algebraic expression is a non-redundant set of cubes.

Non-redundant means that no cube contains another; e.g. $a\bar{b} + c$ is a non-redundant expression while $ab + b$ is a redundant expression because $\{b\} \subseteq \{a, b\}$.

- Definition 2.4. A Boolean function can be represented in the *sum-of-product* (SOP) form or disjunctive normal form.
- Definition 2.5. A SOP expression is called *cube-free* if there exists no literal that appears in all cubes in the expression.

For example, $ab + \bar{a}c$ is a cube-free SOP expression while $ab + bc$ is not.

- Definition 2.6. *Algebraic division* is an operation used to compute a quotient expression Q and a remainder expression R resulting from a given expression F and divisor expression D such that $F = Q \cdot D + R$.
- Definition 2.7. *Boolean division* is an operation used to compute Q , D and R of F (similar to algebraic division), using Boolean algebra rules.
- Definition 2.8. The *Primary divisors* of an expression F , denoted as $D(F)$, are the set of quotients that are derived by dividing F by all possible cubes.
- Definition 2.9. The *kernels* of an expression F , denoted as $K(F)$, is the set of cube-free primary divisors of F .

- Definition 2.10. The *co-kernel* is a cube that is used to derive a kernel.

Consider, for example, the function $F = ae + af + bce + bcf + bde + bdf$. $F/bc = (e + f)$ is a kernel, and $F/b = ce + cf + de$ is not. The co-kernel bc is used to obtain kernel $e + f$.

Each kernel has its own level. The level of a kernel is defined according to the following rules:

1. If a kernel does not contain any other kernel, the level of the kernel is 0.
2. If a kernel contains kernel of level $n - 1$ but does not contain kernels whose level is more than $n - 1$, its level is n .

Consider the function $F = ae + af + bce + bcf + bde + bdf$. Function F can be factorized to obtain $F = (a + b(c + d))(e + f)$. $K^0 = c + d$ is a kernel of level 0, since it does not contain any other kernel. $(e + f)$ is also a kernel of level 0. $K^1 = (a + b(c + d))$, while the function F itself is a level 2 kernel.

2.1 Logic Synthesis Algorithms

Early effort on logic synthesis and optimization algorithms are dated back to the 1950's [16, 17] and 1960's [38]. Although these efforts have much historical importance, their applicability was limited. However, as soon as *Large Scale Integration*

technology became available, the importance of logic synthesis was emphasized. Many algorithms, such as MINI [39] and LSS [40] were proposed.

The advent of PLA (Programmable Logic Array) technology boosted the two-level logic optimization techniques. ESPRESSO [18] is a well-known two-level logic minimization tool.

The need for area minimization forces logic synthesis to consider the multi-level logic representation. The introduction of kernel and kernel extraction techniques in [19, 20] enhances the quality of multi-level logic optimization techniques. The MIS [19] and BOLD [22] are examples of such techniques.

At the beginning of 1990s the area of logic synthesis matured. The most well known logic synthesis tool, SIS, was proposed by Brayton et al. [21]. However, there are some other recently introduced techniques that produce better quality results as compared to SIS. The *Perturb and Simplify* [41] and *Redundancy Addition and Removal* [42] are two such techniques. These techniques are based on the transduction (*transformation and reduction*) method proposed by Muroga et. al. [43].

In addition to the common two-level and multi-level logic representations, there exist some other techniques to represent Boolean functions. These include the *Binary Decision Diagrams* (BDD) [38, 44, 45] and multiplexer based representations [46]. BDD is a directed acyclic graph (DAG) representation of logic functions.

Multi-level logic provides the optimal representation of Boolean functions in terms of area. However, there are some Boolean functions that are more efficient

to implement using XOR-based representation as compared to the multi-level logic. The n -bit parity checker is one such functions. The most well-known XOR-based representation is the Reed-Muller (or AND-XOR) form [47]. There are *fixed (positive or negative)* and *mixed polarity* RM forms. Unfortunately, decomposing Boolean functions using XOR gates is difficult, let alone finding the perfect polarity for it [48].

Recently, with several new power-constrained applications ranging from mobile phones to laptop computers, power dissipation has emerged as another important objective of VLSI circuit design [49, 50, 51]. The optimization of power consumption can be performed at various levels of circuit design, including the logic level. Thus, minimization of power consumption has to be reflected in the logic optimization process. The POSE (Power Optimized Synthesis Environment) [52] is an example of one technique that considers power consumption of the synthesized circuits.

With the increasing demand for high quality, more efficient and less area circuits, circuit design has become a multiobjective optimization problem. Therefore, there should evolve new methodologies for designing logic circuits. These should include all types of representations, such as multi-level, Reed-Muller and multiplexer-based representations. It should also consider all design objectives and/or constraints, such as delay, area and power consumption. Therefore, logic synthesis can be modelled as a search task in the design space. Deterministic algorithms are not favored due to the huge size of the design space. The type of algorithms that could be used to

explore such huge search space size is non-deterministic algorithm. In this context, the Ant Colony Optimization is a recent heuristic that deserves consideration.

2.2 Ant Colony Optimization Algorithm

The Ant Colony Optimization (ACO) algorithm is a new meta-heuristic that has a combination of distributed computation, *autocatalysis* (positive feedback) and constructive greediness to find an optimal solution for combinatorial optimization problems. This algorithm tries to mimic the ants behavior in the real world. Since its introduction, the ACO algorithm has received much attention and has been incorporated in many optimization problems, namely the network routing, traveling salesman, quadratic assignment, and resource allocation problems [14].

The ACO algorithm has been inspired by the experiments run by Goss et al. [53] using a colony of real ants. They observed that real ants were able to select the shortest path between their nest and food resource, in the existence of alternate paths between the two. The search is made possible by an indirect communication known as *stigmergy* amongst the ants. While traveling their way, ants deposit a chemical substance, called *pheromone*, on the ground. When they arrive at a decision point, they make a probabilistic choice, biased by the intensity of pheromone they smell. This behavior has an autocatalytic effect because of the very fact that choosing a path will increase the probability that the corresponding path will be

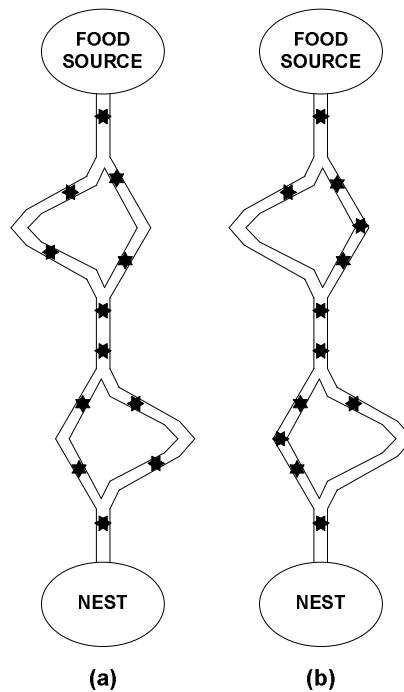


Figure 2.1: Double bridge experiment. (a) Ants start exploring the double bridge. (b) Eventually most of the ants choose the shortest path [9].

chosen again by future ants. When they return back, the probability of choosing the same path is higher (due to the increase of pheromone). New pheromone will be released on the chosen path, which makes it more attractive for future ants. Shortly, all ants will select the shortest path.

Figure 2.1 shows the behavior of ants in a double bridge experiment [9]. In this case, because of the same pheromone laying mechanism, the shortest branch is most often selected. The first ants to arrive at the food source are those that took the two shortest branches. When these ants start their return trip, more pheromone is present on the short branch than the one on the long branch. This will stimulate successive ants to choose the short branch. Although a single ant is

in principle capable of building a solution (i.e., of finding a path between nest and food resource), it is only the colony of ants that presents the “shortest path finding” behavior. In a sense, this behavior is an emergent property of the ant colony.

This behavior was formulated as Ant System (AS) by Dorigo et al. [14]. Based on the AS algorithm, the Ant Colony Optimization (ACO) algorithm was proposed [54]. In ACO algorithm, the optimization problem is formulated as a graph $G = (C, L)$, where C is the set of components of the problem, and L is the set of possible connections or transitions among the elements of C . The solution is expressed in terms of feasible paths on the graph G , with respect to a set of given constraints. The population of agents (ants) collectively solve the problem under consideration using the graph representation. Though each ant is capable of finding a (probably poor) solution, good quality solutions can emerge as a result of collective interaction amongst ants. Pheromone trails encode a long-term memory about the whole ant search process. Its value depends on the problem representation and the optimization objective.

A general outline of the ACO algorithm is presented in Figure 2.2 [54]. Informally, the behavior of ants in ACO algorithm can be summarized as follows. A colony of ants concurrently and asynchronously move through adjacent states of the problem by moving through neighbor nodes of G . They move by applying a stochastic local decision policy which makes use of the information contained in the local node and ant’s routing table. By moving, ants incrementally build solutions

to the optimization problem. When the solution is being built, every ant evaluates the solution and puts the information about its goodness on the pheromone trails of the connection used. This pheromone information will direct the search of future ants, until a feasible solution is found.

```

Algorithm ACO_meta_heuristic();
    while (termination criterion not satisfied)
        ant_generation_and_activity();
        pheromone_evaporation();
        daemon_actions(); {optional}
    end while
end Algorithm

```

Figure 2.2: Ant Colony Algorithm.

The ants in ACO algorithm have the following properties [14]:

1. Each ant searches for a minimum cost feasible partial solution.
2. An ant k has a memory M^k that it can use to store information on the path it followed so far. The stored information can be used to build feasible solutions, evaluate solutions and retrace the path backward.
3. An ant k can be assigned a start state s_s^k and more than one termination conditions e^k .
4. Ants start from a start state and move to feasible neighbor states, building the solution in an incremental way. The procedure stops when at least one termination condition e^k for ant k is satisfied.

5. An ant k located in node i can move to node j chosen in a feasible neighborhood N_i^k through probabilistic decision rules. This can be formulated as follows: an ant k in state $s_r = \langle s_{r-1}, i \rangle$ can move to any node j in its feasible neighborhood N_i^k , defined as $N_i^k = \{j \mid (j \in N_i) \wedge (\langle s_r, j \rangle \in S)\}$ $s_r \in S$, with S is a set of all states.
6. A probabilistic rule is a function of the following.
 - (a) the values stored in a node local data structure $A_i = [a_{ij}]$ called *ant-routing table* obtained from pheromone trails and heuristic values,
 - (b) the ant's own memory from previous iteration, and
 - (c) the problem constraints.
7. When moving from node i to neighbor node j , the ant can update the pheromone trails τ_{ij} on the edge (i, j) .
8. Once it has built a solution, an ant can retrace the same path backward, update the pheromone trails and die.

In order to get more insight about the algorithm, an example of using ACO algorithm for Traveling Salesman Problem (TSP) is given in the following.

Consider, for example, a 5-city TSP problem shown in Figure 2.3. The objective is to find the minimal tour required to visit all the 5 cities. The connectivity matrix of the graph is given in Table 2.1. The values given in the table denotes the distance

(*d*) between each city. Assume that it is a symmetric TSP problem, in which d_{ij} is equal to d_{ji} .

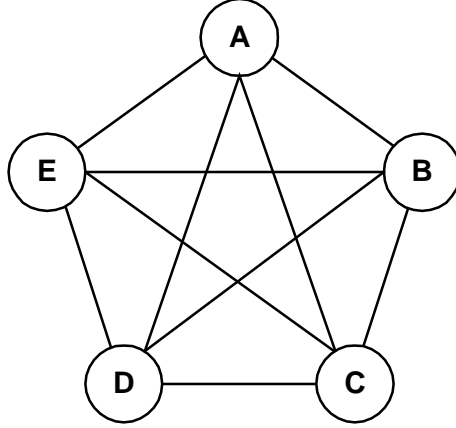


Figure 2.3: Example of a TSP problem.

Table 2.1: Connectivity matrix of TSP example shown in Figure 2.3.

	A	B	C	D	E
A	0	100	125	100	75
B	100	0	50	75	125
C	125	50	0	100	125
D	100	75	100	0	50
E	75	125	125	50	0

Each edge in the graph is given an initial pheromone value (τ) equal to 1. Let heuristic value (η) is equal to the reciprocal of the distance. The probability of selecting an edge is then equal to [54]:

$$p_{ij}^k(t) = \frac{[\tau_{ij}(t)]^\alpha \cdot [\eta_{ij}]^\beta}{\sum_{l \in N} [\tau_{il}(t)]^\alpha \cdot [\eta_{il}]^\beta} \quad (2.1)$$

where N is the set of neighboring cities, and α and β are two parameters that control

the relative weight of pheromone trail and heuristic value. In this example, for the sake of simplicity, the value of α and β are set equal to 1.

Table 2.2 shows the heuristic value (η) for each edge.

Table 2.2: Heuristic value for each edge in Figure 2.3.

	A	B	C	D	E
A	0.000	0.010	0.008	0.010	0.013
B	0.010	0.000	0.020	0.013	0.008
C	0.008	0.020	0.000	0.010	0.008
D	0.010	0.013	0.010	0.000	0.020
E	0.013	0.008	0.008	0.020	0.000

Since there are 5 cities, assume that the size of the colony of ant is 5. Each ant will start their tour from different city. For example, the first ant starts from city A, the second ant starts from city B, and so on. The following explains how the ants construct the solution.

Iteration 1

The first ant starts the tour from city A. There are four neighboring cities to be considered by the ant. The probability of choosing any edge leading to a certain city is calculated using Equation 2.1 and is given in the following table.

B	C	D	E
0.24	0.19	0.24	0.32

Using a stochastic process, i.e., *Roulette Wheel*, the ant choose the next city. Assume

that the ant takes city B as the next city to visit. The ant will update its memory and put city B in its *Tabu List*

When the ant arrives at city B, there are 3 cities left to visit. The probability of choosing these cities is given in the following table.

C	D	E
0.48	0.32	0.19

Assume that city D is taken. The ant will then update its *Tabu List* by adding city D.

There are two neighbors of city D: C and E. The following table shows the probability of choosing each of these cities.

C	E
0.33	0.66

Assume that the ant selects city E. The content of its *Tabu List* is then : A,B,D,E. Since there is one remaining city to visit, the next process will certainly take C. The path that was built by the ant is then: $A \rightarrow B \rightarrow D \rightarrow E \rightarrow C$. The length of this path is $L = AB + BD + DE + EC = 100 + 75 + 50 + 125 = 350$.

The remaining ants will proceed according to the same procedure. The following table summarize the solutions built by all ants.

The last column in Table 2.3 is the *gain* obtained by each ant. Since the longest

Table 2.3: Solutions built by the ant in the first iteration.

Ant	Path	Length of the path (L)	$\Delta\tau = 500/L$
ant1	$A \rightarrow B \rightarrow D \rightarrow E \rightarrow C$	350	1.43
ant2	$B \rightarrow C \rightarrow D \rightarrow E \rightarrow A$	275	1.82
ant3	$C \rightarrow B \rightarrow D \rightarrow E \rightarrow A$	250	2.00
ant4	$D \rightarrow E \rightarrow A \rightarrow B \rightarrow C$	275	1.82
ant5	$E \rightarrow A \rightarrow B \rightarrow C \rightarrow D$	325	1.54

distance between cities is 125. The solution built by the ant must not exceed $4 * 125 = 500$. Thus, the gain of each ant can be formulated as $500/L$, with L is the length of the path of the solution.

When all ants finish their tour. They will track back and update the pheromone along their path by putting additional pheromone ($\Delta\tau$). Note that, the amount of $\Delta\tau$ is proportional to the gain obtained by the ant. The new pheromone value is given by the following.

$$\tau = \tau + \Delta\tau$$

Consider, for example, edge AB was used by ant1, ant4 and ant5. The new pheromone value for edge AB is therefore equal to $1 + 1.43 + 1.82 + 1.54 = 5.79$.

Then, pheromone will evaporate according to the following formula:

$$\tau = (1 - \rho) * \tau$$

Assume that ρ is equal to 0.2. Then the pheromone value on edge AB is equal to $0.8 * 5.79 = 4.63$. The calculation of pheromone value is performed for all edges.

Table 2.4 shows the new pheromone values on each edge at the end of iteration 1.

Table 2.4: Pheromone values for each edge after iteration 1.

	initial pheromone value					new pheromone value				
	A	B	C	D	E	A	B	C	D	E
A	0.00	1.00	1.00	1.00	1.00	0.00	4.63	0.80	0.80	6.54
B	1.00	0.00	1.00	1.00	1.00	4.63	0.00	6.54	3.54	0.80
C	1.00	1.00	0.00	1.00	1.00	0.80	6.54	0.00	0.80	0.80
D	1.00	1.00	1.00	0.00	1.00	0.80	3.54	0.80	0.00	6.45
E	1.00	1.00	0.80	1.00	0.00	6.54	0.80	0.80	6.45	0.00

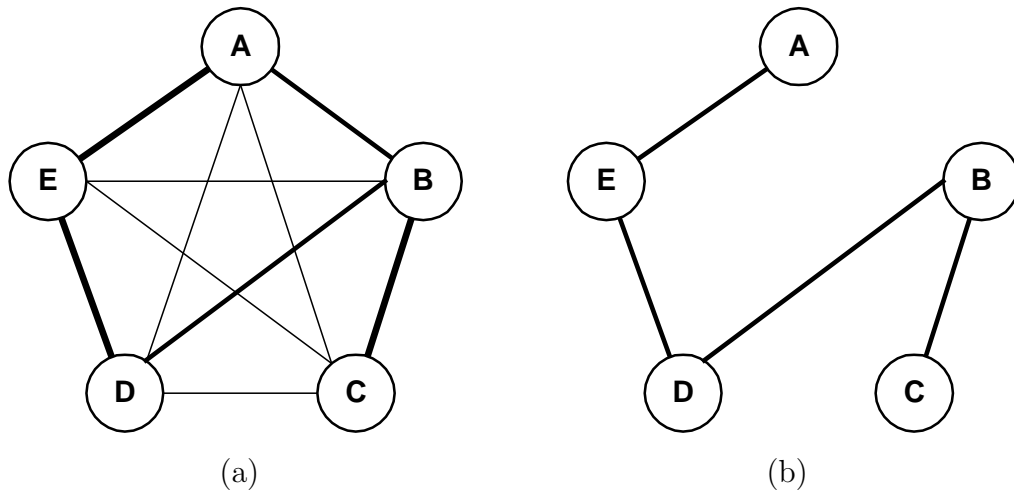


Figure 2.4: (a) Visualization of pheromone values and (b) Best solution built in the first iteration.

Figure 2.4 (a) shows the visualization of pheromone values on the edges. In this figure, the darker the edge, the higher the pheromone. The best solution found by the heuristic in the first iteration is shown in Figure 2.4 (b).

Iteration 2

The same process that were performed in the first iteration is repeated in the second

iteration. However, the initial pheromone values on all edges has changed. Thus, the probability of selecting a certain edge will also change. The higher the pheromone on the edge, the more attractive the edge for an ant to choose.

Assume that all ants have finished their tour construction. The following table summarize the solutions built by all ants.

Table 2.5: Solutions built by the ant in the second iteration.

Ant	Path	Length of the path (L)	$\Delta\tau = 500/L$
ant1	$A \rightarrow E \rightarrow D \rightarrow B \rightarrow C$	250	2.00
ant2	$B \rightarrow C \rightarrow D \rightarrow E \rightarrow A$	275	1.82
ant3	$C \rightarrow B \rightarrow D \rightarrow E \rightarrow A$	250	2.00
ant4	$D \rightarrow E \rightarrow A \rightarrow B \rightarrow C$	275	1.82
ant5	$E \rightarrow A \rightarrow D \rightarrow B \rightarrow C$	300	1.67

The pheromone update and pheromone evaporation procedures are then performed. This will change the value of pheromone on each edges. Table 2.6 shows these values.

Table 2.6: Pheromone values for each edge after iteration 2.

	initial pheromone value					new pheromone value				
	A	B	C	D	E	A	B	C	D	E
A	0.00	4.63	0.80	0.80	6.54	0.00	6.45	0.80	2.47	15.84
B	4.63	0.00	6.54	3.54	0.80	6.45	0.00	15.84	9.21	0.80
C	0.80	6.54	0.00	0.80	0.80	0.80	15.84	0.00	2.62	0.80
D	0.80	3.54	0.80	0.00	6.45	2.47	9.21	2.62	0.00	14.09
E	6.54	0.80	0.80	6.45	0.00	15.84	0.80	0.80	14.09	0.00

Figure 2.5 (a) shows the visualization of pheromone values on the edges. As we can see, the lines representing edge AE, ED and BC are very thick. These lines are thicker than the corresponding ones in the previous iteration (see Figure 2.4).

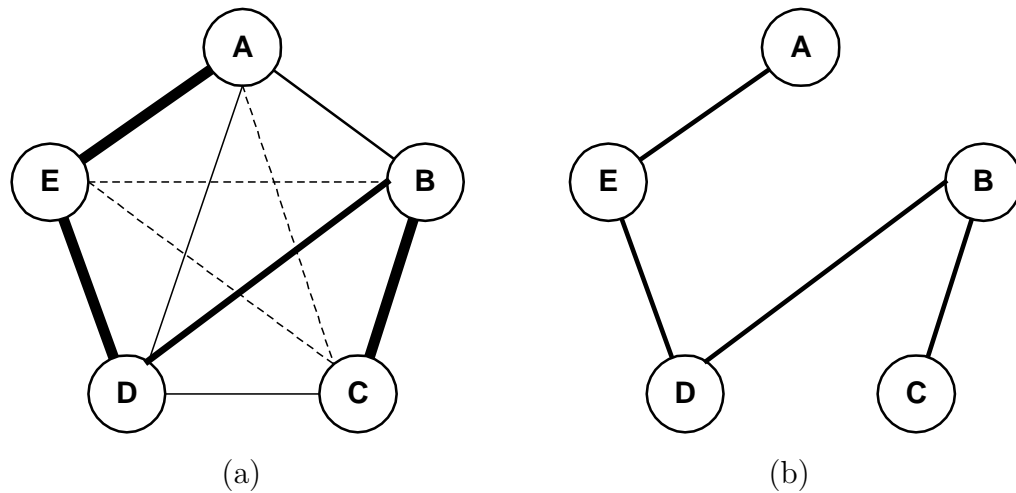


Figure 2.5: (a) Visualization of pheromone values and (b) Best solution built in the second iteration.

The thickness of these lines correspond to their high pheromone values. This is because more ants are using these edges (see Table 2.6). On the other hand, the lines representing edge AC, BE and CE are very thin. Since no ant is using these edges, there is no additional pheromone given. In addition, pheromone evaporation reduces the intensity of pheromone values on these edges. This will make these edges less attractive for future ants.

The algorithm will proceed until a criteria is met. From Figure 2.5(a), it can be seen that the best solution for the given TSP problem will likely be equal to the one illustrated in Figure 2.5(b).

It has been shown that ACO algorithm produced better quality results compared to those obtained by other heuristics when it is applied to combinatorial optimization problems such as TSP and QAP [55]. Unfortunately, only few published works found

in literature that uses ACO algorithm for evolutionary logic design (Coello et al. [6]). Therefore, there is a need for investigating further the use ACO for evolutionary design of digital circuits.

2.3 The Multiobjective Optimization Problem

Constraint satisfaction and multiobjective optimization are two aspects of the same problem. Both involve the simultaneous optimization of a number of functions. Based on the approach used in handling the constraint, there exists *constrained optimization* and *multiobjective optimization*.

Constraints can be expressed in terms of inequalities of the type

$$f(x) \leq g \tag{2.2}$$

where f is a non-linear, real-valued function of the decision variable vector x , while g is a constant value.

Without loss of generality, the constrained optimization problem is that of minimizing a scalar function f_1 of some decision variable vector x in a universe u , subject to a number $n - 1$ of conditions involving x , and eventually expressed as a functional vector inequality of the type

$$(f_2(x), \dots, f_n(x)) \leq (g_2, \dots, g_n) \tag{2.3}$$

where the inequalities are applied component by component. It is assumed that there is at least one point u which satisfies all constraints [56].

A general *multiobjective optimization problem* (MOP) includes a set of n parameters (decision variables), a set of k objectives, and a set of m constraints. Objectives and constraints are functions of the decision variables. The optimization goal is defined in Equations 2.4, and 2.5.

$$\text{maximize } y = f(x) = (f_1(x), f_2(x), \dots, f_k(x)) \quad (2.4)$$

$$\text{subject to } e(x) = (e_1(x), e_2(x), \dots, e_m(x)) \leq 0 \quad (2.5)$$

Where,

$$x = (x_1, x_2, \dots, x_n) \in X \quad (2.6)$$

$$y = (y_1, y_2, \dots, y_k) \in Y \quad (2.7)$$

In this abstract model, x is called the decision vector, y is called the objective vector, X is called the decision space, and Y is called the objective space. The constraints $e(x) \leq 0$ determine the set of feasible solutions. The feasible set X_f is defined as the set of decision vectors x that satisfy the constraints $e(x)$.

In order to select a suitable compromise solution from all alternatives, a decision process is necessary in multiobjective optimization problems (MOP). The decision

process is performed based on the preference articulation. The preference articulation implicitly defines the utility function to differentiate any candidate solutions. Three approaches have been used, namely priorities, weighting coefficients and goal values.

Priorities are real values, which determine the order in which objectives are to be optimized according to their importance. In this technique, all objectives need to be assigned different priorities. However, assigning priorities itself is another difficult problem, mostly for conflicting objectives. Thus, the quality of results obtained from this technique is rather limited.

In the weighting coefficient scheme, all objectives are aggregated into a single function. An example of this approach is the weighted sum scheme given by:

$$\min \left(\sum_{i=1}^k w_i f_i(x) \right)$$

where $w_i \geq 0$ are the weighting coefficients representing the relative importance of the i^{th} objective function of the problem. It is usually assumed that:

$$\sum_{i=1}^k w_i = 1$$

This technique is known for its simplicity. However, since the result of solving optimization model using weighted sum can vary significantly as the weighting co-

efficient change, the perfect tuning of weight values for each objectives become very important. In addition, the different scale and behavior of each objective makes it difficult to determine the perfect weights for each objective and aggregate them into a single function.

The goal values can accommodate a whole variety of constrained and/or multiobjective problem formulations. The goal information is often naturally available from the problem formulation, although not necessarily in an explicit way. The interpretation of such information should be used to differentiate any alternate solutions. The goal values can be easily incorporated with fuzzy logic [15] for solving MOP problem. This will be explained in the following section.

2.4 Fuzzy Logic

Fuzzy Logic was introduced by Lofti A. Zadeh in [57, 58]. During the past decades, fuzzy logic has found numerous applications in the field of engineering and control [59]. In the field of VLSI design, several techniques based on fuzzy logic are reported in the literature [60, 61, 62].

The expressive power of fuzzy logic derives from the fact that it contains not only the classical two-valued and multi-valued logical systems but also probability theory and probabilistic logic. Fuzzy logic deals with approximate rather than precise modes of reasoning. This makes fuzzy logic capable of handling the uncertainty of

data. In addition to that, natural language, which is the basis of fuzzy logic, is more convenient for expressing engineering problems.

In general, fuzzy logic can be viewed as a nonlinear mapping of an input data vector into a scalar output. However, the flexibility of fuzzy logic may create lots of different mapping for a single problem instance. Therefore, a good understanding of the fuzzy set theory, fuzzy reasoning and fuzzy rules is needed.

2.4.1 Fuzzy Set Theory

Unlike in classical (crisp) theory where each element can either belong to the set or not, an element in fuzzy logic may partially belong to a fuzzy set by a certain degree.

A fuzzy set A of universe of discourse X is defined as $A = \{(x, \mu_A(x)) \mid \text{all } x \in X\}$, where X is a space point and $\mu_A(x)$ is a membership function of x being an element of A . A membership function $\mu_A(x)$ is a mapping of x in A that maps X to the membership space M . The range of the membership function is a subset of the non-negative real numbers whose boundaries are finite [63]. Elements with zero degree of membership are normally not listed.

Fuzzy Reasoning

Unlike classical reasoning in which propositions are whether true or false, fuzzy logic establishes approximate truth value of propositions based on linguistic variables and

inference rules [58]. A linguistic variable is a variable whose values are words or sentences in natural or artificial language. It is concerned with the use of fuzzy values that captures the meaning of words, human reasoning and decision-making. An example of linguistic variable is circuit's area. This variable can be expressed by linguistic values like very small, small, average, large and very large circuit, rather than $20 \mu m^2$, $30 \mu m^2$, $50 \mu m^2$, $75 \mu m^2$, and $100 \mu m^2$.

A linguistic variable carries the concept of fuzzy set qualifiers, called *hedges*. Hedges are terms that modify the shape of fuzzy sets. They include adverbs such as *very*, *somewhat*, *quite*, *more or less*, and *slightly*. They are used as modifiers, truth-values, probabilities, quantifiers and/or possibilities of a certain linguistic variable.

Formally, a linguistic variable comprises of five elements [64]:

1. The variable name
2. The primary term set
3. The universe of discourse U
4. A set of syntactical rules that allows composition of the primary terms and hedges to generate the term set
5. A set of semantic rules that assigns each element in the set a linguistic meaning.

Fuzzy Operators

There are two basic types of fuzzy operators. The operators for the intersection, interpreted as the logical “and”, and the operators for the union, interpreted as the logical “or” of fuzzy sets. The intersection operators are known as triangular norms (t-norms), and union operator as triangular co-norms (t-co-norms or s-norms) [63]. Some examples of s-norm operators are given below, (were A and B are the fuzzy sets of universe of discourse X).

1. Maximum. $[\mu_{A \cup B}(x) = \max\{\mu_A(x), \mu_B(x)\}]$.
2. Algebraic sum. $[\mu_{A \cup B}(x) = \mu_A(x) + \mu_B(x) - \mu_A(x)\mu_B(x)]$.
3. Bounded sum. $[\mu_{A \cup B}(x) = \min(1, \mu_A(x) + \mu_B(x))]$.
4. Drastic sum. $[\mu_{A \cup B}(x) = \mu_A(x)$ if $\mu_B(x) = 0$, $\mu_B(x)$ if $\mu_A(x) = 0$, 1 if $\mu_A(x), \mu_B(x) > 0]$.

An s-norm operator satisfies commutativity, monotonicity, associativity and $\mu_{A \cup 0}(x) = \mu_A(x)$ properties.

Following are some examples of t-norm operators.

1. Minimum. $[\mu_{A \cap B}(x) = \min\{\mu_A(x), \mu_B(x)\}]$.
2. Algebraic product. $[\mu_{A \cap B}(x) = \mu_A(x)\mu_B(x)]$.
3. Bounded product. $[\mu_{A \cap B}(x) = \max(0, \mu_A(x) + \mu_B(x) - 1)]$.

4. Drastic product. $[\mu_A \cap_B(x) = \mu_A(x)$ if $\mu_B(x) = 1$, $\mu_B(x)$ if $\mu_A(x) = 1$, 0 if $\mu_A(x), \mu_B(x) < 1]$.

Like s-norm, t-norms also satisfy commutativity, monotonicity, associativity and $\mu_A \cap_1(x) = \mu_A(x)$. Also, the fuzzy complementation operator is defined as follows.

$$\bar{\mu}_B(x) = 1 - \mu_B(x) \quad (2.8)$$

2.4.2 Multi-objective Optimization Using Fuzzy Logic

Approximate reasoning can be made based on linguistic variables and their values. Rules can be generated based on previous experience. The rules are expressed as **If ... Then** statements. Connectives such as AND and OR can be used in approximate reasoning to join two or more linguistic values. The If part (*antecedent*) is a fuzzy predicate defined in terms of linguistic values and fuzzy operators (AND and OR). The Then part is called the *consequent*.

In optimization problems, the linguistic value used in the consequent part identifies the fuzzy subset of good solutions. Therefore, the result of evaluation of the antecedent part identifies the degree of membership in the fuzzy subset of good solutions according to the fuzzy rule in question. If more than one rule is used to perform decision-making, each rule can be evaluated to generate a numerical value. Then, these numerical values from various evaluations of different rules can be combined

to generate a crisp value on a higher level of hierarchy.

Consider the circuit design problem with minimization of area, delay, and power consumption. Three linguistic variables area, delay and power introduced. Then good solutions can be characterized by the following fuzzy rule.

If the circuit has (small area) and (less delay) and (less power consumption) then it is a good solution.

In the traditional fuzzy logic, the minmax operators are used to build the above fuzzy rule. However, it was shown in [65] that these operators can lead to undesirable behavior. This behavior has led to the development of other fuzzy operators such as the *Ordered Weighted Averaging (OWA)* operator explained below.

Ordered Weighted Averaging (OWA) Operator

Generally, the formulation of multi criterion decision functions neither desires the pure “AND-ing” of t-norm nor the pure “OR-ing” of s-norm. The reason for this is the complete lack of compensation of t-norm for any partial fulfillment and complete submission of s-norm to fulfillment of any criteria. Also the indifference to the individual criterion of each of these two forms of operators led to the development of Ordered Weighted Averaging (OWA) operators [66, 67]. This operator allows easy adjustment of the degree of “AND-ing” and “OR-ing” embedded in the aggregation. According to [66, 67], “OR-like” and “AND-like” OWA for two fuzzy sets A and B

are implemented as given in Equations 2.9 and 2.10 respectively.

$$\mu_{A \cup B}(x) = \beta \times \max(\mu_A, \mu_B) + (1 - \beta) \times \frac{1}{2}(\mu_A + \mu_B) \quad (2.9)$$

$$\mu_{A \cap B}(x) = \beta \times \min(\mu_A, \mu_B) + (1 - \beta) \times \frac{1}{2}(\mu_A + \mu_B) \quad (2.10)$$

where β is a constant parameter in the range $[0,1]$. It represents the degree to which OWA operator resembles a pure “OR” or pure “AND” respectively.

2.5 Concluding Remarks

Some background material, definitions and concepts that should be helpful in understanding this thesis work were provided in this chapter. Basic knowledge about logic synthesis algorithm, Ant Colony Optimization (ACO) algorithm, Multi-Objective Optimization Problem (MOP) and Fuzzy Logic were also presented. Next, literature review on existing techniques in ELD is given in Chapter 3.

Chapter 3

LITERATURE REVIEW

In this chapter, literature review of evolutionary logic design is presented. Discussion and observations are also provided.

3.1 Introduction

In recent years, engineers have shown growing interest in **Nature** wishing to imitate the observed processes. The reason for this lies in the fact that living beings exhibit very desirable qualities, such as adaptation and fault tolerance which engineers have been largely struggling to reproduce. This has led to the birth of such field as evolutionary computation.

Recently, a new field of research in which hardware design is pursued as biological organisms has begun to evolve. The new paradigm may radically change the design

procedure and new possibilities for discovering novel designs and/or more efficient circuits may emerge. The new methodology considers a concept for automatic design of electronic systems. Instead of using human made models and techniques, it employs search heuristics to develop efficient designs.

Evolutionary design of digital circuits is a very challenging field. This is due to two reasons: (a) the complexity of the search space and (b) the existence of efficient CAD tools for digital design. Thus, it is difficult to develop new iterative heuristics'-based CAD tools that provide competitive performance when compared to the already existing ones. Nonetheless, the possibility to find new circuit designs and the capacity to contemplate a larger set of specifications are some of the reasons that complement its difficulty [25].

3.2 Classification of Evolutionary Logic Design

Evolvable Hardware (EHW) or *Evolutionary Electronics* is a field of research that focuses on using Evolutionary Algorithms (EAs) in the hardware domain. The scope of this field is vast, ranging from hardware design, fault tolerance, image processing and pattern recognition to robot control [25, 33]. Nevertheless, EHW can be roughly classified into two fields, namely *design EHW* and *adaptive EHW*. Based on the application point of view, EHW is further divided into design of analog and digital circuits. EHW for design of digital circuits is also called *Evolutionary Logic Design*

(*ELD*).

There are three possible representations of digital circuits in *ELD*, namely functional, gate, and transistor level. These representations differ in the degree of complexity of the basic building blocks used. On the functional level, a circuit is represented in terms of high level mapping of digital circuits. The basic building blocks for this representation can be the minterms of a Boolean function or some RTL blocks such as multiplexers. Gate level representation deals with basic logic gates, while transistor level uses CMOS transistors and TTL as their building blocks.

Gate level representation is the most widely used representation in the literature. This is due to the fact that the behavior of the basic building blocks, i.e., logic gates is not as complicated as transistor level representation, as well as providing a simple mapping between the circuit's structure and the representation.

3.3 Existing ELD Techniques

Most of the techniques presented in the following section use Genetic Algorithms (GAs) as the search engine for the *ELD*. Some adequate background on GAs can be found in any book on iterative heuristic such as [15].

3.3.1 EAs Based ELD

Louis [10] introduced the idea of using Evolutionary Algorithms as tools to perform *structure design*, in which digital circuits are viewed as structure of interconnected logic gates. They modelled a given circuit as a matrix. Each cell represents a primitive gate, such as AND, OR, NOT, and XOR gates with their corresponding input. Connecting WIRES are simply gates that transfer one of their inputs to their output. Every cell in a column $i + 1$ can only get its input from cells in column i . This structure is shown in Figure 3.1.

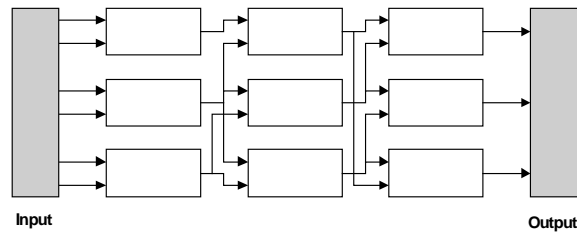


Figure 3.1: A mapping scheme used in [10].

In this figure, gates which are close together in two-dimensional (phenotype) space may be far apart in one-dimensional (genotype) space. This condition creates problems for classical genetic operators such as single-point crossover. Therefore, masked crossover is used to preserve highly fit schemas in the chromosome.

The *masked crossover* makes use of the relative fitness of the children, with respect to their parents. When a child is produced, the masks used to produce it may be modified depending on how well the child does relative to the parents. Initial masks can be generated randomly and will be propagated along with the evolution

process. Mask propagation is controlled by a set of rules that depends on the relative fitness of children to its parents. Thus, three types of children can be defined:

1. Good child: has fitness higher than that of both parents
2. Average child: has fitness between that of both parents
3. Bad child: has fitness lower than that of both parents.

A child's mask is a copy of the dominant parent's mask except for the changes the rules allow. The underlying premise guiding the rules is that when a child is less fit than its dominant parent, the recessive parent contributed bits reduce the fitness of the child.

Using the above mentioned approaches, the authors managed to design some digital circuits, ranging from 2-bit adders to 6-bit parity circuits [10].

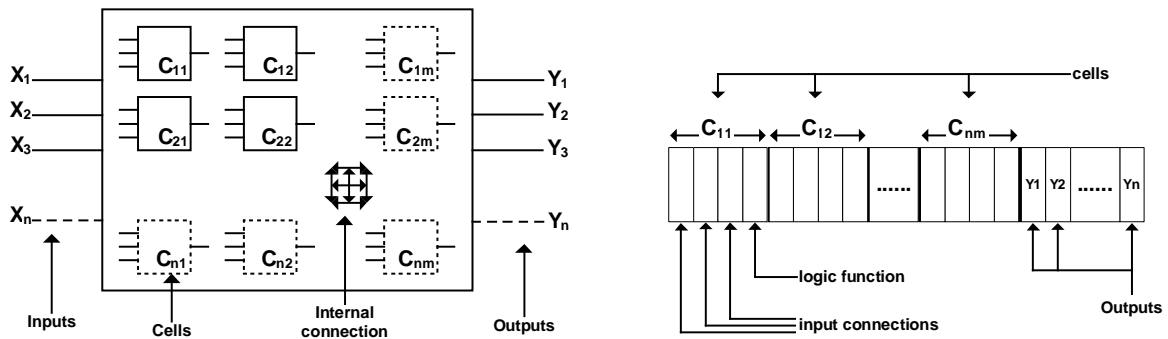


Figure 3.2: Chromosome representation used by Miller et. al., [1, 2, 3, 4, 5].

Miller et al. [3] argued that one aspect of evolution in hardware is geometry. They suggested that the chromosome representation should match the hardware's

geometry configuration. In the case of FPGA, a matrix of $n \times m$ array of logic cells is used as the phenotype representation. The genotype representation, the chromosome, is defined as a set of interconnections together with gate level functionality for cells. This genotype-phenotype mapping is shown in Figure 3.2.

Since the authors were targeting FPGAs, the logic function at each gene of the chromosome can be any of the possible functions realized by a FPGA cell. Table 3.1 lists all possible cell functions.

Table 3.1: Possible cell functions in [1, 2, 3, 4, 5].

Alphabet	Function	Alphabet	Function
0	0	10	$a \oplus b$
1	1	11	$a \oplus \bar{b}$
2	a	12	$a + b$
3	b	13	$a + \bar{b}$
4	\bar{a}	14	$\bar{a} + b$
5	\bar{b}	15	$\bar{a} + \bar{b}$
6	$a \cdot b$	16	$a \cdot \bar{c} + b \cdot c$
7	$a \cdot \bar{b}$	17	$a \cdot \bar{c} + \bar{b} \cdot c$
8	$\bar{a} \cdot b$	18	$\bar{a} \cdot \bar{c} + b \cdot c$
9	$\bar{a} \cdot \bar{b}$	19	$\bar{a} \cdot \bar{c} + \bar{b} \cdot c$

Each gene is a sequence of integers representing the target interconnection of gate's inputs and the gate type. Consider, for example, the case shown in Figure 3.3. The first quadruplet of the chromosome is 0-1-0-10, indicating that the first input of the cell is connected to pin number 0, the second input to pin number 1, and the third input to pin number 0 (the third input is not used) respectively. The gate type is 10, two-input XOR. The interconnection between cells is restricted by the

levels-back parameter, which denotes the number of previous column(s) in the array that a cell can be connected to. If the levels-back parameter is one, then each cell must be connected to its immediate neighbor in the previous column. Cells within any particular column cannot be connected together, and feedback connections are not allowed.

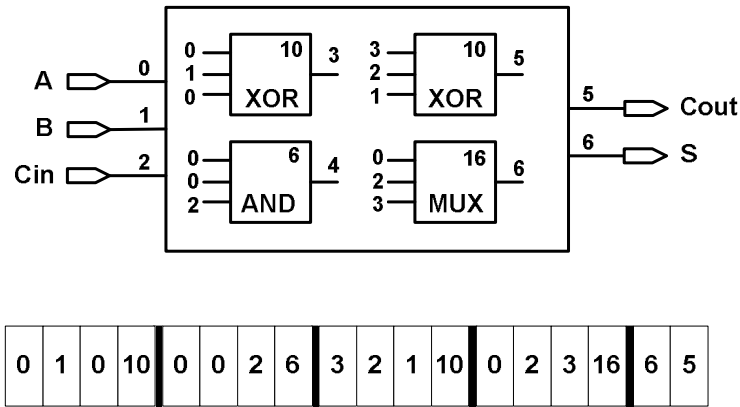


Figure 3.3: Example of genotype-phenotype mapping used in [1, 2, 3, 4, 5].

The authors used Genetic Algorithm in [4] and Evolutionary Strategies in [1] to produce some evolved circuits including those of a full adder and a 3-bit multiplier. They have shown that the obtained circuits require fewer number of gates compared to the ones produced using conventional methods.

Coello [6, 7, 11] used the same chromosome representation of circuits as those used by Louis [10]. Each cell is a gate of the type AND, NOT, OR, XOR or WIRE. Each cell is encoded in a triplet of inputs and gate type, as illustrated in Figure 3.4.

A gate at position (i, j) of the matrix can only be connected to the one at

Input 1	Input 2	Gate type
---------	---------	-----------

Figure 3.4: Encoding of a cell used in [6, 7, 11].

$(i, j - 1)$. This restriction reduces the cardinality of alphabet needed to represent the chromosome, since the integer number to represent each cell is increasing in a column wise only.

The evolution runs in two phases, the first phase is to find a fully functional circuit, and the second one is to find an optimum circuit. The goal of the optimization is to maximize the number of WIRES in the chromosome representation. This translates into less number of gates required to implement a given circuit.

Coello proposed three different implementations of GAs, namely binary GA (BGA), n -cardinality GA (NGA) and multiobjective GA (MGA). In MGA, multiobjective optimization is not applied for optimizing different objectives such as delay, area and power. It is used only to divide the search for correct truth table into several objectives. Each optimization objective concentrates on a single bit in the truth table. In addition, one optimization objective is added to unite all the former ones. Thus, if the length of the truth table is n , then $n + 1$ objectives have to be found by the MGA [36].

Hounsel et al. used a fixed length chromosome for circuit representation [12, 13]. Specific sections of the chromosome are reserved for describing the inputs and outputs of the circuit. Circuit's inputs are encoded in the first section of the

chromosome, while the outputs are defined at the end of the chromosome. Logic elements are referenced by position within chromosome. Figure 3.5 displays the relative location of each encoded section.

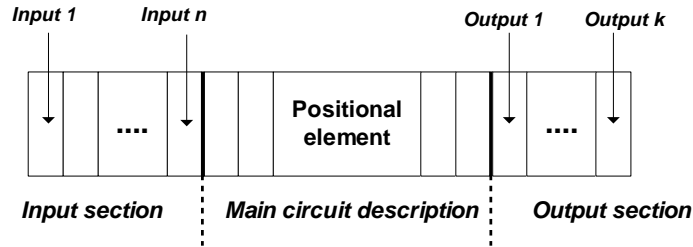


Figure 3.5: Chromosome representation [12, 13].

Each logic element in a circuit is allocated at a specific position within the chromosome. Each position can be a primitive gate or macro block such as multiplexer, adder, etc. Each of these is represented by an ID from a circuit library. Interconnectivity between cells is not restricted to its nearest positional neighbor. Rather, cells are free to connect to other cells at higher positions within the chromosome. Feedback connections are not permitted. Figure 3.6 demonstrates the encoding of a macro block (full-adder) with its connectivity within the chromosome.

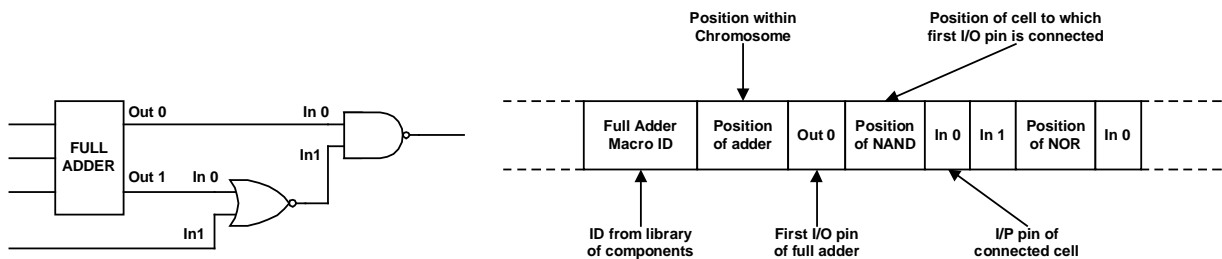


Figure 3.6: Macro blocks and its genotype representation in [12, 13].

Single point crossover is used to generate *offsprings*. Chromosome repair is used

to reconnect any broken interconnection during the operation. This guarantees that an offspring chromosome represents a valid circuit. Mutation is applied to maintain diversity within the population. There are four types of mutation used in the evolution process. These are shown in Figure 3.7.

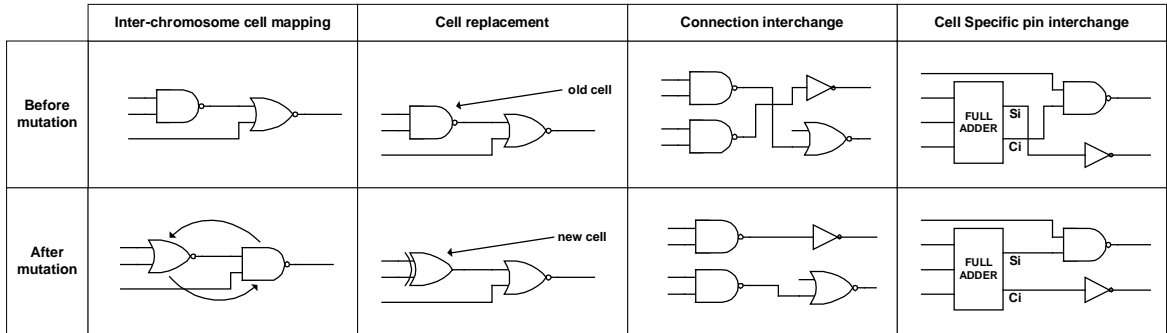


Figure 3.7: Mutation operators proposed in [12, 13].

Evaluation of chromosomes is done by a HDL simulator. The evolved circuit can then be synthesized to provide a technology specific netlist, ready for transfer onto the target FPGA. The evolved circuits have been compared with those designed using conventional techniques. It is shown that some of the evolved circuits have slightly better performance in terms of delay, compared to the circuits produced by conventional methods [12, 13].

3.3.2 ACO Based ELD

ACO-based ELD was proposed by Coello et al. [6]. They used a matrix representation, whereby each cell of the matrix consists of a gate and the gate's corresponding input(s). Each column in the matrix is called a *state* and each cell in a certain

column is called a *sub-state*.

All ants have to construct a tour in each iteration. Ants start their movement from the first column and proceed until they reach the last column. The goal of an ant in constructing a tour is to fill up the matrix. However, ants can only fill the first k (k is equal to the number of circuit's output) number of cells in every column. The other cells are filled randomly.

The selection of which attribute combination (gate type and its corresponding input(s)) to be assigned in a newly visited cell is performed by a stochastic process. For this purpose, all possible combinations of gates and its corresponding inputs are considered. The probability of choosing a certain combination is determined by the *distance* and *pheromone* value. The distance is the increment (or decrement) in the number of correct matchings with the target truth table. The probability is then calculated using the following formula.

$$p_{i,j}^k(t) = f_{i,j}(t) \times h_{i,j} \quad (3.1)$$

where k refers to the ant that is considered, t refers to the current iteration, $f_{i,j}(t)$ is the amount of pheromone between state i and state j , and $h_{i,j}(t)$ is the distance between state i and state j . The selection is then performed by using roulette wheel.

Consider, for example, a two-bit adder circuit. Assume that the size of the matrix used is 6×5 . The number of inputs considered is four (without the carry input)

and the number of outputs is three. First, the ant will select which combination to be assigned at cell(0,0). The probability of choosing each combination of gate and its corresponding inputs are calculated. Assume that the result of selection (using roulette wheel) is WIRE1(3,4). This triplet is then put into cell(0,0). After that, for the second output of the circuit, again, probability values for each combination is calculated. Assume that XOR(3,1) is selected. This combination is then assigned into cell(1,0). Using the same procedure, cell(2,0) is filled. Since there are only three outputs, the rest of the cells in the first column is filled randomly. Figure 3.8 shows the matrix's state for the first column. The shadowed cells are the ones that were filled randomly.

WIRE1(3,6)				
XOR(3,1)				
XOR(2,4)				
OR(3,4)				
AND(4,2)				
WIRE1(1,1)				

Figure 3.8: The matrix's state after the filling of the first column.

By using the same procedure, the ant moves to the second column, the third column and so on, until it reaches the last column. Assume that the result of its movement is shown in Figure 3.9

WIRE1(3,4)	AND(1,6)	OR(1,4)	WIRE1(1,1)	WIRE1(1,1)
XOR(3,1)	OR(5,2)	XOR(4,2)	WIRE1(2,2)	WIRE1(2,2)
XOR(2,4)	WIRE1(3,3)	WIRE1(3,3)	WIRE1(3,3)	WIRE1(3,3)
OR(3,4)	AND(5,2)	OR(6,3)	AND(3,4)	NOT1(2,5)
AND(4,2)	WIRE1(4,2)	XOR(4,4)	OR(3,5)	OR(5,3)
WIRE1(1,1)	XOR(4,4)	OR(3,4)	OR(3,5)	AND(1,3)

Figure 3.9: The matrix's state after the filling of all cells

When the ants finish the tour, the solution obtained is evaluated. Note that not all cells in the matrix are included in the final solution. Figure 3.10 shows an example of tour built by an ant. In this figure, the shadowed cells are the ones that are included in the final solution.

WIRE1(3,4)	AND(1,6)	OR(1,4)	WIRE1(1,1)	WIRE1(1,1)
XOR(3,1)	OR(5,2)	XOR(4,2)	WIRE1(2,2)	WIRE1(2,2)
XOR(2,4)	WIRE1(3,3)	WIRE1(3,3)	WIRE1(3,3)	WIRE1(3,3)
OR(3,4)	AND(5,2)	OR(6,3)	AND(3,4)	NOT1(2,5)
AND(4,2)	WIRE1(4,2)	XOR(4,4)	OR(3,5)	OR(5,3)
WIRE1(1,1)	XOR(4,4)	OR(3,4)	OR(3,5)	AND(1,3)

Figure 3.10: The cells used in the solution by an ant.

All ants will update the pheromone along its track. The pheromone update is performed using the following formula.

$$f_{i,j}(t+1) = (1 - \alpha) \times f_{i,j}(t) + \sum_{k=1}^m f_{i,j}^k \quad (3.2)$$

where $0 \leq \alpha \leq 1$, k is the index of the ant and $f_{i,j}$ of the solution built. The value of $f_{i,j}$ is calculated based on the following conditions:

1. If the circuit is not feasible (i.e., not all outputs match their truth table).

$$f_{i,j}(t) = f_{i,j}(t) + \textit{payoff}$$

2. If the circuit is feasible.

$$f_{i,j}(t) = f_{i,j}(t) + (2 \times \textit{payoff})$$

3. If the circuit is the best feasible solution.

$$f_{i,j}(t) = f_{i,j}(t) + (3 \times \textit{payoff})$$

The value of *payoff* is given by the number of matches produced between the output generated by the circuit built by the agent and the target truth table. When all ants finish their tour, the best solution is saved and the process starts from beginning again. After the maximum number of iterations is reached, the best global solution is returned.

3.3.3 Other Related Work

Multiplexer-based Genetic Programming for logic design was proposed by Coello et al. [68]. A tree structure is used to represent a circuit. An algorithm, the *Cartesian Grid Programming* (CGP), was proposed and used for logic design [69, 34]. A complete automated system for ELD, “The Evolware” was proposed in [70].

Some researchers concentrated on the use of EAs for solving logic synthesis problems. Their work can be classified into three groups. The first group uses EAs to optimize the representation of multi-level logic circuits [71, 72]. The second group works on minimizing the RM representation using EAs [73, 74]. The last group focuses on the optimization of BDD-based representation of logic circuits using EAs [74].

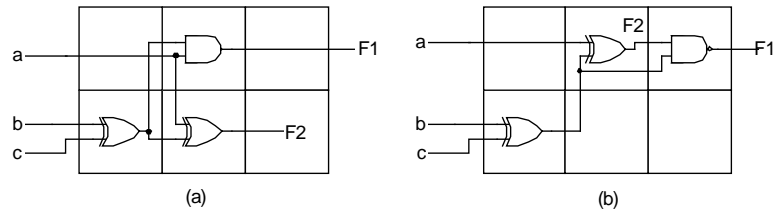


Figure 3.11: Problems that may appear in matrix representation: (a) fitness of $F1 < 1$ (b) fitness of $F2 = 1$.

3.4 Discussion

Several techniques in evolutionary logic design are described in the previous section. Majority of those techniques were able to arrive at solutions that are difficult to obtain using conventional methods. However, there are still many open problems that were not addressed. A number of these problems are listed below.

1. Circuit representation

Most of the published work in evolutionary logic design used a two-dimensional matrix of $n \times m$ to represent a circuit. The position of circuit's outputs will most likely be placed at $\text{cell}(0, m - 1)$. However, it may happen that the best solution can be found at $\text{cell}(i, j)$, $0 < i < n$, $0 < j < m$. But some redundant gates existing between this cell and the output cell may degrade the quality of the solution. The problem becomes complicated even further when the number of circuit's output is more than one. Figure 3.11 illustrates the problem arises from circuit representation.

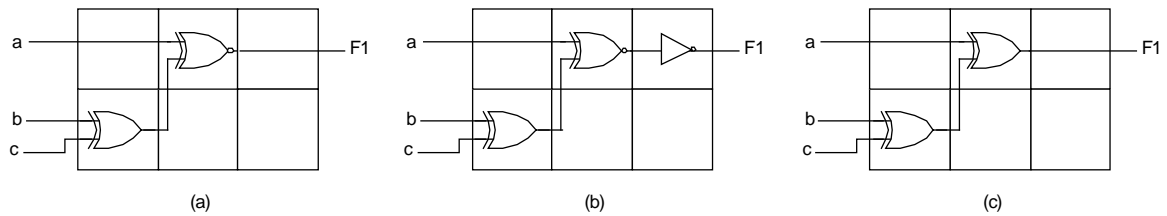


Figure 3.12: An evolved two-bit odd parity circuit. (a) Fitness of $F1 = 0$ (b) Adding an inverter, fitness of $F1 = 1$ (c) Toggle the type of gate (XNOR \rightarrow XOR), fitness of $F1 = 1$

2. Functional fitness calculation

The value of functional fitness depends on the number of correct matchings between the output's pattern of the obtained solution and the truth table of the intended circuit. The higher the number of hits achieved, the higher the value of the functional fitness. This argument is not always true in logic design. A solution that has low functional fitness can be inverted to have a high functional fitness (see Figure 3.12).

3. Don't care values

A key factor in minimization of Boolean functions is the existence of don't care value [20]. However, all techniques presented in ELD have paid no attention to this factor. Their algorithms can only handle completely specified functions. It is believed that the inclusion of don't care values will be indeed beneficial for the ELD.

4. Inverted inputs

Determining the correct phase (positive or negative) for each primary input

has been long addressed in conventional logic design techniques. In fact, for some cases, the use of the complement of some of the primary inputs can lead to more efficient circuit's representation.

5. Objectives of the optimization

Most of the existing techniques used the gate count as their optimization objective. With the increasing need for circuits that have better performance and lower power consumption, the objective of only minimizing gate count is not anymore sufficient. In addition, the term 'gate' or basic module for the evolutionary logic design depends on the definition of the gate library that is used. One may use NAND gates, or a set of AND, OR and XOR gates, or MUXes, or a combination of them. Each of the aforementioned 'gates' has different characteristics in terms of area, delay and input (output) capacitance for different target technologies. Therefore, optimizing the circuits in terms of area (delay and/or power) is more appropriate compared to optimizing it in terms of gate count.

The ACO-based approach proposed in [6] shows some interesting features. The problem associated with the circuit representation depicted in Figure 3.12 can be handled. This is because whenever an ant visits a cell that has truth table equal to the target truth table, the combination that will be selected for the next state will most likely be WIRES. In addition, the number of combinations of attributes is

proportional to the size of the matrix and the number of gate types used. Therefore, the process of assigning attributes to a new cell is a time consuming task.

In order to tackle the abovementioned problems, there are several possible improvements that can be investigated. These are enumerated below.

1. There is no need to fix the position of circuits output in the matrix. The ants can stop anywhere in the matrix, whenever they found the fully functional circuit.
2. The ant can have some intelligence to remember or forget some of the paths that were built. Thus, in agreement with the first assumption, the ant can return the best possible partial solution (sub-circuit) from the current matrix.
3. In order to support the second assumption, the content of the matrix will be dynamically filled. At every iteration, the cells that were included in the best possible partial solution obtained by the ant will be kept, while the other cells will be removed. These empty cells will be filled again in the next iteration.

3.5 Concluding Remarks

In this chapter, several existing techniques in ELD have been presented. The review has given insight on what has been done in this area. The discussion section in this chapter has highlighted the shortcoming of those techniques and provided some

possible improvements. It has led us to propose a new technique in ELD. This is the subject of the next chapter.

Chapter 4

PROBLEM AND COST

FUNCTION FORMULATION

In this chapter, the problem and cost function formulation are discussed. Problem statement, assumptions, inputs and outputs of the designed approach are given.

4.1 Problem Formulation

A Boolean function can be represented in a number of forms. For example, the following are possible representations of the same function.

1. $f = \bar{x}yz + x\bar{y}z + xy\bar{z}$

2. $f = (\bar{x}y + x\bar{y})z + xy\bar{z}$

$$3. f = (x \oplus y)z + xy\bar{z}$$

$$4. f = (x + y)(z \oplus xy)$$

The first representation, is a two-level logic representation, where all implicants are included in the function. If it is assumed that only two input gates are available (XOR gate is assumed as an atomic gate) and that complemented literals are available, then the first representation requires nine literals and eight gates (6 AND gates and 2 OR gates). The second representation, a factored form of function f (multi-level logic), requires eight literals and seven gates (5 AND gates and 2 OR gates). The third representation requires six literals and five gates (3 AND gates, 1 OR gate and 1 XOR gate). The last representation requires five literals and four gates (2 AND gates, 1 OR gate, and 1 XOR gate).

Based on the above analysis, the last representation is considered the best representation for function f , in terms of the number of literals. A human designer, however, cannot easily arrive at this representation. Fortunately, iterative heuristics have shown that they are capable of arriving at such efficient representations. Another major design objective is the delay of the circuits. Two-level logic representation is without doubt the best representation as far as minimum delay is concerned. Therefore, the first representation has the least delay.

Synthesis and optimization of digital circuits in terms of area and/or delay (performance) have been the focus of most research effort in logic synthesis field in

the last two decades. Results of several research efforts to optimize area and performance are available in the literature and are summarized in several papers and books [8, 19, 20, 21, 48]. Nevertheless, with several new power-constrained applications ranging from mobile phones to laptop computers, power dissipation has emerged as a major objective of VLSI circuit design [49, 51]. Several published works on logic synthesis targeting low power are reported in [52, 75, 76, 77, 78].

With the increasing demand of high quality, high performance and less area circuits, the problem of circuit design requires a multiobjective optimization approach. However, it should be noted that optimal representation can be obtained by a careful selection of gate types and an innovative ability to combine these in building a circuit. However, this process is not an easy task. There are 2^{2^n} possible n variables single-output logic functions. This makes the complexity of circuit design problem NP-hard.

Logic Design: A Search in the Design Space

As has been indicated in the preceding sections, the design space of digital circuits could be huge. There are 2^n ($C_1^{2^n}$) possible functions that satisfy $2^n - 1$ out of 2^n correct truth table for an n -input single-output Boolean function. The number of sub-functions that satisfy half of the truth table is $C_{2^n/2}^{2^n}$. For example, there are 12,870 possible sub-functions that satisfy half of the truth table of a four-input Boolean function. The number of intermediate points in the design space that is not

representing the function is even bigger. In addition to that, there exists a number of structures representing each of those points. These different structures represent different design objectives and/or constraints. Exploring the whole search space is impractical. Therefore, the search space sampled by the algorithm must have its size limited.

Determining the size of the search space is a subtle issue. It should be large enough to include a good variety of novel circuit topologies, but also small enough for an iterative heuristic to be able to find good solution(s). Therefore, as stated in [25], some procedures must be followed:

1. The search space sampled by the heuristics must have its size limited. Although it is important to sample wide variety of topologies, some criteria should be chosen to control the number of possible solutions.
2. It is usually necessary to adapt the search techniques to the particularities of the design problem.

4.2 Problem Statement

Formally, the problem considered in this thesis can be stated as follows.

“Given the truth table of a function f of the required circuit and a target technology to work within, design a combinational logic circuit

that performs the function f subject to a set of constraints using Ant Colony Optimization (ACO) Algorithm”

The most efficient structural representation of a circuit will be chosen based on the cost function used. It should be added that this work focuses on design of combinational circuits. There are no memory elements and feedback paths allowed in the circuit’s representation.

4.2.1 Assumptions

Here are some assumptions made before proceeding to the problem and cost function formulation.

1. The set of logic gates used is available. Only two-input single-output logic gates are considered. Wires are gates connecting one of its inputs to the output.
2. The truth table or functional description of the intended Boolean function is available.
3. The technology parameters are given.
4. The circuit is modelled as a matrix. Each cell of the matrix includes the information about the gate type used and the index of cells in the previous column which are connected to both of the gate’s inputs.

4.2.2 Input and Output

The proposed methodology in this thesis considers the following information as inputs:

1. The truth table or functional description of the intended Boolean function is available. The methodology can accept an input file consisting the truth table of the circuit and parameters required by the heuristics. The file uses the format described in Appendix A. The methodology can also accept a PLA file of the circuit. In the case of random circuit experiments, all parameters will be generated automatically, except for the number of variables, number of outputs and number of experiments.
2. The file containing information of gates' parameters is given. The format for this file is given in Appendix A.
3. In order to have a comparison with SIS tools, the SIS environment should be available to the system.

The outputs produced are as follows:

1. Structural representation of the logic gates in the matrix.
2. The quality measures of the final representation in terms of power consumption, delay, number of gates used and area requirements.

The cost function that is used in this thesis includes area, delay and power consumption of the circuits. The formulation of these cost function is explained below.

4.3 Cost Function Modeling

This section discusses the modeling of cost functions in terms of gate count, area, delay and power consumption.

4.3.1 Gate Count Cost Function

Each type of gate has different size, depending on the number of transistors used to implement its function. The size of a NOT gate is different than the size of a NAND gate. Thus, the number of gates cannot be used to estimate the area of a given circuit. However, the increasing applicability of semi-custom VLSI circuits complements that argument. In FPGAs, for example, a number of logic functions can be implemented in one cell, regardless whether it is a NAND gate, an AND gate or even a multiplexer. Therefore, for some target technology, the number of gates can be used as one of the objective for optimization.

If G is the set of possible gate types and $g_i \in G$, the cost for gate count can be formalized as follows.

$$Cost_{gate_count} = \sum gt_i \quad (4.1)$$

Where

$$gt_i = \begin{cases} 1 & \text{if } g_i \in G, g_i \neq WIRE \\ 0 & \text{otherwise} \end{cases} \quad (4.2)$$

4.3.2 Area Cost Function

The size of a VLSI circuit consists of the area for logic gates (blocks) and the interconnection wires. With the advanced technology used for implementing VLSI circuits, the size of transistors become smaller and smaller. Thus, the area requirement for interconnection wire becomes significant. However, the length of interconnection wires in VLSI circuits is determined by routing algorithms. Therefore, in this thesis, only area from logic gates is used to estimate the overall size of the circuit. The size of these gates is obtained from a VLSI design library.

Formally, the cost for area of VLSI circuits can be stated as follows.

$$Cost_{area} = \sum_{g_i \in G, g_i \neq WIRES} A(g_i) \quad (4.3)$$

Where $A(g_i)$ is the area of gate g_i and $g_i \in G$.

4.3.3 Delay Cost Function

The overall performance of a VLSI circuit depends upon how fast it can process signals, i.e., its clock speed. The propagation delay of signals in VLSI circuits consists of two elements: switching delay of gates and interconnect delay. Due to

improved technology, libraries with considerably low switching delay are available. This fact and the increased gate density on the chip make the interconnect delay a prominent factor in the overall circuit delay.

If a path π consists of nets $\{v_1, v_2, \dots, v_n\}$, then, the delay T_π along π is expressed by the following Equation.

$$T_\pi = \sum_{i=1}^{n-1} (CD_i + ID_i) \quad (4.4)$$

Where CD_i is the switching delay of the cell driving gate v_i and ID_i is the interconnect delay of net v_i .

Using the RC delay model, ID_i depends on the load factor, interconnect resistance and load capacitance, as shown in Equation 4.5.

$$ID_i = (LF_i + R_i) \times C_i \quad (4.5)$$

Where LF_i is the load factor of the driving block (which is independent of the layout), R_i is the interconnect resistance of net v_i , and C_i is the load capacitance of cell i .

The load capacitance C_i of gate i comprises the interconnect capacitance at the output node of gate i and the sum of the capacitances of the input nodes of the

gates driven by gate i .

$$C_i = C_i^r + \sum_{j \in M_i} C_j^g \quad (4.6)$$

Where C_j^g is the capacitance of the input node of a gate j driven by gate i and C_i^r represents the interconnect capacitance at the output node of cell i .

The overall circuit delay is determined by the delay along the longest path (the most critical path) in the layout. If the most critical path is denoted by π_c then, the cost function for the circuit delay can be given as follows.

$$Cost_{delay} = T_{\pi_c} = \max_j \{T_{\pi_j}\} \quad \forall j \in \{1, 2, \dots, K\} \quad (4.7)$$

Where K represents the total number of critical paths determined by a timing analysis program.

4.3.4 Power Consumption Cost Function

In a standard CMOS circuit, the total power consumption can be given by the following Equation.

$$P_t = \sum_{i \in M} \left(\frac{1}{2} \cdot C_i \cdot V_{DD}^2 \cdot f \cdot S_i \cdot \beta \right) + \sum_{i \in V} Q_{SC_i} \cdot V_{DD} \cdot f \cdot S_i + I_{leak} \cdot V_{DD} \quad (4.8)$$

In Equation 4.8, P_t is the total power consumption, V_{DD} is the supply voltage,

S_i is the switching probability at the output node of cell i , i.e., the number of transitions per clock cycle at the output of gate i and f is the clock frequency.

The first term in the above equation gives the dynamic power consumption during charging or discharging of a node in the circuit. Here, M is the set of all nodes in the circuit, C_i denotes the total capacitance of node i whereas β is a technology dependent constant. The second term in Equation 4.8 gives the power consumption due to the short circuit current. Here, V is the set of all wires connecting V_{DD} to ground during output transition, Q_{SC_i} represents the charge carried by the short circuit current per transition. The third term represents the static power dissipation due to leakage current I_{leak} .

In the VLSI circuits with well designed logic gates, the dynamic power consumption contributes about 90% to the total power consumption [79]. Hence, most of the reported work is focused on minimizing the dynamic power consumption. Also, in the case of standard-cell placement, the cells are obtained from the technology library and nothing can be done to reduce the power consumption due to the second and the third term in Equation 4.8. Due to this fact, the emphasis in this work is on optimizing the dynamic power consumption. Since the first term is dominant, Equation 4.8 can be approximated as follows.

$$P_t \simeq \sum_{i \in M} \frac{1}{2} \cdot C_i \cdot V_{DD}^2 \cdot f \cdot S_i \cdot \beta \quad (4.9)$$

Assuming the clock frequency and input voltage to be fixed, the total power consumption of the circuit becomes a function of the total capacitance and the switching probabilities as shown below.

$$P_t \simeq \sum_{i \in M} C_i \cdot S_i \quad (4.10)$$

Thus, the estimate of cost of the overall power consumption in VLSI circuits can be approximated as follows.

$$Cost_{power} = \sum_{i \in M} S_i \cdot C_i \quad (4.11)$$

4.4 Weighted Sum Fitness Function Calculation

The fitness of a solution contains two parts, namely functional fitness and objective fitness. The functional fitness deals with the functionality of the solution, i.e., how good the solution is in satisfying the truth table of the intended Boolean function. The objective fitness determines the quality of solution in terms of delay, area, and/or power consumption.

4.4.1 Functional Fitness

Several functional fitness formulations are reported in the literature [25]. The commonly used one is the ratio of the number of correct hits to the length of the truth

table. If FF denotes the functional fitness, then the formulation below is applied.

$$FF = \frac{\text{Number of hits}}{\text{Length of the truth table}} \quad (4.12)$$

The solution has to be ‘inverted’ if the value of FF is less than 0.5. Therefore, the formulation of *normalized FF* (FF_n) below is applied.

$$FF_n = \text{Max}\{FF, 1 - FF\} \quad (4.13)$$

4.4.2 Objective Fitness

The objective fitness ($OF(i)$) is a measure of the quality of solution in terms of optimization objectives such as area, delay, gate count, and power consumption. It consider two aspects: constraints satisfaction and multiobjective optimization. In order to indicate whether a solution is satisfying a certain constraint, objective fitness is formulated as follow.

$$OF(i) = \frac{\text{Cost}(i)}{\text{Cost}(i) + \text{Constraint}(i)} \quad (4.14)$$

For example, objective fitness of the solution in terms of area is:

$$OF(\text{area}) = \frac{\text{Cost}(\text{area})}{\text{Cost}(\text{area}) + \text{Constraint}(\text{area})} \quad (4.15)$$

With this formulation, a circuit satisfying the constraint in terms of area will have $OF(area)$ greater than or equal to 0.5. Any solution that has $OF(area)$ less than 0.5 will not be considered. The constraint values are given by the user. It states the upper bound for specific optimization objectives. Since there are four attributes to optimize, there is objective fitness for each of these attributes. These are computed using Equation 4.14.

The weights assigned to each attributes, w_i , indicates the emphasis of the optimization process. For example, for area optimization, w_{area} can be set equal to three while other weights are set to one, each. It is also possible to have more than one optimization objectives. For example, if we want to build a circuit with less area and less delay, w_{area} and w_{delay} can be set equal to k while w_{gc} and w_{power} are set equal to l , $k > l, k > 1, l \geq 0$. Note that some other weighting scheme can be applied.

The weighted sum objective fitness function calculation can be expressed as follows.

$$OF = \frac{\sum_{i \in obj} W_i \cdot OF(i)}{\sum_{i \in obj} W_i} \quad (4.16)$$

Where obj represents the set of optimization objectives.

4.5 Fuzzy Fitness Function Calculation

In this section a fuzzy-based fitness function is formulated. Similar to the weighted sum approach, the overall fitness of a solution consists of two parts: functional fitness and objective fitness. In this approach membership functions are used and these membership functions will be aggregated into a single function using a fuzzy operator.

4.5.1 Functional Fitness

Using Equation 4.13, the value of functional fitness lies in the range $[0.5, 1]$. Thus the membership function for functional fitness is trivial. It is shown in Equation 4.17.

$$\mu_{func}(x) = \begin{cases} x & \text{if } 0.5 \leq x \leq 1 \\ 0 & \text{otherwise} \end{cases} \quad (4.17)$$

4.5.2 Objective Fitness

In order to build the membership function for all objectives, estimated value for lower bound and/or upper bound of the objective is required.

Each characteristic of the circuit (area, delay and power consumption) can be used either as constraint or objective. The membership function for each case (objective or constraint) will be different. This will be discussed next.

Area as Optimization Objective

The lower bound on area can be estimated by referring to the VLSI circuit design and logic synthesis principles. For any n -input single-output circuit, the minimum area for the given circuit is equal to the area of $n - 1$ 2-input gates representing binary tree structure. Since any circuit can be implemented using NAND gates and NAND gates happen to be the smallest among other gate (except NOT gate), then the minimum area is:

$$min_{area} = (n - 1) \times Area(NAND\ gate)$$

In order to guide the search intelligently, the maximum value must be carefully estimated. For this purpose, SIS tools [21] are used to obtain circuits with minimum area. In this context, *rugged.script* is used to generate the circuits' netlist files. These files are then fed to our own tool to obtain the estimated value for area, delay and power consumption. The reason behind this is twofold. Firstly because the delay optimization in SIS does not consider switching delay (see Equation 4.5). Secondly, SIS does not consider power optimization.

Since we want to obtain circuits better than SIS, these values (area, delay, and power) are used as the target values. In the case of area as optimization objectives, the target area is equal to the area of circuits obtained by SIS and denoted as tg_{area1} (see Figure 4.1). Thus, the membership function for area as optimization objectives

is:

$$\mu_{area_obj} = \begin{cases} 1 & 0 \leq area \leq min_{area} \\ 1 - \frac{(area - min_{area})}{tg_{area1} - min_{area}} & min_{area} \leq area \leq tg_{area1} \\ 0 & otherwise \end{cases} \quad (4.18)$$

The shape of the membership function is depicted as the bold line shown in Figure 4.1.

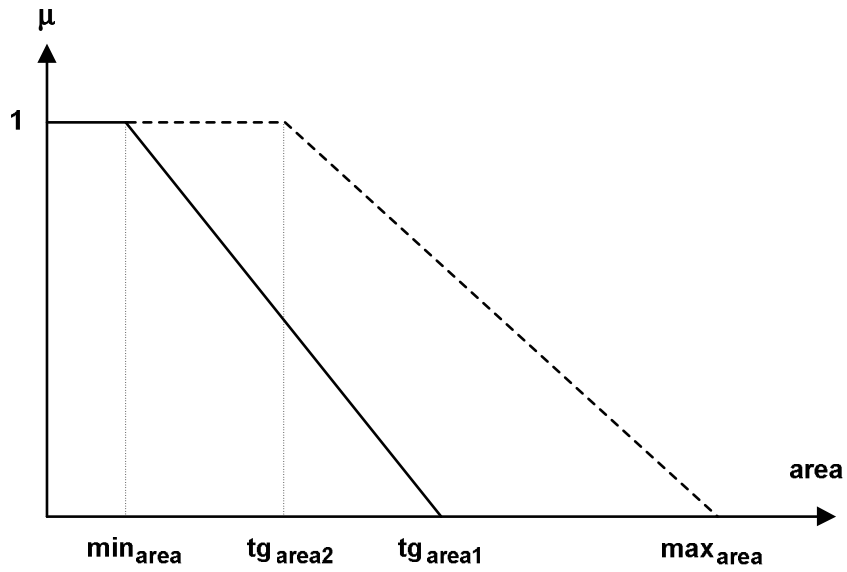


Figure 4.1: Membership function for area.

Area as Constraint

In this case, the area of circuit obtained from SIS is used as target value. For this purpose, the max_{area} and tg_{area2} should be defined. The following settings are applied, $tg_{area2} = k_1 \times tg_{area1}$ and $max_{area} = k_2 \times tg_{area1}$, $k_1, k_2 \in \mathfrak{R}$, $0 < k_1 \leq$

1, $k_2 \geq 1$. The membership function is then:

$$\mu_{area_con} = \begin{cases} 1 & 0 \leq area \leq tg_{area1} \\ 1 - \frac{area - k_1}{max_{area} - k_1} & 1 \leq area \leq max_{area} \\ 0 & otherwise \end{cases} \quad (4.19)$$

The shape of the membership function is depicted as dashed line shown in Figure 4.1.

Delay as Optimization Objective

The minimum delay (min_{delay}) is estimated as the delay of two-level logic consisting of NAND gates without considering the switching delay. The tg_{delay1} is estimated from circuit generated by SIS with *delay.script* executed. The membership function for delay as optimization objectives is:

$$\mu_{delay_obj} = \begin{cases} 1 & 0 \leq delay \leq min_{delay} \\ 1 - \frac{delay - min_{delay}}{tg_{delay1} - min_{delay}} & min_{delay} \leq delay \leq tg_{delay1} \\ 0 & otherwise \end{cases} \quad (4.20)$$

The shape of the membership function is depicted as bold line shown in Figure 4.2.

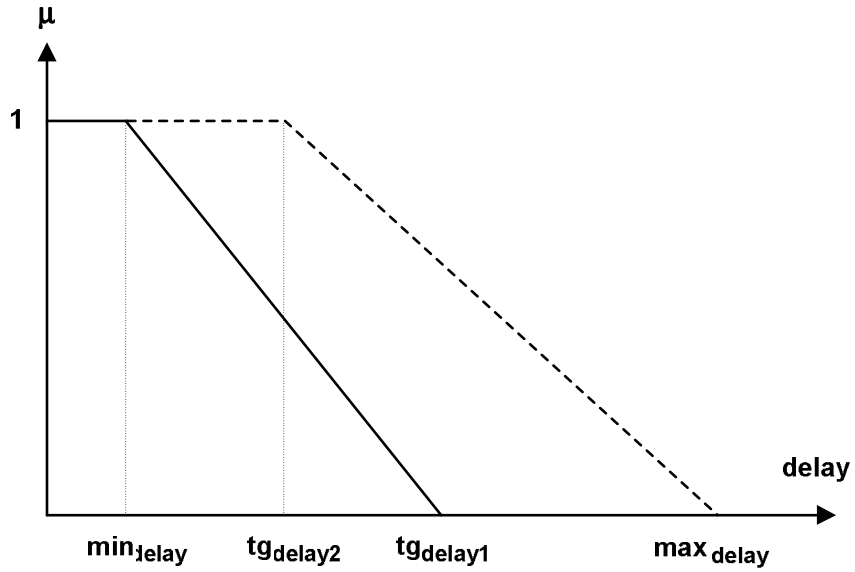


Figure 4.2: Membership function for delay.

Delay as Constraint

In this case, the following settings are applied, $tg_{delay2} = k_1 \times tg_{delay1}$ and $\max_{delay} = k_2 \times tg_{delay1}$, $k_1, k_2 \in \mathfrak{R}$, $0 < k_1 \leq 1$, $k_2 \geq 1$. The membership function is then

$$\mu_{delay_con} = \begin{cases} 1 & 0 \leq delay \leq tg_{delay1} \\ 1 - \frac{delay - k_1}{\max_{delay} - k_1} & 1 \leq delay \leq \max_{delay} \\ 0 & otherwise \end{cases} \quad (4.21)$$

The shape of the membership function is depicted as dashed line shown in Figure 4.2.

Power as Optimization Objective

The minimum power (min_{power}) is estimated as the power consumption of minimum area circuit in which each gate has the least switching activity (see Equation 4.8). It is assumed that for a given truth table, the output of each gate will be ‘1’ only once. Thus the minimum power consumption (switching activity) can be estimated as follows.

$$min_{power} = 2 \cdot \frac{\text{length of truth table} - 1}{(\text{length of truth table})^2} \cdot \text{capacitance}(NAND)$$

The tg_{power1} is estimated from minimum area circuit generated by SIS. The membership function for power as optimization objectives is:

$$\mu_{power_obj} = \begin{cases} 1 & 0 \leq power \leq min_{power} \\ 1 - \frac{power - min_{power}}{tg_{power1} - min_{power}} & min_{power} \leq power \leq tg_{power1} \\ 0 & otherwise \end{cases} \quad (4.22)$$

The shape of the membership function is depicted as bold line shown in Figure 4.3.

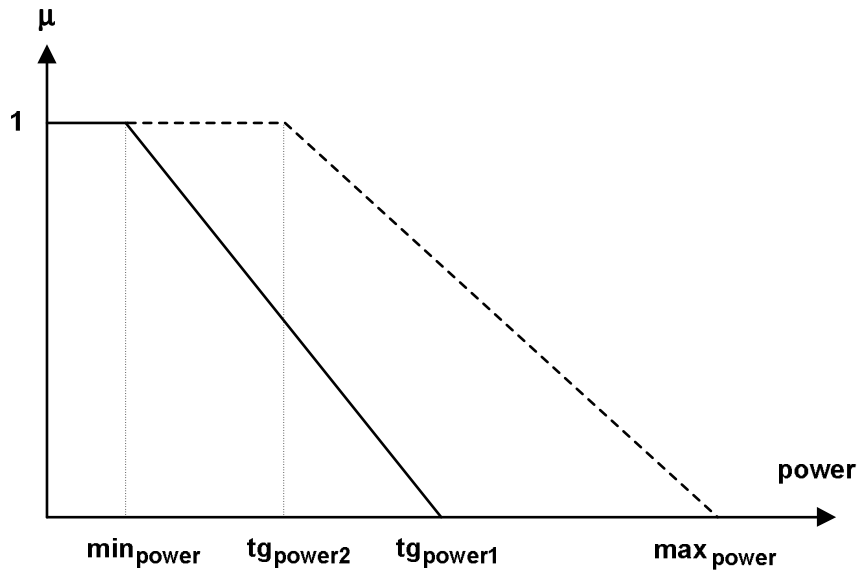


Figure 4.3: Membership function for power.

Power as Constraint

The following settings are applied, $tg_{power2} = k_1 \times tg_{area1}$ and $max_{power} = k_2 \times tg_{power1}$, $k_1, k_2 \in \mathfrak{R}$, $0 < k_1 \leq 1$, $k_2 \geq 1$. The membership function is:

$$\mu_{power_con} = \begin{cases} 1 & 0 \leq power \leq tg_{power1} \\ 1 - \frac{power - k_1}{max_{power} - k_1} & 1 \leq power \leq max_{power} \\ 0 & otherwise \end{cases} \quad (4.23)$$

The shape of the membership function is depicted as dashed line shown in Figure 4.3.

OWA operator is used to aggregate the above membership functions to calculate the objective fitness. The choice of which type of membership function used (either

objective or constraint) depends on the course of the current action. For example, for minimization of area with delay and power as constraint, the μ_{area_obj} , μ_{delay_con} and μ_{power_con} are considered. The objective fitness is then calculated as

$$\begin{aligned} \mu_{obj}(x) = & \beta \times \min(\mu_{area_obj}, \mu_{delay_con}, \mu_{power_con}) \\ & +(1 - \beta) \times \frac{1}{3}(\mu_{area_obj} + \mu_{delay_con} + \mu_{power_con}) \end{aligned} \quad (4.24)$$

Overall Fitness

The formulation of overall fitness (OvF) calculation is shown in Equation 4.25. The W_f is the weight for functional fitness. The value of this weight must be chosen intelligently. The value of W_f must be large enough in order to have better functionality of the circuit. However, it should not be too large in order to get better quality solution in terms of design objectives.

$$OvF = W_f \cdot FF + (1 - W_f) \cdot OF \quad (4.25)$$

We proposed two strategies to choose the value of W_f , namely *static* and *dynamic* approaches. In the static approach, the value W_f will be the same throughout all iterations. Initial experiments showed that the setting of $0.5 < W_f < 0.9$ is appropriate.

In dynamic approach, the value of W_f will be changed during iteration. It will start with a defined minimum value $MinW_f$. If there is a stagnation in the search,

i.e., the value of FF does not change after certain number of iterations, the value of W_f will be increased. In order to check whether stagnation occurs or not, an FF counter must be asserted. The pseudocode in Figure 4.4 below shows the procedure of dynamic approach.

Dynamic WF

$MinW_f$ Minimum allowed W_f value
 $MaxW_f$ Maximum allowed W_f value
 MAXITER Maximum iteration
 CountMax Maximum counter for FF stagnation

```

counter = 0
 $W_f = MinW_f$ 
Begin
  If (counter > CountMax) and ( $W_f < MaxW_f$ )
     $W_f = W_f + \frac{MaxW_f - MinW_f}{MAXITER}$ 
    .....
    .....
    curfit =  $FF$  of solution
    If curfit = oldfit
      counter = counter + 1
    If curfit > oldfit
      oldfit = curfit
End

```

Figure 4.4: Dynamic W_f calculation.

Based on the calculation of functional fitness, three different OVF calculations exists. These are:

1. Original: The normal value of FF is used.
2. Normalized: The value of FF_n is used instead of FF .

3. Normalized-Penalized: The value of FF_{np} is used instead of FF .

$$\text{With } FF_{np} = FF_n - (1 - FF_n).$$

Performance evaluation of these three approaches will be carried out in the experiments. Results and discussion will be given in Chapter 6 and 7.

4.6 Concluding Remarks

This chapter and the following chapter are the core of this thesis. In this chapter, the evolutionary logic design problem has been formulated. The problem statement and cost function formulation for the proposed algorithm are also detailed. In the following chapter, the proposed algorithm for ELD based on ACO algorithm will be discussed.

Chapter 5

ACO ALGORITHM FOR COMBINATIONAL LOGIC DESIGN

In Chapter 3, literature review was presented. Problem and cost function formulation have been discussed in Chapter 4. In this chapter, the proposed algorithms for ACO-based ELD are presented.

5.1 Introduction

A logic circuit can be modelled as a graph of interconnected modules. There exists a number of possible graphs representing a given circuit. These graphs differ in their

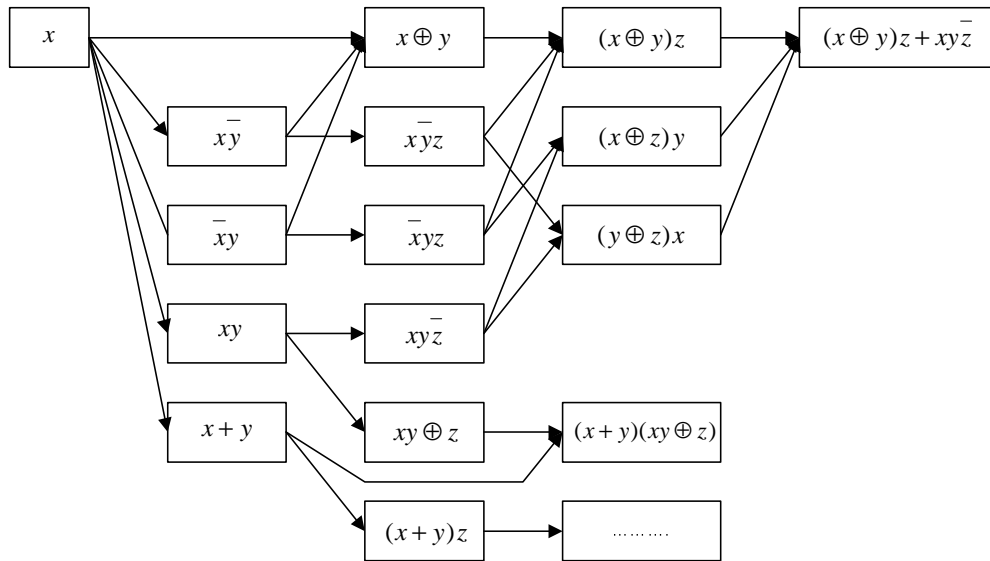


Figure 5.1: Figure Illustrating some of the possible paths in function f .

characteristics, i.e., area, delay, and power. As mentioned in the previous chapter, the number of these graphs could be huge. In this context, the ACO algorithm can be used as an engine to search the best solution according to a given cost function.

Consider the Boolean function $f = \bar{x}yz + x\bar{y}z + xy\bar{z}$. This function can be represented in a number of forms. These representations can be transformed into a directed acyclic graph G . Figure 5.1 shows some of the possible paths starting from literal x and ending with two different representations of f .

Using ACO algorithm, the best solution can be found by traversing graph G . Assume that the objective of the tour construction is to find the shortest path representing function f . Each ant starts its tour from node x . At each node, the ant will select the next node to visit. The probability of selecting an edge leading to a specific node is determined by a pheromone value (τ) and a heuristic value (η)

on the edge. The pheromone value implies the preference of search obtained from knowledge of past generation, while the heuristic value represent the objectives of optimization process.

When the ant reaches a node with no successor, it will track back and put additional pheromone on all visited edges. The additional pheromone will in turn guide the next generation of ants towards preferable solution.

Since the objective is to find the shortest path representing function f , the ant that finds the path $x \rightarrow (x+y) \rightarrow (x+y)(xy \oplus z)$ would return the best representation of function f .

The number of paths shown in Figure 5.1 is more than eleven. The actual number of paths is large. It is impractical to traverse all those paths. Therefore, some modifications in ACO algorithm are needed to handle this large search space. This will be detailed in the next section.

5.2 Modified-ACO (MACO) for Logic Design

In this section, the modified ACO algorithm is presented. It starts with the circuit encoding, followed by the procedures of the modified ACO algorithms.

5.2.1 Circuit Encoding

A circuit is modelled as a matrix M of size $n \times m$. Each cell of the matrix contains a triplet of *attributes* consisting of the type of gate used and its corresponding inputs, i.e., the row indices of the preceding column (see Figure 5.2).

Input 1	Input 2	Gate type
----------------	----------------	------------------

Figure 5.2: Representation of a cell in the matrix.

The value of input 1 and input 2 indicates the row indices from which the current cell is getting its input from. The value of the gate type indicates the type of the gate being assigned to that cells assuming a predetermined set of gate types (see Table 5.1). The input of a gate at position (i, j) can only be connected to the output of a cell at $(i', (j - 1))$ and i' can be any row index in column $(j - 1)$.

Table 5.1: Gate ID, gate name and output of the gate, considering input a and b .

Gate ID	Gate	Output
0	WIRE1	a
1	WIRE2	b
2	NOT1	\bar{a}
3	NOT2	\bar{b}
4	AND	$a \cdot b$
5	OR	$a + b$
6	XOR	$a \oplus b$
7	NAND	$\overline{a \cdot b}$
8	NOR	$\overline{a + b}$
9	XNOR	$\overline{a \oplus b}$

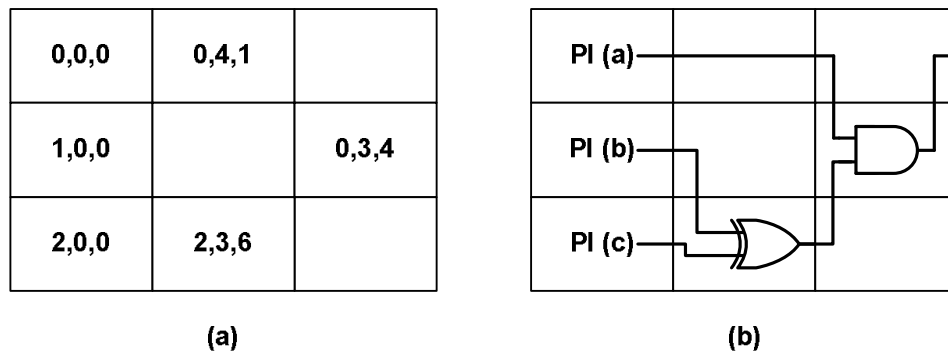


Figure 5.3: Example of a circuit and its encoding.

Consider the example shown in Figure 5.3. Cell(1,2) whose attribute is (0,3,4) is an AND gate (according to Table 5.1). The first input of the AND gate of this cell is connected to the output of cell(0,1), which is a WIRE, and the second input is connected to the output of cell(2,1).

5.2.2 Modifications of the Ant Colony Algorithm

It is assumed that all ants originate from a dummy cell called nest (see Figure 5.4). Each ant visits a cell in a column and moves to a cell in the next column, until it reaches the last column or a cell that has no successor. The idea is to find a correct and optimal path consisting of logic gates to implement the required truth table and satisfying the cost function.

Nevertheless, it is possible that the current matrix contains no solution, even if the size of the matrix is large. In fact, enlarging the matrix will be counter productive because the time for traversing the paths will exponentially increase. In order to tackle this problem, the size of the matrix can be kept small enough

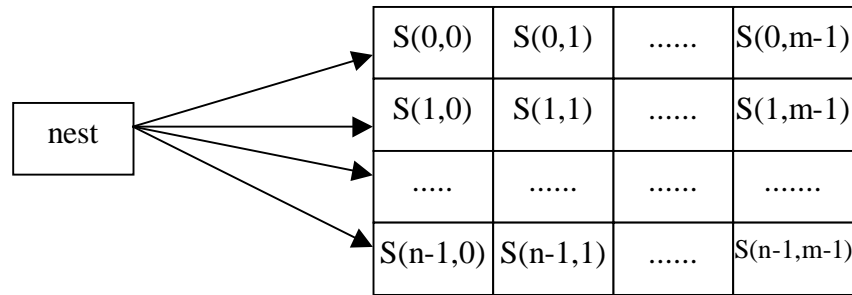


Figure 5.4: Nest cell and matrix M for ant to be traversed.

to reduce the time complexity, but the content of the matrix will be dynamically changed during the iteration.

At first, the matrix will be randomly filled. After the ants finish their tour, the solution provided will be evaluated. All cells that are included in the best solution of the current matrix will be kept. Note that, this solution may not represent the intended function. All un-needed cells will be removed. These empty cells will be filled up again in the next iteration. The ants will then traverse the new matrix and return the best possible solution. If the stopping criteria is not met, the same procedure will be repeated. Figure 5.5 shows the pseudocode of the approach.

The *Filling* and *Removing* cells procedures in MACO algorithm shown in Figure 5.5 are performed to handle the limitation of ACO algorithm due to the huge search space of circuit design problem. To further accommodate some improvements mentioned in Section 3.4, the following modifications are suggested:

1. The Intelligent Ant
2. The Veteran Ant

Algorithm Modified ACO (MACO)

```

Begin
  For  $0 < i < iteration$ 
    Filling_the_Matrix
    Ant_Activity
    Removing_Unfit_Cells
  EndFor
End

```

Figure 5.5: Modified ACO algorithm for logic design.

The Intelligent Ant

The original ACO algorithm works on a clearly defined graph where the number of nodes and/or edges is mostly static and the quality of best solution is unknown. On the other hand, the result of ELD must be a functionally correct circuit optimized according to the cost function. While traversing the matrix, each ant must seek good solution in terms of circuit's functionality first. Since the length of the tour is limited by the size of the matrix, the ant should have intelligence to select which part of its tour that provides the best solution in terms of functional fitness. The remaining path will be removed from its memory. Using this approach, the ant will provide better partial solution in every iteration and that the best solution would emerge at the end of the iterative process.

The Veteran Ant

In the original ACO algorithm, all ants will die after finishing their tour. Then, a new generation of ants is born and use the information of the pheromone trail to construct their tour. However, if the number of ants is too small to cover all the existing paths, the quality of new solutions can be worse compared to the old one. Using larger number of ants will give higher probability of obtaining better or at least equal solution. However, this will add computation time significantly.

In addition, since the content of the matrix will be dynamically changed, it is important that the best partial solution is kept in every iteration. This can be done by *saving* the paths found by the best ants. Therefore, unlike the original ACO algorithm, after finishing their tour, some of the best ants will be selected and upgraded to act as *veteran ant* (*Vant*). All ants will die, except the veterans. These veteran ants will bring their information and ‘lead’ new generation of ants to find the solution.

For the following reasons, the number of veteran ants used can be more than one.

1. In order to get the function $f = G(f_1, f_2)$, both f_1 and f_2 must be available and connected through a Boolean operator (a gate) G . If the number of veteran ants is one, only one partial solution will be saved in each iteration. Both f_1 and f_2 may be available in the matrix at the same time. Thus, saving f_2 as

well as f_1 (using two veteran ants) will increase the possibility of obtaining the solution faster.

2. There exist a number of different structural representations for a Boolean function f . The number of sub-functions of f is even bigger. Finding which is the best representation for sub-function f_k is difficult. Some of the f_{k_i} can lead to a good solution, but some of them may lead to a worse solution. Thus, saving more than one veteran ant can reduce the possibility of getting stuck in local optimal solutions.

Using more *Vants* mean more information saved in each iteration. This can help the search process. However, this can be counter productive since more *Vants* means more cells locked during iteration. This will reduce the space for exploring new solutions. In this thesis, the number of *Vant* used is two.

As mentioned before, the solution approach has three main steps, namely: *filling*, *traversing* and *removing*. These three steps will be repeated a number of times until one of the stopping criteria is met. The details for each of these steps are given in the following subsections.

5.2.3 Filling the Matrix

The purpose of this step is to fill empty cells in the matrix with randomly generated attributes. The possible gate type is defined in the gate library. In this procedure,

the truth table and functional fitness of the cell will be calculated as well. Figure 5.6 shows the pseudocode of the procedure **filling_the_matrix**.

```

Procedure Filling_the_Matrix();

/* row          maximum number of rows allowed */
/* column       maximum number of columns allowed */

Begin
  For  $0 \leq j < column$ 
    For  $0 \leq i < row$ 
      If Cell[i][j] is empty
        Cell[i][j].gate = random gate from library
        Cell[i][j].input[0] = random integer < row
        Cell[i][j].input[1] = random integer < row
        Calculate_truth_table();
        Calculate_functional_fitness();
      EndIf
    EndFor
  EndFor
End

```

Figure 5.6: Procedure Filling_the_Matrix.

5.2.4 Ant Activity

The *Ant Activity* procedure contains three parts: the movement of ants, evaluation of solutions built and the pheromone update. These are discussed next.

Pheromone and Trail Actualization

As mentioned earlier, each ant starts its tour from a dummy cell called nest and moves to any of the cell in the first column. Next, the ant will move to the second column, and so on, until it reaches a cell that has no successor. The selection of which edge to traverse is determined by a stochastic process using *Roulette Wheel*. The probability to choose a specific edge depends on pheromone value (τ) and heuristic value (η) of the edge. The probability of selecting next node is formulated below [54]:

$$p_{ij}^k(t) = \frac{[\tau_{ij}(t)]^\alpha \cdot [\eta_{ij}]^\beta}{\sum [\tau_{il}(t)]^\alpha \cdot [\eta_{il}]^\beta} \quad (5.1)$$

The value of α and β imply the preference of the search, whether it depends more on pheromone value or heuristic value, respectively. Every newly created cell will be given an initial and small amount of pheromone value. This value will be updated in every iteration made by the ant.

Heuristic Value (η)

The heuristic value (η) depends on the distance of functional fitness values between cells, and formulated as follows.

$$d = FF_n(i + 1) - FF_n(i) \quad (5.2)$$

$$\eta = d + 0.5 \quad (5.3)$$

The addition of 0.5 in the calculation of η is meant to normalize the value of η into $[0,1]$. A decrease in functional fitness means that the value of η is in the range of $[0,0.5)$, while an increase in functional fitness makes the value of η in the range of $(0.5, 1]$

Tour Evaluation

While traversing the matrix, every ant carries information of the paths traversed so far, e.g., the row index of all cells that were visited. If an ant reaches a cell that has no successor, it will evaluate and select which part of its tour results in the best functional fitness value. The value of OF and OvF of the solution will be evaluated.

Pheromone Update

When all ants finished their tour, pheromone update is performed. However, only a certain number of ‘the best’ ants can update the pheromone along their paths. These best ants are the *Vants* mentioned earlier. The pheromone update is performed using the following:

$$\tau(t) = \tau(t) + \lambda \cdot OvF(t) \quad (5.4)$$

where $OvF(t)$ denotes the overall fitness of the solution that the ants built and λ is a constant.

After the pheromone is updated, the pheromone evaporation procedure is performed using the following formula.

$$\tau(t) = (1 - \rho) \times \tau(t), \quad \text{with } \rho = (0, 1] \quad (5.5)$$

In case of multiple outputs circuits, multiple colonies of ants will be used. In this context, each colony of ants is assigned to find a specific output of the circuit. All colonies will share the same matrix. The possibility of using the same sub-functions is established by sharing the pheromone value among different colonies.

5.2.5 Removing the Unfit Cell

After the ants finish their tour, the matrix M will be checked to see which cells are worth keeping. Each cell can assume two different status, namely l (locked) and r (removed). The status of a cell is determined by the following rules:

1. A cell is locked if
 - (a) it is included in the best path

(b) it is feeding another locked cell

2. A cell is removed otherwise

The cells that assume r status will be removed at the end of the current iteration. These empty cells will be then filled up by **Filling_the_Matrix** procedure in the beginning of the next iteration. The example below shows how the algorithm works.

Example 1

Consider, for example, a function $f = \bar{a}\bar{b}c + \bar{a}b\bar{c} + a\bar{b}\bar{c} + abc = a \oplus b \oplus c$. Assume the first **Filling_the_Matrix** is shown in Figure 5.7 (the nest node is not shown).

Let's take a look at some of the cells in detail. Assume that the initial value of τ is 1, and the value of $\alpha = \beta = 1$.

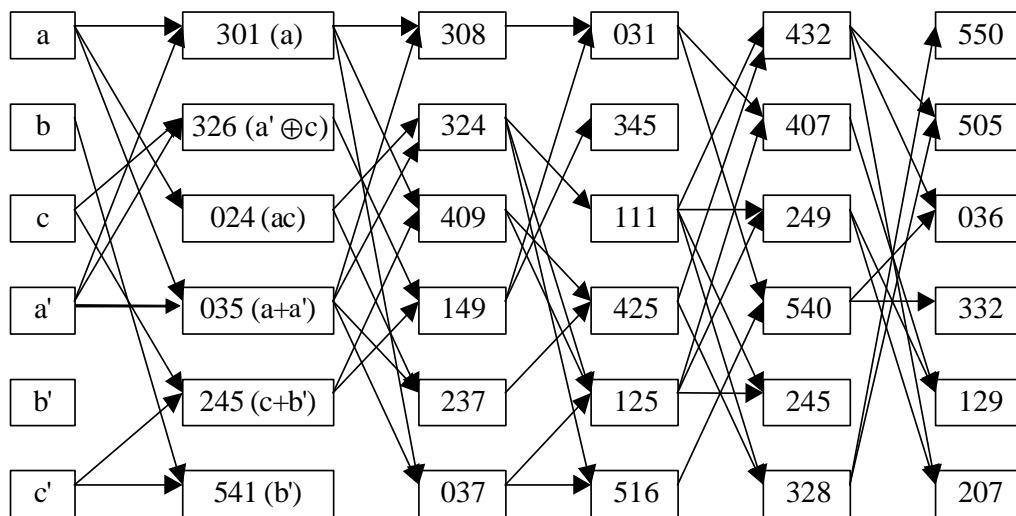


Figure 5.7: Result of Filling the Matrix Procedure in the First Iteration for Example 1.

1. Cell (0,0)

This is a primary input whose literal is a . The fitness of the node is 0.5. There are three edges originating from this node, namely to cell (0,1), cell (2,1) and cell (3,1). These cells have fitness 0.5, 0.5 and 0.5, respectively. Heuristic values η for edges to those cells are 0.5 each. Sum of $\tau^1 \times \eta^1 = (1 \times 0.5) + (1 \times 0.5) + (1 \times 0.5) = 1.5$. Recall to Equation 5.1, the values of p for these edges are:

$$(a) \ p_{cell(0,1)} = (1 \times 0.5) / 1.5 = 0.33$$

$$(b) \ p_{cell(2,1)} = (1 \times 0.5) / 1.5 = 0.33$$

$$(c) \ p_{cell(3,1)} = (1 \times 0.5) / 1.5 = 0.33$$

2. Cell (1,0)

This is a primary input whose literal is b . The fitness of the node is 0.5. There is one edge originating from this node, namely to cell (5,1). This cell has fitness 0.5. Heuristic value η for edge is 0.5. Sum of $\tau^1 \times \eta^1 = (1 \times 0.5) = 0.5$. Therefore, the value of p for the edge is 1.

3. Cell (0,1)

The node is the result of combination of output from cell(0,0) and cell (3,0) using WIRE1, which corresponds to literal a . The fitness of the node is 0.5. There are two edges originating from this node, namely to cell (2,2) and cell (5,2). These cell have fitness 0.75 and 0.5, respectively. Heuristic values η for

these edges are 0.75 and 0.5. Sum of $\tau^1 \times \eta^1 = (1 \times 0.75) + (1 \times 0.5) = 1.25$.

Then, the value of p for these edges are

$$(a) p_{cell(2,2)} = (1 \times 0.75) / 1.25 = 0.6$$

$$(b) p_{cell(5,2)} = (1 \times 0.5) / 1.25 = 0.4$$

4. Cell (5,1)

This is a primary input whose literal is a . The fitness of the node is 0.5. There is no edge originating from the node. Thus, if an ant visits the node, the tour of the ant will stop here.

5. Cell (2,2)

The node is the result of combination of output from cell(0,1) and cell (4,1) using XNOR gate, which corresponds to $((c+b') \oplus a)$. The fitness of the node is 0.75. There are two edges originating from this node, namely to cell (3,3) and cell (4,3). Those cell have fitness 0.75 and 0,75 respectively. Heuristic values η for these edges are 0.75 and 0.75. Sum of $\tau^1 \times \eta^1 = (1 \times 0.75) + (1 \times 0.75) = 1.5$.

The values of p for these edges are

$$(a) p_{cell(3,3)} = (1 \times 0.75) / 1.5 = 0.5$$

$$(b) p_{cell(4,3)} = (1 \times 0.75) / 1.5 = 0.5$$

Let's assume that there are two ants that find solutions whose fitness are 0.75.

The paths for these ant are:

1. ant1: fitness = 0.75

path: cell (5,5) → cell (0,4) → cell (2,3) → cell (1,2) → cell (2,1) → cell (4,0)

2. ant2: fitness = 0.75

path: cell (5,5) → cell (0,4) → cell (3,3) → cell (2,2) → cell (0,1) → cell (0,0)

Thus, the new pheromone value for those cells are (assume that $\lambda = 0.5$):

1. Pheromone update by ant1

$$\Delta\tau = \lambda \cdot f(t) = 0.5 \times 0.75 = 0.5 \times 0.75 = 0.375$$

$$\tau(\text{cell } (5,5)) = \tau(\text{cell } (0,4)) = \tau(\text{cell } (2,3)) = \tau(\text{cell } (1,2)) = \tau(\text{cell } (2,1)) =$$

$$\tau(\text{cell } (4,0)) = 1 + 0.375 = 1.375$$

2. Pheromone update by ant2

$$\Delta\tau = \lambda \cdot f(t) = 0.5 \times 0.75 = 0.375$$

$$\tau(\text{cell } (5,5)) = \tau(\text{cell } (0,4)) = 1.375 + 0.375 = 1.75$$

$$\tau(\text{cell } (3,3)) = \tau(\text{cell } (2,2)) = \tau(\text{cell } (0,1)) = \tau(\text{cell } (0,0)) = 1 + 0.375 = 1.375$$

Note that cells(5,5) and cell(0,4) acquire more pheromones since more ants visit them in their tour. The pheromone value in each of cell will be:

Note that the bold and underscored values are the cells that were included in the best tour.

<u>1.375</u>	<u>1.375</u>	1.000	1.000	<u>1.75</u>	1.000
1.000	1.000	<u>1.375</u>	1.000	1.000	1.000
1.000	<u>1.375</u>	<u>1.375</u>	<u>1.375</u>	1.000	1.000
1.000	1.000	1.000	<u>1.375</u>	1.000	1.000
<u>1.375</u>	1.000	1.000	1.000	1.000	1.000
1.000	1.000	1.000	1.000	1.000	<u>1.750</u>

After the pheromone was updated, it will decay using the following rules.

$$\tau = (1 - \rho) \times \tau, \text{ with } \rho = (0, 1]$$

Assume that the value of ρ is 0.8. The pheromone value of each cell will be:

<u>1.100</u>	<u>1.100</u>	0.800	0.800	<u>1.400</u>	0.800
0.800	0.800	<u>1.100</u>	0.800	0.800	0.800
0.800	<u>1.100</u>	<u>1.100</u>	<u>1.100</u>	0.800	0.800
0.800	0.800	0.800	<u>1.100</u>	0.800	0.800
<u>1.100</u>	0.800	0.800	0.800	0.800	0.800
0.800	0.800	0.800	0.800	0.800	<u>1.400</u>

All cells that are included in the paths of ‘the best ants’ will assume status lock.

In addition, the cell that is feeding a locked cell will be locked. After removal of the unfit cells, matrix M will consist the cells shown in Figure 5.8.

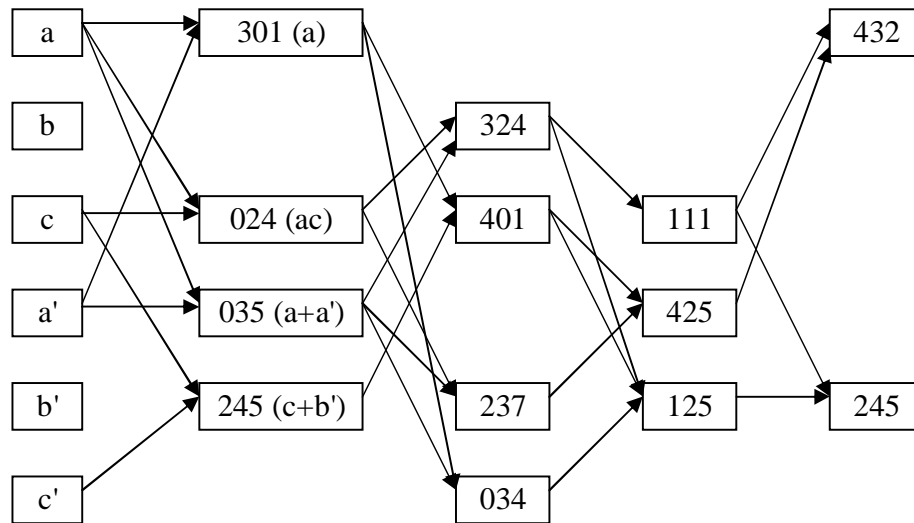


Figure 5.8: Removing of cells in the first iteration.

Filling the matrix, second iteration.

All empty cells in the matrix will be filled with randomly generated attributes.

Assume that the result of *filling_the_matrix* is shown in Figure 5.9.

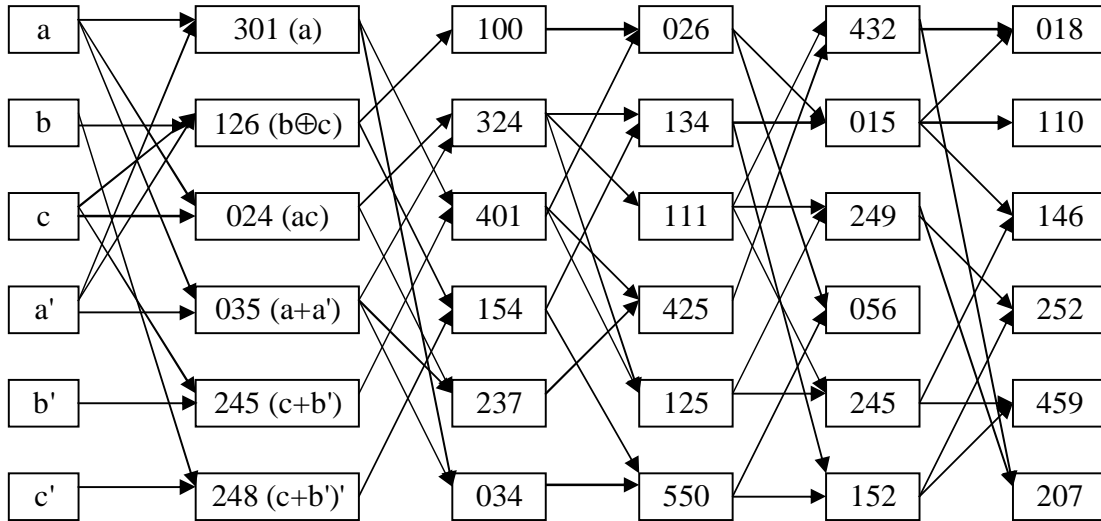


Figure 5.9: Filling the matrix in the second iteration

Suppose that there are three ants that found the best solutions.

1. ant1 : fitness = 1

path : Cell (0,0) → cell (0,1) → cell (2,2) → cell (0,3) → cell(3,4)

2. ant2 : fitness = 1

path : Cell (1,0) → cell (1,1) → cell (0,2) → cell (0,3) → cell(3,4)

3. ant3 : fitness = 1

path: Cell (3,0) → cell (3,1) → cell (5,2) → cell (5,3) → cell(3,4)

Note that the first two ants are basically building the same circuit. However, if intelligent ants are used, ant1 and ant2 can stop at cell(0,4) and discard other succeeding cells included in the path. Since ant1 and ant2 requires shorter path compared to ant3, the solution built will be returned by these two ants.

5.3 Improved-Modified ACO algorithm

Initial experiments showed that some further improvements can be made to increase the performance of the MACO algorithm. In this section, three modifications are presented.

5.3.1 Dynamic Search Space

Assuming that the size of the matrix M used to represent the circuit is 5 x 5 and the interconnection between cells are fixed. Since there are ten types of gates available, the total number of combination in the matrix M will be 10^{25} . If the interconnections between cells are made random, this number will increase even bigger. However, if the size of the matrix M is too small, the search space is limited. Then the quality of solution obtained may suffer.

In this section, a dynamic search space is proposed. The idea is to have a bigger search space only when it is required. At the beginning of first iteration, the matrix is set to its initial size. In the course of any iteration, the size of the matrix may be

increased or decreased. Obviously, there should be a limit on the maximum number of rows and columns of the matrix. It is assumed that the minimum size of the matrix is $NV \times NV$, with NV as the number of variables of the intended function. The maximum size of the matrix is $(k_1 \cdot NV) \times (k_2 \cdot NV)$, $k_1, k_2 > 0$. Since logic circuits have a tree-like structure, the number of rows required to implement the circuits is generally bigger than the number of columns. In other words, $k_1 > k_2$.

Row Adjustment

Row Utilization (RU) is defined as the largest ratio of the number of locked cells in a certain column to the number of rows, or can be formulated as follows:

$$LC = \text{number of locked cells}$$

$$RU = \max\left\{\frac{LC_i}{\text{number of row}}\right\} \quad 0 \leq i < \text{number of column}$$

Additional row(s) will be introduced if RU is greater than $MARU$ (Maximum Allowable Row Utilization). The value of $MARU$ can be determined through experiments. The setting of $0.75 < MARU < 0.9$ were used.

Last Row (LR) is defined as the largest row index of the locked cell in the matrix. The value of LR will be used to reduce the number of rows in the matrix.

Column Adjustment

Column Utilization (CU) is defined as the ratio of the length of best ant's tour to the number of columns, or can be formulated as follows:

$$CU = \frac{\text{length of the best path}}{\text{number of column}}$$

Additional column(s) will be introduced if *CU* is greater than *MACU* (Maximum Allowable Column Utilization). The value of *MACU* can be determined through experiments.

When the best partial solution is returned, the number of columns will be set equal to the length of best ant's tour. The pseudocode in Figure 5.10 explains how the row and column adjustments are performed in the proposed algorithm.

5.3.2 Perturbation

Perturbation can be performed to further avoid getting stuck in local optimal. The procedure of perturbation imitates the *Selection* and *Allocation* procedures in Simulated Evolution (SE) [15]. First, a goodness measure of each cell is calculated. The formulation of the goodness measure of a cell is given next.

```

Row and Column Adjustment;
/* row      number of row */
/* column   number of column */
/* maxrow   maximum number of row allowed */
/* maxcolumn maximum number of column allowed */

Begin
  For  $0 < i < iteration$ 
    Filling_the_Matrix
    Ant_Activity
    ....
    If ( $RU > MARU$ ) and ( $row < maxrow$ )
       $row = row + 1$ 
    If ( $CU > MACU$ ) and ( $column < maxcolumn$ )
       $column = column + 1$ 
    ....
     $row = LR$ 
     $column = length\ of\ the\ best\ path$ 
    Removing_Unfit_Cells
  EndFor
End

```

Figure 5.10: The Use of Row and Column Adjustment.

Goodness Measure

A goodness measure of a cell is determined by a combination of FF_n s of the cell and FF_n s of the neighboring cells, and its position (column) in the current matrix. Consider cell(i, j) and its surrounding neighbors shown in Figure 5.11. Functional fitness (FF_n) of cell(i, j) is affected by the FF_n s of its inputs, cell($p1, j - 1$) and cell($p2, j - 1$) and is affecting the FF_n of cell($q, j + 1$). Thus, the balance of functional fitness (BFF) for cell(i, j) is calculated as follows.

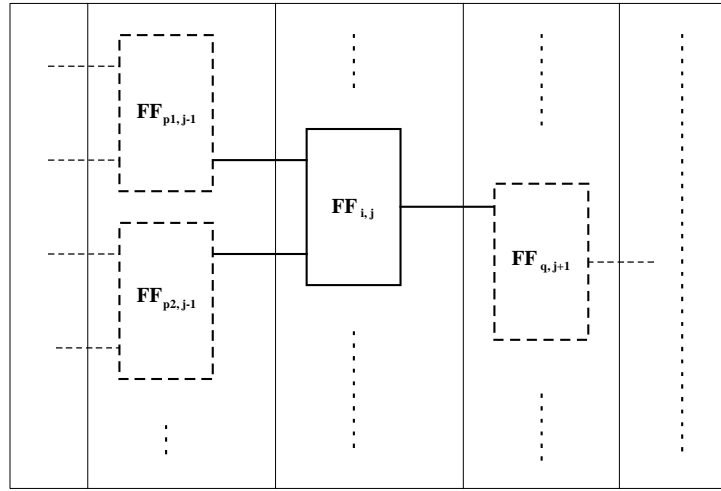


Figure 5.11: How the Neighboring Cells Affect the FF_n of Cell(i, j).

P = set of predecessor cells

S = set of successor cells

$$BFF = \frac{\sum_{k \in P} (FF_n(i,j) - FF_n(k,j-1)) + \sum_{k \in S} (FF_n(k,j+1) - FF_n(i,j))}{\text{Number of neighbors}}$$

If FF_n of the cells in the first column, i.e., the literals, are assumed to be 0.5 and the $FF_n(sol)$ is FF_n of the solution, then the *expected* FF_n (EFF) of cell(i, j) is equal to:

$$EFF = 0.5 + \frac{(FF_n(sol) - 0.5) \cdot j}{\text{length of best_ant}}$$

The goodness of the cell is then calculated as:

$$G = FF_n + BFF$$

A random number RN is then generated. The maximum value of this random

number is set equal to the value of EFF . If $G \geq RN$, the cell will be kept. Perturbation will be performed otherwise.

The move is carried out by replacing the gate type of a cell by a new random type of gate. The perturbed solution is then evaluated. The perturbed solution is considered a new solution if its quality, according to the cost function, is better compared to the original solution.

Perturbation;

Row and Column Adjustment;

```
/* row          number of row */
/* column      number of column */
/* M           current solution */
/* M'          temporary solution */
```

Begin

```
M' ← M
```

```
For  $0 \leq j < column$ 
```

```
  For  $0 \leq i < row$ 
```

```
     $RN = rand() \% ((int) EFF)$ 
```

```
     $G = BFF + FF_n$ 
```

```
    If  $G < RN$ 
```

```
      cell[i][j].gate = assign random gate
```

```
      Calculate truth table cell[i][j]
```

```
      Calculate fitness cell[i][j]
```

```
    EndIf
```

```
  EndFor
```

```
EndFor
```

```
Calculate fitness of M'
```

```
If M'.fitness > M.fitness
```

```
M ← M'
```

```
End
```

Figure 5.12: Perturbation Procedure.

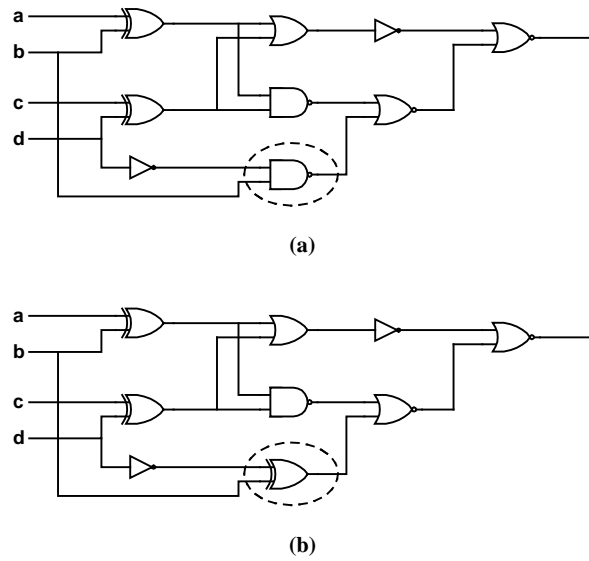


Figure 5.13: Effect of perturbation on functional fitness value (a) $FF_n = 0.9375$ (b) $FF_n = 1$.

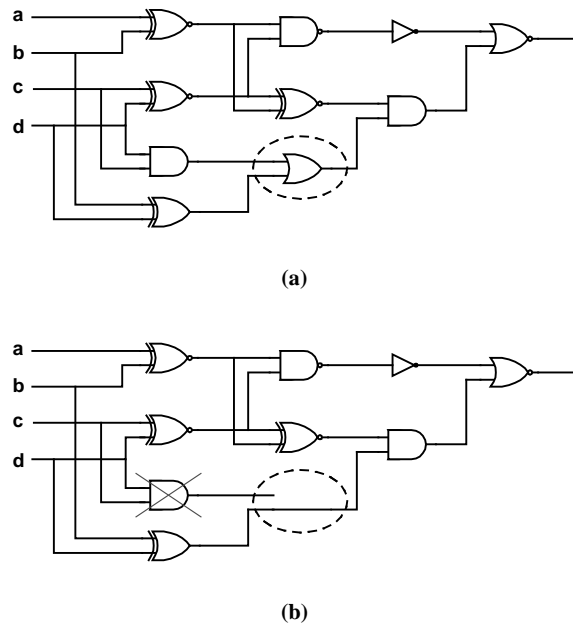


Figure 5.14: Effect of perturbation on objective fitness (a) gate count = 10 (b) gate count = 8.

Perturbation can affect both functional fitness and objective fitness of solutions. Figure 5.13 shows an example of how perturbation affect the functional fitness. By changing the circled NAND gate into an XOR gate, the FF of the solution is changed from 0.9375 into 1. In Figure 5.14, changing the circled OR gate into a WIRE reduce the number of gate count (area) of the solution. Note that both solutions have the same FF s.

When the maximum number of iterations is reached, but no functionally correct circuit is produced, the search process can be continued using the *residual function*. This is discussed below.

5.3.3 Residual Function

Given suitable time to evolve, the proposed algorithm could find the target truth table. However, it could happen that after a given maximum number of iterations, functionally correct circuits are not produced. In this case, two approaches can be used, either to have another run of the algorithm, or to extend the search by using current solution as initial state for the heuristic. No modifications are needed to perform the first approach. The second approach requires some modifications so that the extension of the search is performed intelligently. This section addresses the approach used for extending the search in ELD.

Extending the Search

The goal of ELD is to produce functional and optimized circuits. A solution whose functional fitness is 0.9 is not considered as a good solution. However, in terms of evolution process, it is 90% functional. Given the time to evolve, it is hoped that by extending the search into a more directed solution space, the fully functional circuits can emerge from this solution.

Consider, for example, the target truth table (F) for the algorithm to be generated is 10010011. Assume that after maximum iteration is reached, the best solution returned by the algorithm has the truth table (f_1) 10010000. The functional fitness of the solution is ‘only’ 0.75. Assume that the searching process is continued by targeting *residual* truth table (f_2) 00000011. Then, if f_2 is obtained, both f_1 and f_2 can be *merged* using an OR gate to build the intended truth table F . Since the search space for f_2 is likely to be smaller than the search space for F , the possibility to find f_2 is greater compared to F .

The residual function f_2 is obtained by *decomposing* function F to f_1 OR f_2 . The *decomposition* procedure in Boolean algebra allows the use of *don't care values* (*). Thus, the truth table of f_2 will be *00*0011. The don't care values will allow us to explore richer solution space. In addition to that, the target solutions will increase, since there are four representations for f_2 : 00000011, 00010011, 10000011, and 10010011. This makes the searching process more promising. The procedure of

how the decomposition is performed is discussed below.

Decomposition Rules

Decomposition plays an important part in the conventional logic design algorithms. The idea is to divide a Boolean function into some lower complexity sub-functions, so that the overall representation can be minimized. Decomposition can be formulated as follows. Given F as a Boolean function, find f_1, \dots, f_k so that $F = G(f_1, \dots, f_k)$, where G is a Boolean operator (a gate). The sub-functions f_1 or f_k can be decomposed further to obtain simpler functions.

Decomposition can be performed in many ways. Since only two inputs gate are used, there are three types of decomposition considered, namely: OR, AND and XOR decomposition. These names denote the gate used for the decomposition. Thus, decomposition process can be formulated as follows.

Given Boolean function F and known sub-function f_1

AND decomposition : find f_2 so that $F = f_1 \cdot f_2$

OR decomposition : find f_2 so that $F = f_1 + f_2$

XOR decomposition : find f_2 so that $F = f_1 \oplus f_2$

Unfortunately, not all functions can be decomposed using AND or OR decomposition. There is a need of a procedure to check whether a function is decomposable by AND (OR) decomposition or not. Table 5.2 and Table 5.3 show the value of

Table 5.2: AND decomposition table.

F	f_1	f_2	Meaning	Coding
0	0	*	don't care	2
0	1	0	logic 0	0
1	0	-	can't happen	3
1	1	1	logic 1	1

f_2 for different input pattern of F and f_1 for AND and OR decomposition, respectively. If the value of f_2 is '-' (can't happen condition), then the function F is not decomposable using f_1 .

Table 5.3: OR decomposition table.

F	f_1	f_2	Meaning	Coding
0	0	0	logic 0	0
0	1	-	can't happen	3
1	0	1	logic 1	1
1	1	*	don't care	2

In contrast with the AND and OR decomposition, function f_2 can always be produced by decomposing F to f_1 by XOR decomposition, since $f_2 = F \oplus f_1$. However, in XOR decomposition, the f_2 will be in the form of completely specified functions, i.e., the truth table of f_2 does not have don't cares values, as shown in Table 5.4. Thus, it is possible that f_2 is more complex than f_1 (or F) itself.

Merging the solutions

Using the concept of residual function, the algorithm will work in at least two stages. The first stage is to find f_1 , while the second one is to find f_2 . At the end of the second stage, f_1 and f_2 will be merged to obtain a new solution. Consider,

Table 5.4: XOR decomposition table.

F	f_1	f_2	Meaning	Coding
0	0	0	logic 0	0
0	1	1	logic 1	1
1	0	1	logic 1	1
1	1	0	logic 0	0

for example, a function F with truth table 1000111111100101. Assume that the first stage of the algorithm found f_1 whose truth table is 0000111110100101 (see Figure 5.15 (a)). Assume that OR decomposition is used. Using OR decomposition table, truth table of f_2 is then 1000*****1*00*0*. Assumed that the second stage of the algorithm find f_2 with truth table 1000001001000001, shown in Figure 5.15 (b). With OR gate as operator, the function F' obtained from merging f_1 and f_2 is shown in Figure 5.15 (c).

If $F' = F$, it means that the algorithm found the functionally correct circuits. However, it is possible that f_2 was not found and $F' \neq F$. In this case, another stage of decomposition must be performed. The new f_2 will be calculated by using F' as f_1 . This process is continued until the maximum number of decomposition

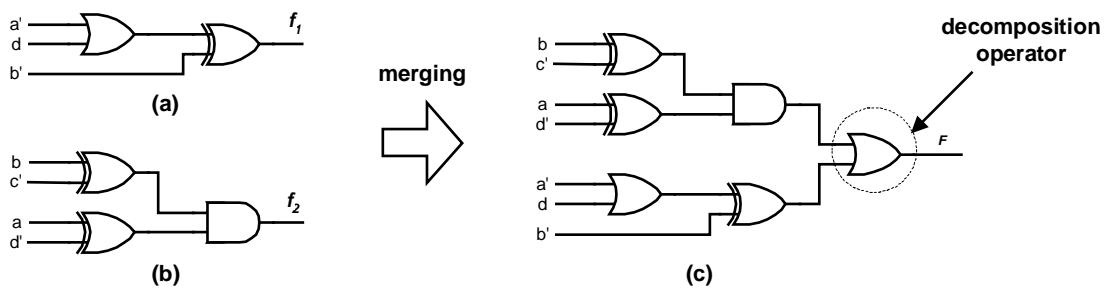


Figure 5.15: Example of using the residual function.

```

Decomposition()

If ( $s = 0$ ) and (solution. $FF = 1$ )
    Return solution

Else
    If ( $s > 0$ )
        Merge( $f_1, f_2, G, F'$ )
        If ( $F' = F$ )
            Return solution
        EndIf

     $f_1 \leftarrow$  solution
    If ( $s = 0$ )
         $G =$  OR gate
    ElseIf ( $s = 1$ )
         $G =$  AND gate
    Else
        If Check_decompose( $F, f_1, \text{OR}$ )  $> 0$ 
             $G =$  OR gate
        ElseIf Check_decompose( $F, f_1, \text{AND}$ )  $> 0$ 
             $G =$  AND gate
        Else  $G =$  XOR gate
    EndIf

    Decompose( $F, f_1, G, f_2$ )

EndIf

```

Figure 5.16: Decomposition procedure.

stages allowed is reached.

In order to get the benefit of the don't care values, both of AND and OR decomposition get higher priority compared to the XOR decomposition. The justification is that the unneeded minterms from f_1 can be removed using AND decomposition and the required minterms can be added using the OR decomposition. Note that the "can't happen" condition will be treated as normal don't cares. If both decompositions fail, the XOR decomposition is performed. Figure 5.16 shows the pseudocode of decomposition procedure.

Improved Modified ACO (IMACO) algorithm

```

/* MAXITER      Maximum iteration */
/* MAXSTAGE     Maximum decomposition stage */

  For  $0 < s < MAXSTAGE$ 
    For  $0 < i < MAXITER$ 
      Filling_the_Matrix();
      Ant_Activity();
      Removing_Unfit_Cells();
      Perturbation();
    End
    Decomposition();
  End
  Return best solution
End

```

Figure 5.17: Improved-Modified ACO algorithm for logic design.

Putting It All Together

Having the perturbation and decomposition procedures incorporated, the improved modified ACO (IMACO) algorithm for logic design is presented in Figure 5.17.

The IMACO algorithm is more complex compared to the previous one (see Figure 5.5). However, the probability of obtaining better quality result is higher. Experimental results and comparison between the proposed algorithms will be given in the next chapter.

5.4 Concluding Remarks

In this chapter, a Modified Ant Colony Optimization (MACO) algorithm for the design of digital logic circuits is introduced. The need for a modification to the original ACO algorithm is discussed. Moreover, an improved version of the MACO algorithm that includes the use of perturbation and residual function is also proposed. In the next chapter, performance evaluation, experiments and results of the proposed algorithm are presented.

Chapter 6

EXPERIMENTS AND RESULTS

This chapter and the following one are dedicated to experiments and results obtained from applying the proposed algorithms. This chapter concentrates on the evaluation of different possible schemes, while the next chapter will present comparison with existing techniques.

6.1 Experimental Setup

A number of procedures needed for conducting the experiments are first introduced. This includes the setting of inputs, tools and parameters.

Input: In order to perform the experiments, some benchmark circuits are used as test cases. The benchmark consists of twenty randomly generated truth tables of different complexity in addition to twelve circuits obtained from ISCAS'85 bench-

mark. All circuits are in PLA format. Using this format, the proposed algorithm can accept don't care inputs as mentioned in Section 3.4. Details of these circuits are given in Appendix A. Table 6.1 shows a summary of these circuits.

Table 6.1: Summary of circuits used for the experiments.

Circuits used	Single Output		Multiple Output		Notes
	Number of circuits	Specification	Number of circuits	Specification	
Random	20	Number of inputs: 2 - 6	-	-	-
ISCAS'85	3	Number of inputs: 3 - 7	9	Number of inputs: 3-7	arithmetic circuits: majority, parity, adder and multiplier
				Number of outputs: 2-10	

Technology parameters used in the experiments is obtained from MOSIS 0.25 μ library [80]. These parameters are written into a text file using a certain format. This can be seen in Appendix A.

Parameters for the Algorithm: Performance of iterative heuristics depends on the fine-tuning of its parameters. Otherwise mentioned explicitly, in general, these parameters listed below are used. Note that NV is the number of variables for a specific circuit.

- $\alpha = 1$
- $\beta = 1$
- $\rho = 0.1$
- Number of ants = $10 * NV$
- Number of generations = $2 * NV$
- Maximum number of iterations = $500 * NV$

- Number of runs = 20
- Minimum size of the matrix = $NV \times NV$
- Maximum size of the matrix = $(k_1 \cdot NV) \times (k_2 \cdot NV)$, $2 \leq k_2 < k_1$
- Maximum number of decomposition stages = 6

Four types of experiments are carried out to measure the performance of the proposed algorithms. These include experiments for different fitness function calculation, effect of dynamic search space, effect of perturbation and decomposition, and different optimization objectives. The quality of solutions are measured according to the area, delay and power of the circuits. These metrics are measured in μm^2 , ps and pW units, respectively.

6.2 Performance of Different Fitness Calculation

The objective of this experiment is to know which fitness function calculation works best for the proposed algorithms. This includes the selection of weighting scheme and calculation of FF .

6.2.1 Effect of Different Weighting Scheme

As mentioned in Chapter 4, two approaches can be used to select the value of WF , namely: static and dynamic. These are examined below.

For the purpose of this experiment, the size of the matrix is set as $(2 \cdot NV) \times (2 \cdot NV)$. The circuits used as test cases are those having four or five inputs. In

addition to the quality of results in terms of cost function, a measure called *design rate* is used for comparison. Design rate is defined as the percentage of functionally correct circuits delivered by the algorithm from the whole runs of experiment using a given maximum number of iterations.

Table 6.2, Table 6.3 and Table 6.4 show the experimental results, assuming the value of WF is 0.5, 0.75 and 0.875, respectively.

Table 6.2: Experimental results for $WF = 0.5$.

Circuit	design rate	Best result		
		Area	Delay	Power
circuit1	55	15066	5.94	6.572
circuit2	70	15066	5.94	6.572
circuit3	45	10692	3.05	3.818
circuit4	100	1458	0.01	0.666
circuit5	25	12150	3.90	5.076
circuit6	55	10935	3.34	3.818
circuit7	60	12393	6.66	4.732
circuit8	100	7290	2.96	3.161
circuit9	0	-	-	-
circuit10	5	12393	5.32	4.483

Table 6.3: Experimental results for $WF = 0.75$.

Circuit	design rate	Best result		
		Area	Delay	Power
circuit1	100	14823	5.89	6.57
circuit2	100	14823	5.89	6.57
circuit3	70	11421	3.35	3.82
circuit4	95	1458	0.01	0.67
circuit5	85	12150	3.90	5.08
circuit6	100	10935	3.34	3.82
circuit7	85	12636	6.66	4.73
circuit8	100	7290	2.96	3.16
circuit9	65	17496	5.42	5.27
circuit10	35	12393	5.32	4.48

Table 6.4: Experimental results for $WF = 0.875$.

Circuit	design rate	Best result		
		Area	Delay	Power
circuit1	100	14094	5.55	5.28
circuit2	95	14823	5.89	6.57
circuit3	85	10692	3.05	3.82
circuit4	90	1458	0.01	0.67
circuit5	85	12150	3.90	5.08
circuit6	100	10935	3.34	3.82
circuit7	100	12393	6.27	4.48
circuit8	100	7290	2.96	3.16
circuit9	80	16038	6.00	5.27
circuit10	25	12393	5.32	4.48

It was expected that the setting of WF equal to 0.5 will give the best solution in both FF and OF . However, this happened to be a wrong assumption. Indeed, the setting of $WF = 0.5$ is the worst among the others. The average design rate for this setting is only 51.5%, which is quite low. It gives 100% design rate only for small circuits (circuit4 and circuit8) and even fails to deliver working circuit for circuit9. The reason behind this is that the algorithm was trying to satisfy both FF and OF at the same time during the course of iteration. It is more difficult for the algorithm to move to a new solution with higher FF if its OF is low. Thus, the algorithm will spend more time with solutions that have low FF value, which in turn reduces the possibility of delivering correct circuits.

In terms of design rate, both the setting of $WF = 0.75$ and $WF = 0.875$ are much better compared to $WF = 0.5$. The average design rate is 82.5% and 86% respectively. In terms of OF , the setting of $WF = 0.875$ gives the best results

compared to other settings. This happens because the algorithm reached the solution having FF equal to 1 in the early stages of iteration.

The highest value that can be assigned to WF is equal to $MAXWF = \frac{L}{L+1}$, with L is the length of the truth table. The proof is the following.

The overall fitness function (see Equation 4.13) can be rewritten as.

$$OvF * (M + N) = FF * M + OF * N \quad (6.1)$$

Note that FF and OF are fractions in $[0, 1]$, with

$$FF = \frac{H}{L}$$

where H is the number of hits and L is the length of the truth table.

If M is set equal to L , the first term in Equation 6.1 will be equal to H , which is a decimal number. By setting N equal to 1, the second term in Equation 6.1 will stay as a fraction. Since the value of M determines the importance of FF in contrast to OF , the ratio of M to N is equal to $L : 1$. Setting M equal to a value larger than L will not give any effect since the second term of Equation 6.1 is already a fraction. The value of $MAXWF$ is then

$$\frac{M}{M + N} = \frac{L}{L + 1}$$

If the value of WF is increased, the importance of OF will decrease. Consider, for example, the use of $MAXWF$ as WF . During the iterations, solutions that have higher number of matching truth table will be taken, regardless of the value of OF . The value of OF will be considered if there exist two solutions having the same value of FF . In this case, the solution having higher OF will be considered.

Table 6.5: Experimental results for dynamic WF .

Circuit	design rate	Best result		
		Area	Delay	Power
circuit1	90	14823	5.89	6.57
circuit2	95	15066	5.94	6.57
circuit3	50	10692	3.05	3.82
circuit4	90	1458	0.01	0.67
circuit5	75	12150	3.90	5.08
circuit6	95	10935	3.34	3.82
circuit7	100	12393	5.05	4.38
circuit8	100	7290	2.96	3.16
circuit9	55	15066	5.42	5.27
circuit10	25	12393	5.32	4.48

For small circuits, it is better to use higher WF values as shown in Table 6.2, Table 6.3 and Table 6.4. However, for larger circuits, the use of higher WF values can be counter productive. Because, it may happen that a solution having high FF with low OF value is obtained. However, low OF value means less in satisfying the objectives, i.e., the solution may have large area, or delay, or power. Consider, for example, in the case of larger area. The solution will require quite a number of cells to be locked during the iterations. If this happened quite often, it will be difficult for the algorithm to escape local optimal because the number of empty cells in the

matrix to explore new solution space will be less. An answer for this problem is the use of dynamic WF (see Chapter 4).

The experimental results for dynamic WF is shown in Table 6.5. For the purpose of the experiment, a minimum WF value is set equal to 0.5 while the maximum value is set to 0.9. As can be seen from the table, the design rate of this approach is lower compared to the one with $WF = 0.875$. In terms of OF , the use of dynamic WF leads to worse or similar results for small circuits, i.e., circuit1 to circuit8. However, as the size of the circuits is increased, i.e., circuit9, the use of dynamic WF leads to results that are better compared to those obtained using static WF .

6.2.2 Effect of Different FF Calculations

Using dynamic WF , performance of different functional fitness calculations is carried out using larger circuits. Recall to Chapter 4, there are three types of functional fitness calculations considered, original (FF), normalized FF (FF_n), and normalized-penalized FF (FF_{np}). Table 6.6 shows results of the experiments.

The original FF calculation suffers a lot for larger circuits. It fails to deliver working circuits for three out of seven cases. The normalized FF (FF_n) also fails for those same circuits. However, the design rate for FF_n is better compared to FF . This is due to the ‘normalization’ done to the calculation of FF . By normalizing FF , the algorithm will find both the intended Boolean function and the inverted Boolean function. Whichever comes first will be considered.

Although it fails to deliver working circuits for circuit12, the normalized-penalized FF (FF_{np}) is the best compared to the other two. Note that, circuit12 is one example that needs to be highlighted since the size of the circuit is quite large. It will be shown later that this circuit can be generated using the concept of residual functions.

Table 6.6: Results obtained for different FF calculations.

Circuit	Design Rate		
	Original FF	Normalized (FF_n)	Normalized-penalized (FF_{np})
circuit9	55	60	80
circuit10	25	45	40
circuit11	10	20	55
circuit12	0	0	0
circuit13	25	55	50
circuit14	0	0	20
circuit15	0	0	25

From this time onward, except if it is mentioned explicitly, the experiments will be carried out using dynamic WF with FF_{np} .

6.3 Dynamic Search Space

The purpose of this experiment is to show how the use of dynamic matrix size affects the performance of the proposed algorithm. Table 6.7 shows a comparison in terms of design rate and execution time for both static matrix size (SM) and dynamic matrix size (DM) approaches.

In terms of design rate, DM clearly outperforms SM . In addition to that,

circuit12 that was not generated using *SM* was delivered by *DM*. In terms of execution time, *DM* was superior compared to *SM* for small circuits (circuit1 to circuit8) by up to 25% time saving. Note that both approaches use the same number of iterations. The difference in execution times is caused by the different sizes of the search space explored by both approaches. For bigger circuits, *DM* provides faster execution time for circuit9 and circuit10, with 37.5% and 42.5% time saving as compared to the ones obtained using the *SM*. For the remaining circuits, *SM* requires less computation time compared to *DM*. Consider the case of circuit13. The execution time of *DM* is three times higher compared to the one for *SM*. For this circuit, it was observed that the algorithm can achieve solutions having *FF* equal to 0.969 in a very short time. However, it was very difficult to obtain solutions higher *FF* value. Therefore, the design rate for the circuits is low in *SM*. On the other hand, when local optima is observed, *DM* will increase the size of the matrix. This will in turn increase the execution time of the algorithm. However, the probability of obtaining functionally correct circuits will increase. In other words, the design rate of *DM* is higher as compared to the one of *SM*.

Table 6.8 shows a comparison of quality of solutions in terms of area obtained using *SM* and *DM*. Except for circuit12, *DM* provides better circuits in six out of fourteen cases, with 1% to 13% reduction in area. Both approaches produce the same quality of circuits in the remaining cases.

For large circuits, i.e., circuit9 to circuit15, except for circuit14, *DM* produces

Table 6.7: Experimental result for static and dynamic matrix in terms of design rate and computation time.

Circuit	design rate		time	
	SM	DM	SM	DM
circuit1	100	100	21.00	15.27
circuit2	100	100	20.95	15.30
circuit3	100	100	21.10	14.53
circuit4	100	100	4.30	3.50
circuit5	100	100	20.60	17.03
circuit6	100	100	20.70	14.80
circuit7	100	100	21.10	16.27
circuit8	100	100	21.15	12.90
circuit9	80	100	131.44	82.13
circuit10	40	100	134.13	77.07
circuit11	55	93	39.36	57.63
circuit12	0	13	-	151.50
circuit13	50	100	39.20	121.43
circuit14	20	87	132.75	208.13
circuit15	25	93	132.60	188.64

Table 6.8: Area result obtained using static and dynamic matrix size.

Circuit	SM	DM	Ratio
circuit1	14823	12879	0.87
circuit2	14823	13122	0.89
circuit3	10692	10692	1.00
circuit4	1458	1458	1.00
circuit5	12150	13365	1.10
circuit6	10935	10935	1.00
circuit7	12150	12393	1.02
circuit8	7290	7290	1.00
circuit9	15066	15066	1.00
circuit10	12393	11178	0.90
circuit11	17739	17496	0.99
circuit12	0	45684	~
circuit13	20169	19683	0.98
circuit14	22842	26730	1.17
circuit15	21870	20655	0.94

better or equal quality results compared to *SM*. In circuit14, the area of the obtained circuit using *DM* is higher compared the one obtained using *SM*. However, the design rate of *SM* for this circuit is 20% compared to 87% using *DM*. In other words, compared to *SM*, *DM* has much higher probability of arriving at solutions.

6.4 Residual Function

The MACO algorithm depicted in Figure 5.5 failed to deliver some large circuits, i.e., circuit18 up to circuit20. The use of residual function, as included in IMACO algorithm (see Figure 5.17), for these circuits is found necessary. Table 6.9 shows experimental results for these circuits considering residual function. Note that circuit12 is added in addition to those of large circuits since this circuit is one of the hard to implement circuits as indicated in the previous sections.

Table 6.9: Results obtained using IMACO algorithm.

Circuit	design rate	Best result			Average result			time
		Area	Delay	Power	Area	Delay	Power	
circuit12	70	45684	14.30	17.36	83891.08	21.80	28.51	1920.85
circuit18	55	63666	23.83	22.01	81162.00	26.09	26.85	1046.70
circuit19	50	54432	11.34	19.68	78570.00	21.14	25.56	1241.50
circuit20	55	60264	12.43	20.23	73483.20	23.78	25.68	1016.00

As can be seen from the table, all considered circuits in the experiment were delivered by the algorithm. In addition, an improvement in the design rate for circuit12 was observed. The design rate for this circuit is 70%, as compared to 13% in the previous experiment (see Table 6.7). However, as has been expected,

the execution time for IMACO algorithm is increased tremendously. The execution time of IMACO algorithm is up to 5 times as compared to the MACO algorithm.

6.5 Different Optimization Objectives

The cost function considered in this work includes area, delay and power consumption of the circuits. Three sets of experiments are performed. These are:

1. Area optimization with delay and power as constraints (AODPC)
2. Delay optimization with area and power as constraints (DOAPC)
3. Power optimization with area and delay as constraints (POADC)

Basically, since fuzzy logic is used to aggregate the cost functions, the algorithm will try to find solutions that are optimized for area, delay and power at the same time. The term constraints used above is used to imply that the solutions obtained must have area (delay or power) less than or equal to the stated maximum value.

AODPC

In order to understand how the optimization is performed, it is important to observe the behavior of the proposed algorithms during the course of experiments. Figure 6.1 shows the behavior of OVF , FF and OF (overall fitness, functional fitness and objective fitness) against time during one of the experiment performed for circuit1.

As can be seen from the figure, the value of FF increases with time. Since the circuit is relatively small in size, the functionally correct circuit (FF equal to one) is found in less than 50 iterations. In contrast with FF , the value of OvF will never be one, unless if the circuit contain only wires. In fact, the value of OvF depends on the value of FF and OF .

The value of OF may increase or decrease during the course of iterations. Figure 6.2 shows the behavior of fitness function for the first 50 iterations. As can be seen from the figure, at about iteration number 25, the value of OF was decreasing. However, the value of FF is increasing. As mentioned in the previous chapter, whenever solution with higher FF value is obtained, the move to the new solution is preferable. However, if there is no increase in FF , optimization in OF will be carried out.

The optimization of OF is performed according the fuzzy rule applied in the experiment. Figure 6.3 and Figure 6.4 show the behavior of OF during the first 50 iterations and 150 iterations, respectively. The value of area, delay and power are normalized to the highest value achieved during the iterations.

As can be seen from Figure 6.3, the value of OF at iteration number 40 reaches its lowest value because the value of area, delay and power reach their largest value at the same time. However, after iteration number 40, the value of OF is increasing (see Figure 6.3 and Figure 6.4). This means that the optimization in terms of objective functions is performed.

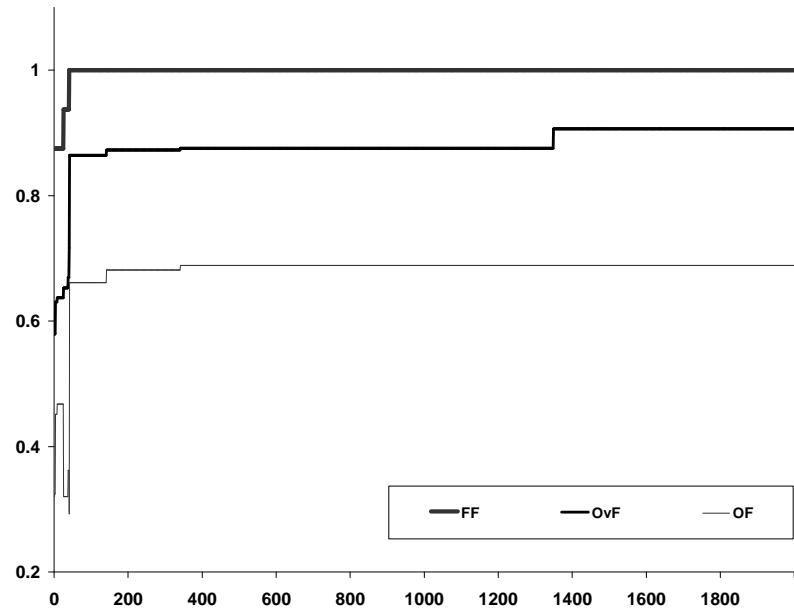


Figure 6.1: Behavior of functional fitness function for circuit1 in the first 2000 iterations using AODPC.

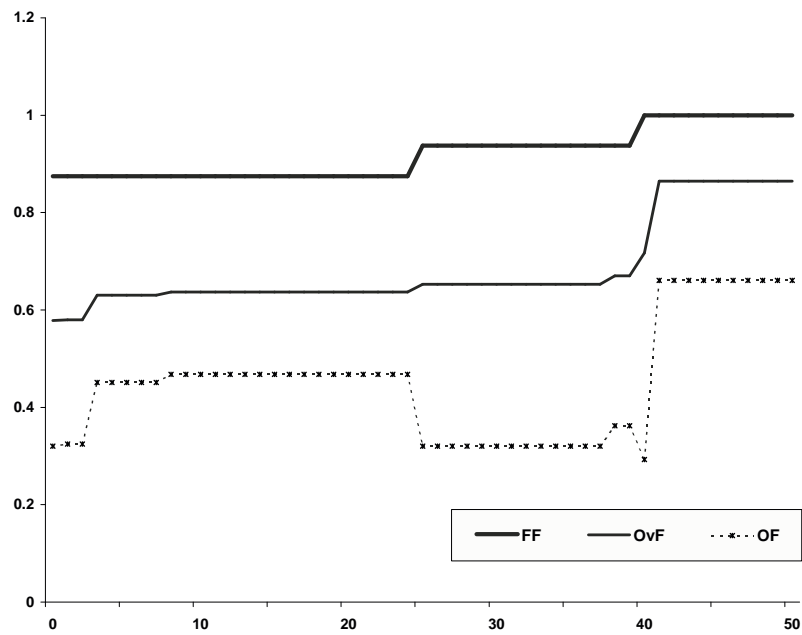


Figure 6.2: Behavior of functional fitness function for circuit1 in the first 50 iterations using AODPC.

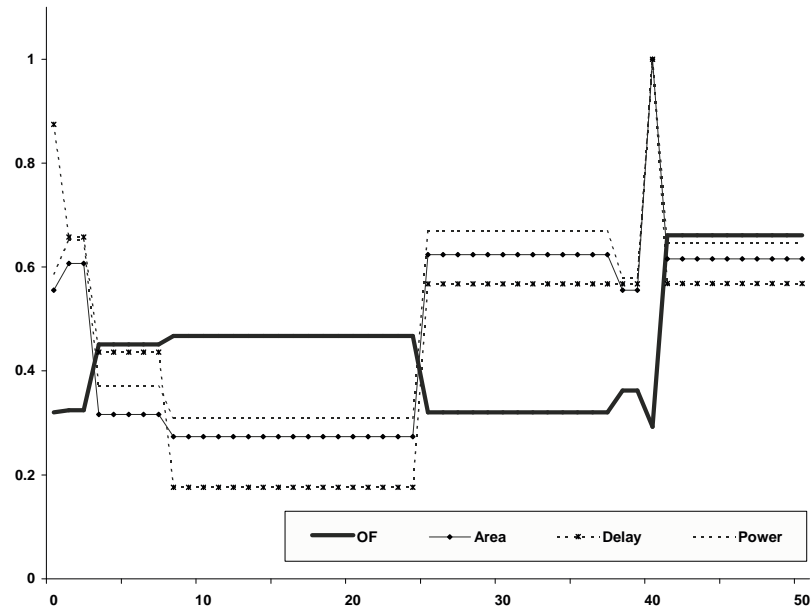


Figure 6.3: Behavior of objective fitness function for circuit1 in the first 50 iterations using AODPC.

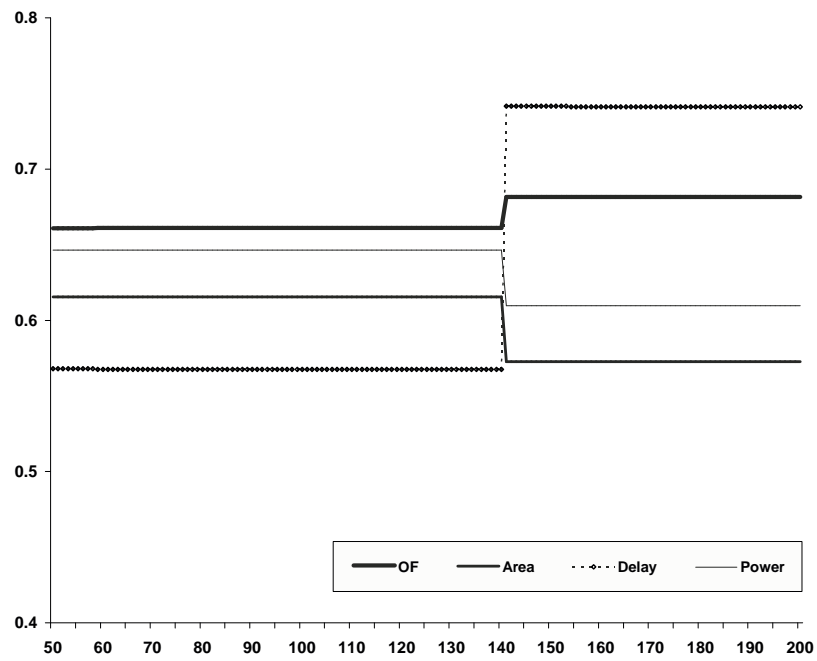


Figure 6.4: Behavior of objective fitness function for circuit1 in iteration 50 to iteration 200 using AODPC

In AODPC, it is expected that the circuits obtained will have less area as compared to the ones produced by other set of experiments. Figure 6.4 illustrates this behavior. As can be seen in the figure, at about iteration number 140, new solution with less area is accepted although it has higher delay compared to the old solution.

Table 6.10: Results of different optimization objectives.

Circuit	AODPC			DOAPC			POADC		
	area	delay	power	area	delay	power	area	delay	power
circuit10	11178	5.42	4.06	12393	5.32	4.48	11178	5.42	4.06
circuit11	17253	5.91	7.22	22599	5.61	9.30	18225	6.29	6.95
circuit12	45684	14.30	17.36	57591	13.88	20.56	45684	14.30	17.36
circuit18	63666	23.83	22.01	77760	16.68	28.75	64638	20.04	21.09
majority	13851	4.57	5.06	16038	4.19	5.02	14580	4.53	4.72
xor8	20655	5.90	9.32	20655	5.90	9.32	20655	5.90	9.32
xor9	23328	8.84	10.65	27216	8.84	11.48	23814	9.57	10.65
add2	24300	11.48	9.96	31347	8.96	11.46	25029	13.30	9.57
add3	49086	21.96	18.47	53703	12.98	21.48	54675	14.36	20.55
mul2	12636	3.56	4.66	18225	2.96	5.99	14823	4.44	4.66
mul3	59292	15.03	17.54	74358	13.14	21.65	73386	16.33	19.11
con1	38151	6.70	13.74	38394	6.24	12.65	42282	9.79	13.97

The results of the experiments for a number of selected circuits are shown in Table 6.10. The table shows the value of area, delay and power for the best solution obtained by different set of experiments. In order to measure the performance of the algorithm for different objectives, the results in this table are normalized with respect to the results of AODPC experiment.

DOAPC

Table 6.11 shows the normalized value of DOAPC. As can be seen from this table, the percentage of improvement in delay varies. The improvement is, however, mostly accompanied by additional area and power consumption. Figure 6.5 shows the normalized area, delay and power for DOAPC. As can be seen in the figure, the value of normalized delay is always less than one. It means that for the given single-output circuits, DOAPC provides circuits with better or at least the same delay as compared to the ones produced by AODPC.

Table 6.11: Results of DOAPC experiments normalized with respect to results of AODPC.

Circuit	Area	Delay	Power	% area	% delay	% power
circuit10	1.11	0.98	1.10	-10.87	1.79	-10.36
circuit11	1.31	0.95	1.29	-30.99	5.01	-28.84
circuit12	1.26	0.97	1.18	-26.06	2.97	-18.42
circuit18	1.22	0.70	1.31	-22.14	30.02	-30.62
majority	1.16	0.92	0.99	-15.79	8.29	0.69
xor8	1.00	1.00	1.00	0.00	0.00	0.00
xor9	1.17	1.00	1.08	-16.67	0.00	-7.83
add2	1.29	0.78	1.15	-29.00	21.98	-15.07
add3	1.09	0.59	1.16	-9.41	40.90	-16.29
mul2	1.44	0.83	1.29	-44.23	16.76	-28.56
mul3	1.25	0.87	1.23	-25.41	12.59	-23.40
con1	1.01	0.93	0.92	-0.64	6.82	7.91

For multiple output circuits, i.e., the longest delay appear in the circuits is considered (see Table 6.10). Figure 6.6 shows the normalized area, delay and power for multiple output circuits. It is observed that the value of normalized delay is always less than one. In general, DOAPC has performed its objective by producing circuits with better delay as compared to the one produced by AODPC.

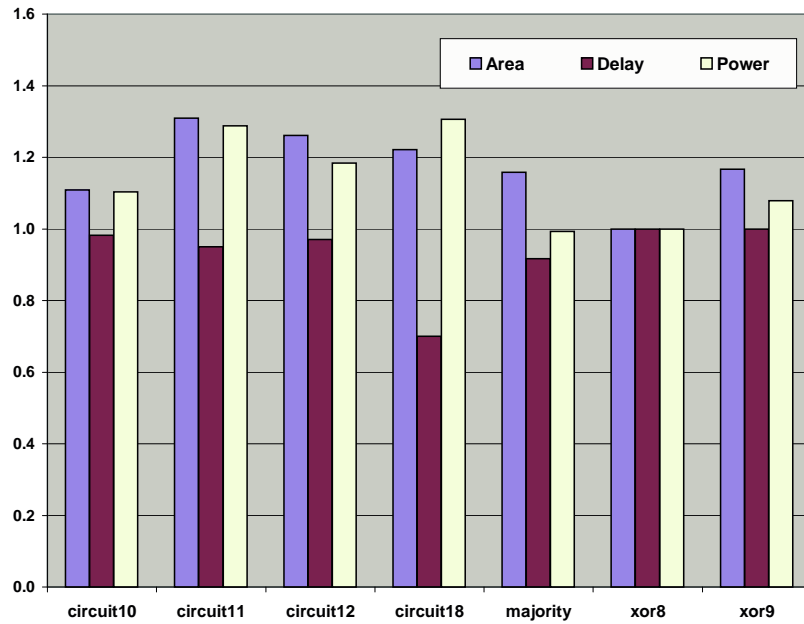


Figure 6.5: Normalized results of DOAPC for single output circuits.

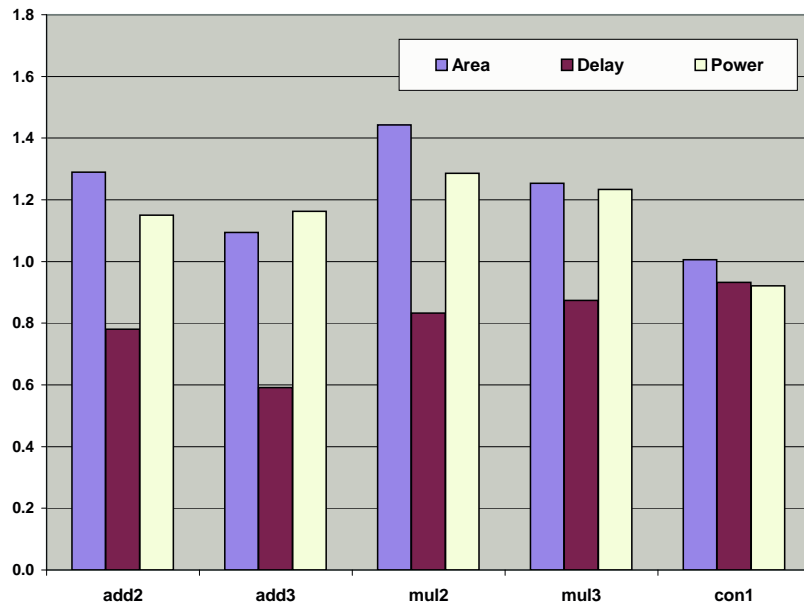


Figure 6.6: Normalized results of DOAPC for multiple output circuits.

POADC

Table 6.12 shows the normalized value of POADC. As can be seen, the percentage of improvement for power is less compared to the percentage of improvement for delay in DOAPC. Figure 6.7 shows the normalized area, delay and power in POADC for single output circuits. It is observed that the value of normalized power for these circuits are less or at least equal to one, which means the optimization of power is achieved.

Table 6.12: Results of POADC experiments normalized with respect to results of AODPC.

Circuit	Area	Delay	Power	% area	% delay	% power
circuit10	1.00	1.00	1.00	0.00	0.00	0.00
circuit11	1.06	1.06	0.96	-5.63	-6.36	3.73
circuit12	1.00	1.00	1.00	0.00	0.00	0.00
circuit18	1.02	0.84	0.96	-1.53	15.94	4.20
majority	1.05	0.99	0.93	-5.26	0.88	6.59
xor8	1.00	1.00	1.00	0.00	0.00	0.00
xor9	1.02	1.08	1.00	-2.08	-8.24	0.00
add2	1.03	1.16	0.96	-3.00	-15.86	3.96
add3	1.11	0.65	1.11	-11.39	34.62	-11.24
mul2	1.17	1.25	1.00	-17.31	-24.54	0.00
mul3	1.24	1.09	1.09	-23.77	-8.66	-8.92
con1	1.11	1.46	1.02	-10.83	-46.12	-1.64

Figure 6.8 shows the normalized area, delay and power for multiple output circuits. The figure shows some discouraging results. Improvement in power are observed for add2 (2-bit adder) and mul2 (2-bit multiplier) circuits. POADC however, failed to produce circuits with better power consumption in contrast to AODPC.

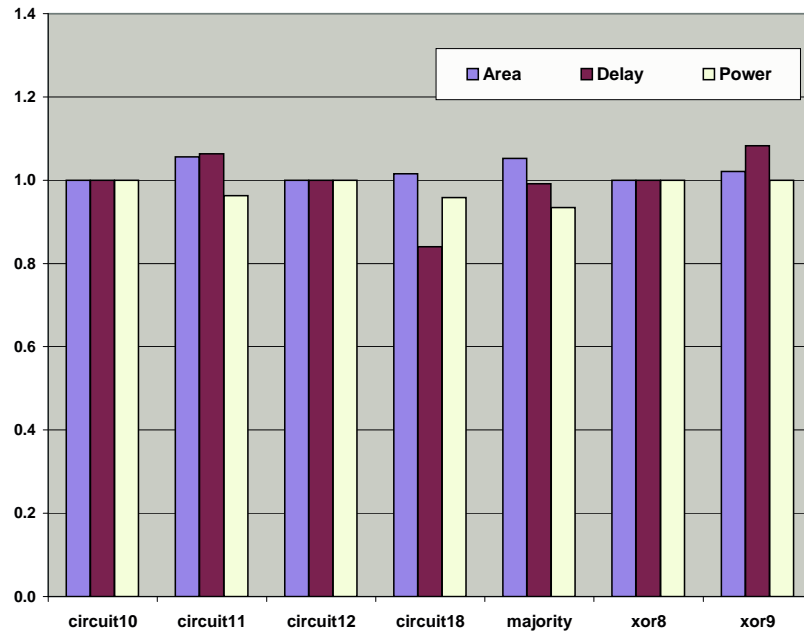


Figure 6.7: Normalized results of POADC for single output circuits.

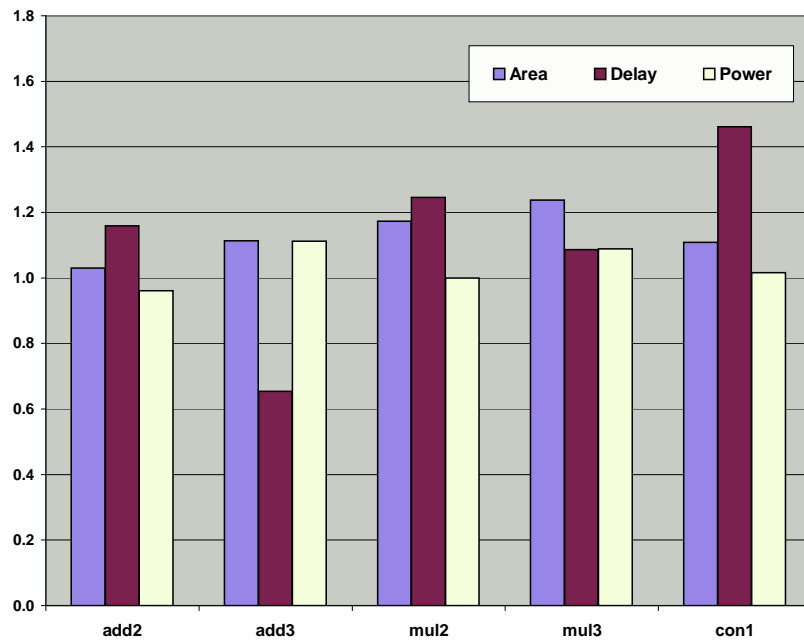


Figure 6.8: Normalized results of POADC for multiple output circuits.

From the three sets of experiments it was observed that the performance of POADC is the worst. There is no much improvement in power consumption as expected. The reason behind this behavior is twofold:

1. By using OWA operator of fuzzy logic, the optimization of area, delay and power are performed at the same time.
2. Power consumption of a given circuit is proportional to the number of gates it has. Thus, in agreement with point 1, the quality of obtained circuits in POADC are generally the same with the ones produced by AODPC.

6.6 Concluding Remarks

In this chapter, performance of the solution approach was evaluated. It began with the performance of different fitness function calculations and continued with the dynamic search space and improved-modified ACO algorithm. The approach was able to arrive at acceptable solutions in all test cases. The performance of different set of experiments has also been presented. Comparison of the solution approach with the existing technique is presented in the next chapter.

Chapter 7

COMPARISON WITH EXISTING TECHNIQUES

In this chapter, a comparison of the results obtained using the introduced techniques is presented.

7.1 Comparison with Existing ACO-based Technique

In this section, the results of our experiments are compared to the results obtained from the existing ACO-based technique proposed by Coello [6]. Since this technique tries to minimize the use of gate count only, the comparison is performed using the results of AODPC of the proposed algorithm. This includes comparison in terms of

Table 7.1: Comparison with Coello [6] in terms of *design rate*.

Circuit	Coello [6]	MACO
circuit1	70	100
circuit2	70	100
circuit3	90	100
circuit4	100	100
circuit5	30	100
circuit6	100	100
circuit7	50	100
circuit8	100	100
mul2	100	100

design rate, quality of results and performance of the algorithm.

7.1.1 Comparison of Design Rate

Table 7.1 shows comparison of both Coello's [6] technique and the proposed algorithm in terms of design rate. For this purpose, the same test cases were used. It should be noted that the technique described in [6] failed to deliver any valid results for large single-output circuits.

Since the test cases are relatively small, the MACO algorithm is used. As can be seen from Table 7.1, the MACO algorithm outperformed the existing ACO-based technique in terms of design rate. The average design rate for MACO algorithm is 100% as compared to 78.89% for Coello [6].

7.1.2 Comparison of the Quality of Solutions

Table 7.2 shows a comparison of the quality of solutions in terms of gate count, area, delay and power consumption as a result of using both techniques. The table shows that there are significant improvements in terms of area for all cases, except for circuit4 that contains a single gate only. The highest improvement is obtained in circuit5, which is 60.98%. Except for circuit7 and mul2, the solutions provided by MACO are better in terms of delay and power. In addition to that, although AODPC is targeting area minimization, some improvements in terms of gate count are also observed.

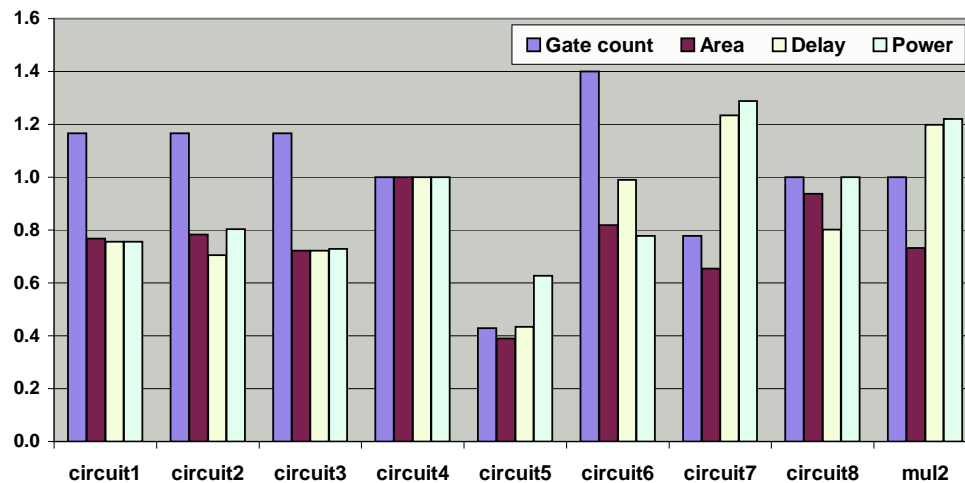


Figure 7.1: Results of MACO normalized with respect to Coello [6].

Figure 7.1 shows the results of MACO algorithm for the given test cases. Note that the results are normalized with respect to Coello's [6] technique. It can be seen that the normalized area for these circuits are always ≤ 1 which means that the obtained circuits require less area compared to the ones produced by Coello's [6].

Table 7.2: Comparison with Coello [6] in terms of area, delay and power.

Circuit	Coello [6]						MACO						% Improvement		
	Gate count	Area	Delay	Power	Gate Count	Area	Delay	Power	Gate Count	Area	Delay	Power			
circuit1	6	16767	7.36	6.57	7	12879	5.57	4.97	-16.67	23.19	24.34	24.33			
circuit2	6	16767	7.36	6.57	7	13122	5.18	5.28	-16.67	21.74	29.55	19.60			
circuit3	6	14823	4.22	5.24	7	10692	3.05	3.82	-16.67	27.87	27.83	27.17			
circuit4	1	1458	0.01	0.67	1	1458	0.01	0.67	0.00	0.00	0.00	0.00			
circuit5	14	29889	12.81	8.09	6	11664	5.57	5.08	57.14	60.98	56.55	37.26			
circuit6	5	13365	3.37	4.91	7	10935	3.34	3.82	-40.00	18.18	0.98	22.21			
circuit7	9	18954	4.53	3.39	7	12393	5.59	4.37	22.22	34.62	-23.37	-28.79			
circuit8	3	7776	3.69	3.16	3	7290	2.96	3.16	0.00	6.25	19.78	0.03			
mul2	7	17253	2.97	3.82	7	12636	3.56	4.66	0.00	26.76	-19.78	-22.05			

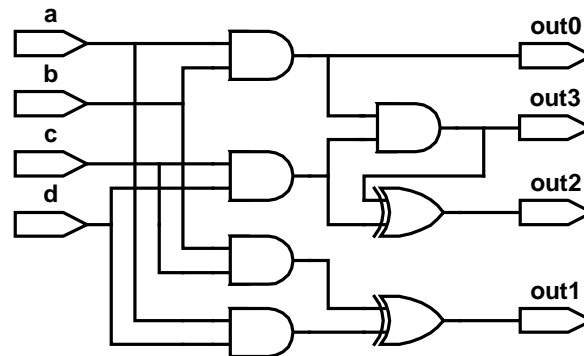


Figure 7.2: 2-bit Multiplier obtained by Coello [6].

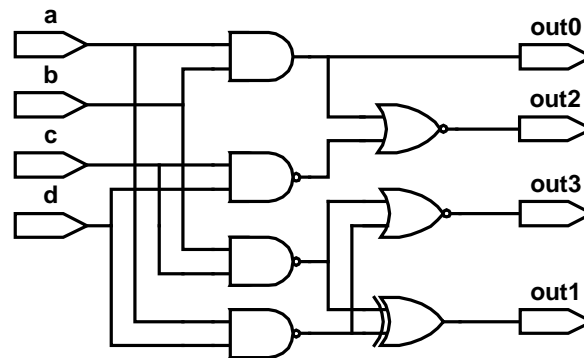


Figure 7.3: 2-bit Multiplier obtained by MACO.

Case study: 2-bit multiplier

Figure 7.2 and Figure 7.3 show the 2-bit multiplier circuits obtained from Coello [6] and MACO respectively. Each circuit consist of seven gates. However, as can be seen from the figures, MACO results in the use of NAND and NOR gates in contrast to AND and XOR gates. Since both NAND and NOR gates requires less area, the circuits obtained by MACO has less area in contrast to the one produced by Coello [6]. In addition, as can be seen in Figure 7.2, output out2 of the circuit

has the longest delay, i.e., the level of out2 is 3. However, the highest level in the circuit produced by MACO is 2. Thus, delay of the circuit produced by MACO will be less than the one produced by Coello [6].

7.1.3 Comparison of Execution Time

Here comparison of execution time for both techniques is conducted. The experiments were carried out using P4 2GHz CPU, 512 MB RAM. Although the length of execution time depends on some variables such as the number of iterations, size of the matrix and the number of gate types, comparison is performed in order to contrast the performance of both techniques.

Table 7.3 shows the average execution time for the given test cases. It is shown that for single-output circuits (except circuit4), MACO results in a saving of more than 70% in execution time. Since circuit4 requires only one gate, the deterministic-like approach of [6] provides faster execution time in contrast to MACO. In addition to that, Coello's approach is worse when it comes to multiple-output circuits. As can be seen in the case of mul2 circuit, MACO saves 98% execution time as compared to [6].

Table 7.3: Comparison with Coello [6] in terms of execution time.

Circuit	Coello [6]	MACO	% time
circuit1	61.43	15.27	75.15
circuit2	61.43	15.17	75.31
circuit3	49.70	14.67	70.49
circuit4	0.40	3.50	-775.00
circuit5	76.00	16.97	77.68
circuit6	50.70	14.83	70.74
circuit7	75.60	16.10	78.70
circuit8	50.40	12.70	74.80
mul2	2876.29	57.20	98.01

7.2 Comparison with Existing Conventional Techniques

In this section, comparison of the proposed algorithm with an existing conventional technique is given. For this purpose, SIS tools are used. However, SIS does not consider load capacitance in their delay calculation and does not consider power optimization. Therefore, the results obtained from SIS are in the form of *netlist* files. These netlist files will be used as input to the cost function calculation procedures of the proposed algorithm to determine the area, delay and power of the circuits obtained.

Area Optimization

In order to compare the performance of the proposed algorithm based on area optimization, AODPC experiment was performed. The results from SIS are the area optimized circuits obtained by executing *rugged.script*, mapped for area minimization. Both SIS and the proposed algorithm use the same gate library.

Since the circuits used as test cases are large circuits, the results obtained using IMACO algorithm are considered. Table 7.4 shows the results for single-output circuits using both techniques. The table shows that except for circuit20, IMACO produces circuits with lesser area than SIS. The highest improvements are obtained for 8-bit and 9-bit odd parity circuits. Parity circuits are best implemented using XOR (XNOR) gates. Unfortunately, SIS is unable to perform XOR decomposition. Thus, the parity circuits obtained by SIS will require larger area as compared to the ones obtained by IMACO.

Table 7.4: Comparison of IMACO and SIS in area optimization for single output circuits.

Circuit	IMACO			SIS			% Improvement		
	Area	Delay	Power	Area	Delay	Power	Area	Delay	Power
circuit11	17253	5.91	7.22	17496	7.08	6.01	1.39	16.51	-20.02
circuit12	45684	14.30	17.36	52731	17.34	19.11	13.36	17.51	9.16
circuit18	63666	23.83	22.01	69984	21.16	25.19	9.03	-12.63	12.64
circuit19	54432	11.34	19.68	54918	18.00	19.83	0.88	37.01	0.78
circuit20	60204	12.43	20.23	60021	12.36	22.53	-0.30	-0.51	10.21
majority	13851	4.57	5.06	14823	6.28	5.41	6.56	27.18	6.48
xor8	20655	5.90	9.32	27945	27.69	10.82	26.09	78.70	13.89
xor9	23328	8.84	10.65	33048	33.25	12.65	29.41	73.40	15.83

Figure 7.4 shows the graphical view of the results obtained from IMACO. Note that these results are normalized with respect to the ones obtained using SIS. As can be seen the normalized area for these test cases are ≤ 1 , which shows that the IMACO algorithm produces circuits better or equal to SIS in terms of area. However, the table shows that IMACO produces circuits that are better not only in terms of area, but also in terms of delay and/or power consumption.

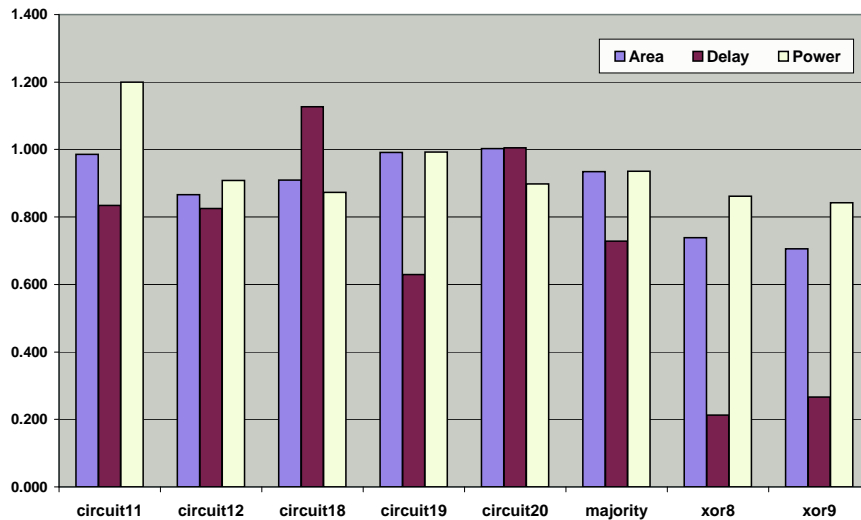


Figure 7.4: Results of IMACO with AODPC for single output functions, normalized to SIS.

The results for multiple outputs circuits for area optimization are shown in Table 7.5. As shown in the table, the improvement in area varies. The highest improvements are observed for multiplier circuits and cm82a circuits. However, MACO failed to deliver better circuits in terms of area for large multiple output circuits (the reason behind this will be explained later). The graphical view of MACO results, normalized with respect to SIS is shown in Figure 7.5.

Table 7.5: Comparison of MACO and SIS in area optimization for multiple output circuits.

Circuit	MACO			SIS			% Improvement		
	Area	Delay	Power	Area	Delay	Power	Area	Delay	Power
add2	24300	11.48	9.96	29889	17.22	11.38	18.70	33.31	12.48
mul2	12636	3.56	4.66	18225	6.59	5.56	30.67	45.94	16.21
cm42a	38880	7.45	13.25	40824	8.86	13.65	4.76	15.95	2.90
cm82a	25272	10.45	9.96	39609	19.54	14.88	36.20	46.53	33.03
mul3	59292	15.03	17.541	112752	43.39	37.75	47.41	65.36	53.53
add3	49086	21.96	18.474	42282	24.99	15.68	-16.09	12.13	-17.79
cm138a	37908	8.919	11.878	39366	11.65	11.48	3.70	23.43	-3.42
con1	38151	6.698	13.741	31590	8.64	11.21	-20.77	22.46	-22.55

Table 7.5 shows that the improvements in the case of add3 and con1 circuits are negative. The reason behind this can be attributed to the procedure employed by MACO to find multiple output circuits. As indicated in Chapter 5, MACO used multiple colonies of ants to find a multiple output function. The sharing between different outputs was assumed to be established by the sharing of pheromone between colonies of ant. For simple multiple output circuits such as multipliers, this assumption is true. However, the experiments proved that the sharing of pheromone itself is not enough to imply the sharing of common sub-functions mostly for large multiple output circuits or multiple output circuits having excessive common sub-functions. Therefore, the sharing of sub-functions between solutions built by the ants has to be measured. This should be used to guide the search further. It will be interesting to investigate this in the future work.

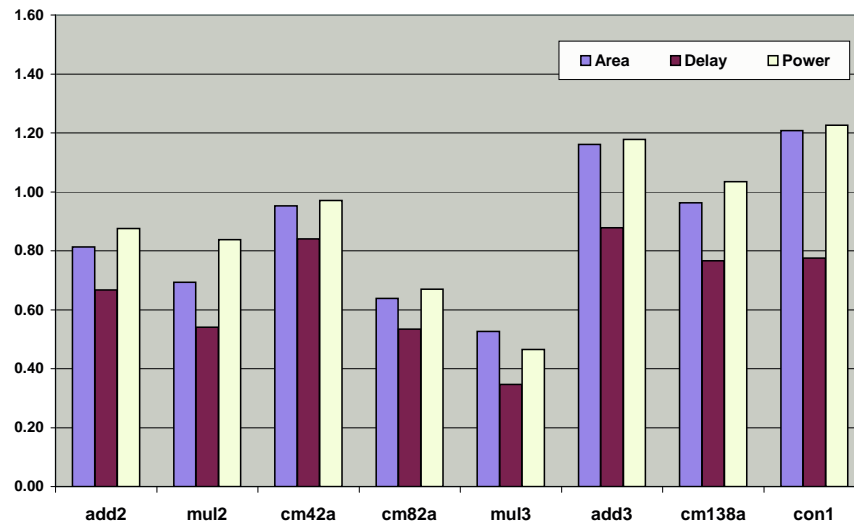


Figure 7.5: Results of MACO with AODPC for multiple outputs functions, normalized to SIS.

Delay Optimization

For delay optimization, the results obtained using SIS are those obtained by executing *delay.script*, mapped for delay minimization. Both the proposed algorithm and SIS used the same gate library during the experiments. The test cases used are the same circuits used for area optimization in the previous section. Table 7.6 and Table 7.7 show the results for single output circuits and multiple output circuits, respectively.

Table 7.6: Comparison of IMACO and SIS in delay optimization for single output circuits.

Circuit	IMACO			SIS			% Improvement		
	Area	Delay	Power	Area	Delay	Power	Area	Delay	Power
circuit11	22599	5.61	9.30	33291	7.39	9.42	32.12	24.01	1.35
circuit12	57591	13.88	20.56	69741	14.21	20.84	17.42	2.36	1.33
circuit18	77760	16.68	28.75	113238	17.51	33.55	31.33	4.74	14.32
circuit19	54432	11.34	19.68	75087	13.69	22.74	27.51	17.19	13.47
circuit20	84564	15.83	32.46	91854	17.54	27.43	7.94	9.75	-18.34
majority	16038	4.19	5.02	18711	7.53	5.40	14.29	44.34	7.11
xor8	20655	5.90	9.32	32805	9.53	11.65	37.04	38.11	20.04
xor9	27216	8.84	11.48	41067	15.42	14.15	33.73	42.64	18.85

Table 7.7: Comparison of MACO and SIS in delay optimization for multiple output circuits.

Circuit	MACO			SIS			% Improvement		
	Area	Delay	Power	Area	Delay	Power	Area	Delay	Power
add2	31347	8.957	11.463	50787	11.77	14.63	38.28	23.90	21.64
mul2	18225	2.96	5.99	25272	4.33	7.16	27.88	31.57	16.30
cm42a	46170	6.396	15.267	43740	8.46	12.23	-5.56	24.41	-24.80
cm82a	48843	7.75	17.09	64638	19.01	18.94	24.44	59.23	9.78
mul3	74358	13.138	21.645	174231	31.66	47.16	57.32	58.51	54.10
add3	53703	12.979	21.484	118827	19.20	35.21	54.81	32.40	38.98
cm138a	38880	10.428	12.689	53217	15.84	14.69	26.94	34.15	13.60
con1	38394	6.241	12.654	40338	10.09	12.02	4.82	38.14	-5.30

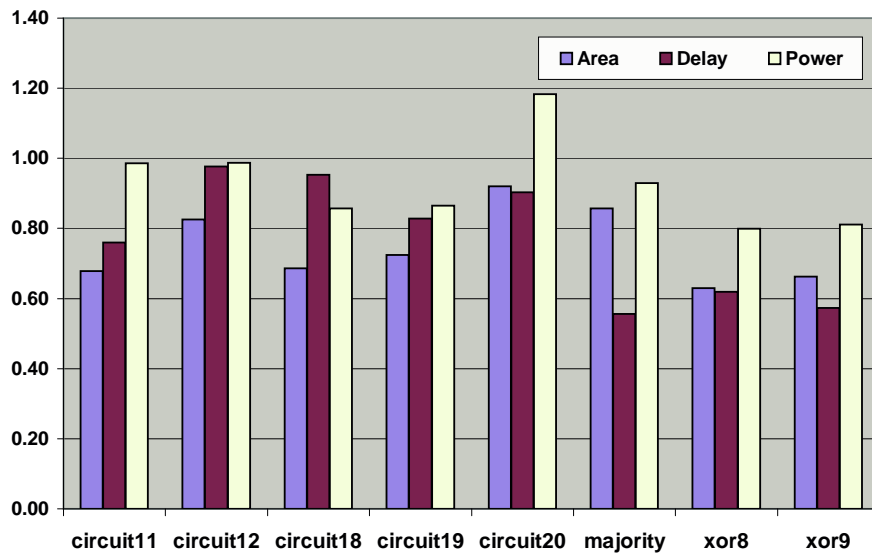


Figure 7.6: Results of IMACO with DOAPC for single outputs functions, normalized to SIS.

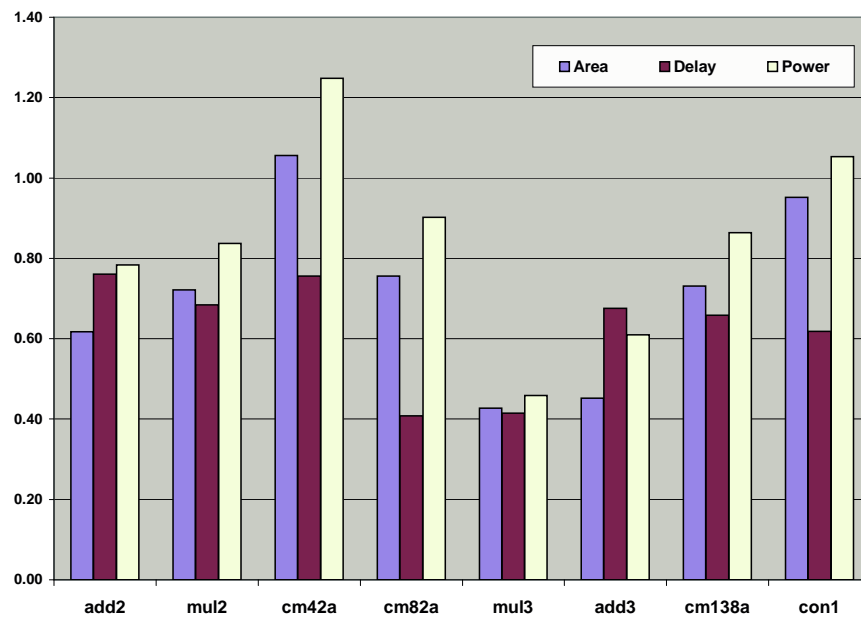


Figure 7.7: Results of MACO with DOAPC for multiple outputs functions, normalized to SIS.

The tables show that the improvement in delay range from 2.36% (circuit12) up to 59.23% (cm82a). In addition to that, significant area improvement of delay optimized circuit is also observed. The graphical view of these results normalized with respect to SIS is given in Figure 7.6 and Figure 7.7 for single output function and multiple output functions, respectively.

As can be seen from the tables and figures above, in contrast with AODPC, the results of DOAPC is very positive. The experiments show that the results obtained from DOAPC is better compared to the ones obtained from SIS in all cases. The reason behind this is the following. As mentioned in Chapter 2, ACO can be easily modeled as a shortest path finding problem. Since delay can be considered proportional to the length of the path, ACO algorithm, which is the basis for MACO, provides a good computational tool for delay optimization problems.

7.3 Comparison with other Techniques

In this section, the proposed algorithm is compared to some other ELD techniques. This includes a GA-based ELD and SimE-based ELD.

7.3.1 Comparison with GAs

The proposed algorithm is compared to the existing GA-based technique. Table 7.8 shows the comparison of MACO and GA [7]. The test case used is the first ten

randomly generated circuits. It should be noted that GA failed to deliver any circuit bigger than those represented in the table.

The table shows that, except for circuit4, the proposed algorithm performs better than GA in terms of area, delay and power. The highest improvement is obtained in the case of circuit8, i.e., 90.29% area improvement, 78.41% delay improvement, and 86.09% power improvement. Since circuit4 consists of one gate only, it can be said that in general, MACO outperforms GAs.

Table 7.8: Comparison with GAs [7] technique in terms of area, delay and power.

Circuit	Coello [7]			MACO			% Improvement		
	Area	Delay	Power	Area	Delay	Power	Area	Delay	Power
circuit1	18954	6.92	6.61	12879	5.57	4.97	32.05	19.57	24.77
circuit2	21870	6.18	6.61	13122	5.18	5.28	40.00	16.13	20.06
circuit3	19926	4.34	5.15	10692	3.05	3.82	46.34	29.84	25.86
circuit4	1458	0.01	0.66	1458	0.01	0.67	0.00	0.00	0.00
circuit5	27945	8.76	7.89	11664	5.57	5.08	58.26	36.46	35.67
circuit6	40338	13.24	14.21	10935	3.34	3.82	72.89	74.77	73.13
circuit7	83835	21.74	28.85	12393	5.59	4.37	85.22	74.28	84.85
circuit8	75087	13.69	22.73	7290	2.96	3.16	90.29	78.41	86.09
circuit9	104004	20.25	30.76	15066	5.42	5.27	85.51	73.23	82.85
circuit10	97686	21.40	28.44	11178	5.42	4.06	88.56	74.67	85.72

Figure 7.8 shows the results of MACO algorithm for the given test cases. These values are normalized with respect to the results obtained using GAs. It can be seen that the area, delay and power of the solutions obtained by MACO are always ≤ 1 .

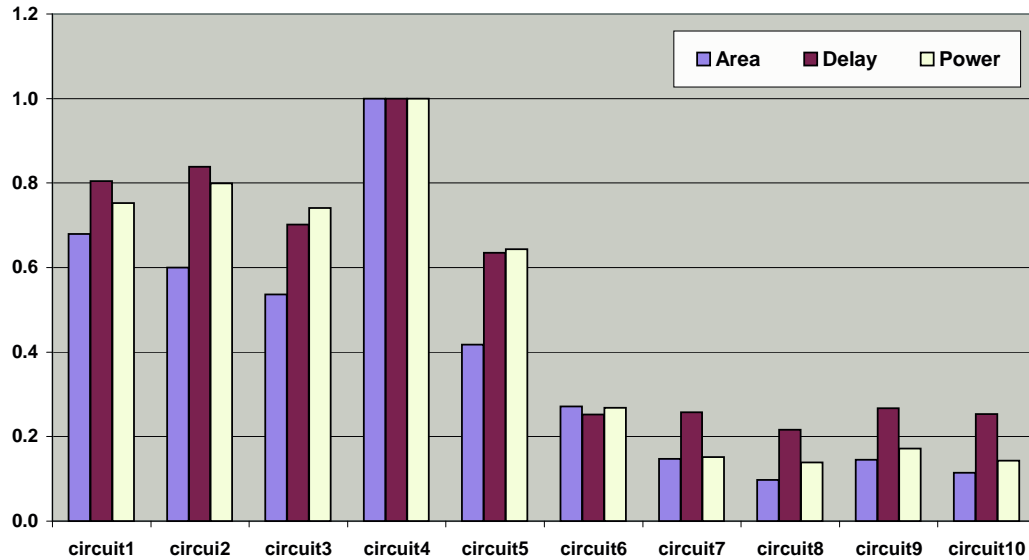


Figure 7.8: Comparison with GA: normalized area, delay and power are always ≤ 1 .

Comparison in terms of execution time is given in Table 7.9. The percentage of improvement is $\approx 99\%$. The table clearly shows that MACO algorithm is superior as compared to GAs in terms of execution time. This result is not surprising since GAs is a population-based heuristic. The time needed to find the solutions depends not only on the number of iterations but also the size of the population used.

Table 7.9: Comparison with GA [7] technique in terms of execution time.

Circuit	Coello [7]	MACO	% Improvement
circuit1	8100	15.27	99.81
circuit2	12240	15.17	99.88
circuit3	11052	14.67	99.87
circuit4	11160	3.50	99.97
circuit5	21132	16.97	99.92
circuit6	30780	14.83	99.95
circuit7	49068	16.10	99.97
circuit8	57240	12.70	99.98
circuit9	44784	83.21	99.81
circuit10	61704	78.96	99.87

There exists other powerful iterative heuristics that have been used for solving optimization problem in VLSI design. One such heuristic is Simulated Evolution (SimE) [15]. Below, the proposed algorithm is compared to SimE-based ELD technique [81].

7.3.2 Comparison with SimE

Table 7.10 and Table 7.11 show a comparison of the proposed algorithm with SimE-based technique for area optimization and delay optimization, respectively.

Table 7.10: Comparison with SimE technique in terms of area, delay and power for area optimization.

Circuit	MACO			SimE			% Improvement		
	Area	Delay	Power	Area	Delay	Power	Area	Delay	Power
circuit1	12879	5.57	4.97	12879	3.90	4.97	0.00	-42.75	0.00
circuit2	13122	5.18	5.28	13122	5.18	5.28	0.00	0.00	0.00
circuit10	11178	5.42	4.06	9963	6.42	3.33	-12.20	15.58	-21.98
circuit14	24786	7.25	9.20	23814	6.80	9.20	-4.08	-6.59	0.00
circuit16	12393	5.71	4.26	9720	8.50	4.30	-27.50	32.78	0.88
circuit17	10692	4.43	4.39	10692	4.43	4.39	0.00	0.00	0.00
add2	24300	11.48	9.96	24300	11.48	9.96	0.00	0.00	0.00
add3	49086	21.96	18.474	40265	26.73	14.83	-21.91	17.85	-24.57
mul2	12636	3.56	4.66	12636	3.56	4.66	0.00	0.00	0.00
mul3	59292	15.03	17.541	74358	13.14	21.65	20.26	-14.40	18.96
cm42a	38880	7.45	13.25	38456	9.44	12.60	-1.10	21.08	-5.17
cm82a	25272	10.45	9.96	25029	11.84	9.24	-0.97	11.78	-7.89
b1	13851	1.53	5.91	11206	2.91	2.78	-23.60	47.46	-112.45
con1	38151	6.698	13.741	30233	6.90	14.23	-26.19	2.93	3.44
rd53	35235	15.32	14.00	38073	14.75	15.34	7.45	-3.88	8.75

Table 7.11: Comparison with SimE technique in terms of area, delay and power for delay optimization.

Circuit	MACO			SimE			% Improvement		
	Area	Delay	Power	Area	Delay	Power	Area	Delay	Power
circuit1	14823	3.86	6.41	15360	4.20	5.80	3.50	8.14	-10.47
circuit2	17739	3.70	7.16	16870	3.88	6.90	-5.15	4.54	-3.70
circuit10	12393	5.32	4.48	13771	5.50	4.77	10.01	3.22	6.02
circuit14	30132	9.75	10.63	24786	7.25	9.20	-21.57	-34.52	-15.47
circuit16	13122	5.71	4.26	10340	7.60	5.22	-26.91	24.82	18.35
circuit17	12150	4.43	4.72	12354	5.30	5.38	1.65	16.47	12.23
add2	31347	8.957	11.463	35270	9.37	12.66	11.12	4.41	9.45
add3	53703	12.979	21.484	53703	12.98	21.48	0.00	0.00	0.00
mul2	18225	2.96	5.99	18225	2.96	5.99	0.00	0.00	0.00
mul3	74358	13.138	21.645	74358	13.14	21.65	0.00	0.00	0.00
cm42a	91854	7.072	32.885	42768	5.19	15.02	-114.77	-36.37	-118.97
cm82a	48843	7.75	17.09	55872	14.25	18.56	12.58	45.61	7.95
b1	14580	1.49	6.24	12745	2.08	7.05	-14.40	28.61	11.49
con1	38394	6.241	12.654	30233	6.90	14.23	-26.99	9.55	11.08
rd53	53946	15.45	19.00	40201	13.10	15.98	-34.19	-17.90	-18.88

It can be seen in Table 7.10 that in eight out of fifteen cases, SimE produced better circuits in terms of area. The worst solution produced by MACO is obtained for circuit16, where the area improvement is -27.5%. There are only two cases in which MACO produced circuits having better area, namely rd53 and mul3 circuits.

These results support our previous observation. The sharing of common sub-functions that should be established by the sharing of pheromone trail, is not working as expected. It is believed that there should be a new method to incorporate the sharing of sub-functions in addition to the pheromone trails. It will be interesting to further investigate this idea.

On the other hand, MACO algorithm provides some positive results in terms of delay optimization. As shown in Table 7.11, in nine out of fifteen cases, MACO

provides better circuits in terms of delay. The highest improvement is obtained for cm82a circuit. There are only three cases, in which SimE provides better results in terms of delay. These results also support our previous observation in delay optimization. Since ACO algorithm is basically a shortest path finding, MACO works best for delay optimization.

7.4 Concluding Remarks

In this chapter, the results obtained using the introduced techniques were compared with those obtained using the existing techniques. The proposed algorithms are better in terms of design rate, quality of solution and execution time compared to the existing ACO-based techniques. The proposed algorithms were also compared to existing conventional tools, represented by SIS. It was observed that the area optimization applied by the introduced algorithms performs better in most of the cases, except for some multiple output circuits. However, the performance of delay optimization of the proposed algorithms was better as compared to SIS.

Chapter 8

CONCLUSIONS AND FUTURE DIRECTIONS

The dramatic increase in designer productivity over the past decade in the area of VLSI (Very Large Scale Integration) circuit design can be attributed to the development of sophisticated computer-aided design tools. The improvement in computer aided design has been made possible by the advances in the field of logic synthesis.

In conventional logic design techniques, circuit designers begin with a precise specification in the form of truth tables or Boolean expressions. These expressions are manipulated by applying logic synthesis algorithms, such as factorization and kernel extraction to minimize circuit representations. The outcome of logic synthesis algorithms will be either in two-level, multi-level, or Reed Muller representations. On the other hand, iterative heuristics work on larger space. Through the process

of assemble-and-test, candidate solutions are built and evaluated. At the end, the optimum solution could evolve from this process.

This thesis offered a perspective for the automatic design of digital circuits through evolutionary techniques. The use of assemble-and-test via iterative heuristics has enabled the sampling of larger search space in circuit design problems. In addition, modern issues in digital circuit design, such as low power and high performance are addressed.

8.1 Conclusion

In this thesis, ACO-based evolutionary logic design techniques have been introduced. The performance of the introduced algorithms have been compared to those of existing conventional and evolutionary techniques.

Here are the concluding statements regarding the thesis work:

1. The introduced techniques successfully address the issue of circuits design, considering modern design issues such as area, delay and power through the use of iterative heuristics, multiobjective optimization and fuzzy logic.
2. It was observed that the introduced techniques have outperformed some of the existing techniques in evolutionary logic design. The comparison is based on the quality of solutions and time requirements.

3. Comparison with existing conventional techniques (represented by SIS) showed that the introduced techniques produced better quality results in terms area, delay and power for most of the test cases.
4. The improvement obtained using the introduced techniques in delay optimization is better than area optimization.

8.2 Future Directions

Some possible directions for future work could be stated as follows:

1. Investigation of how to incorporate the sharing of sub-functions into the ACO algorithm.
2. Investigation of the incorporation of some rules from logic synthesis domain such as *kernel extraction* in order to improve the performance of the introduced techniques.
3. Investigation of the use of some other iterative heuristics and possible hybridization scheme can be performed in order to further improve the quality of solutions.

Although the experiments have shown some good results, currently, the goal of evolutionary logic design system is still far. The most stumbling block for evolutionary techniques is the time taken to produce solutions. Approaches to improve

the execution time of current techniques such as parallelization are thus important to explore. In addition, the advance of technology could allow us to use faster and better machine as the platform for evolutionary logic design systems. Thus, the dream of automated and efficient circuit design systems can be reached.

Appendix A

File Format and Circuit Used as Test Cases

The following are the format of the required input files and the list of circuits used as test cases during the experiments.

A.1 Library File Format

The gates' parameters are obtained from CMOS MOSIS 0.25 μ m library. These includes the following information:

1. The number of transistors (TRCOUNT)
2. The size of the gate (AREA)
3. The switching delay of the gate (BDELAY)
4. The input capacitance (CIN)

5. The output capacitance (COUT)
6. The load factor (LF)

Except for inverters and wires, there is more than one value for input capacitance. In this regards, the higher value is considered. The same applied for the load factor.

The following shows the format of the library files used.

<GATE NAME> <TRCOUNT> <AREA> <BDELAY> <CIN> <COUT> <LF>

Using the above format, the library file considered in this thesis is given next.

WIRE	0	0	0	0	0	0
NOT	2	1215	3	2.661	0.005	516
AND	6	2187	9	2.661	0.005	553
OR	6	1944	11	2.661	0.004	567
XOR	10	3159	12	5.321	0.006	688
NAND	4	1458	5	2.661	0.007	444
NOR	4	1458	7	2.661	0.005	694
XNOR	10	2916	12	5.321	0.004	551

A.2 Input File Format

The proposed algorithms use PLA files as input. The parameters required by the proposed algorithms are then generated automatically. However, if the circuits' specification is not in the form of PLA files, the input file required by the algorithm must contain the following information.

Field	Description
maxrun	The number of maximum runs to be performed by the algorithm
maxiter	The number of maximum iterations for a single run
objtype	The optimization objective of the current action. (0 = gatecount, 1 = area, 2 = delay, and 3 = power)
ifdweight	Static (0) or dynamic (1) weight is employed
weight	The value W_f at the beginning of the iteration
ifphase	Positive (0) or negative (1) phase is used. In positive mode, all literals are uncomplemented. In negative mode, some literals can be in the complemented forms, depending on its functional fitness. (not used, default = 0)
dataset	The number of input dataset. Useful for generating truth table for arithmetic circuits such as adders, multipliers. For example, a 2-bit adder has dataset value equal to 2. (not used, default value = 1)
numvar	Number of inputs
numout	Number of outputs
invin	Set to '1' if complemented literals are used in addition to uncomplemented ones. (default = 0)
row	The number of rows at the beginning of the iteration
level	The number of columns at the beginning of the iteration
iflocal	Set to 1 if local search is employed (not used)
gatemode	The type of library used. Values are within [0-7]
gcmx	Set the maximum number of gates allowed for a circuit (not used)
gcmin	Set the minimum number of gates allowed for a circuit (not used)
numant	Set the number of ants used

Field	Description
maxgen	Set the maximum number of generations of ant
gamma	Set the constant for pheromone update calculation
rho	Set the pheromone evaporation rate
range_tau	Set the maximum range of pheromone values allowed
ttf[0]	The string of truth table of the first output of the circuit
ttf[1]	The string of truth table of the second output of the circuit (if available)
ttf[k]	The string of truth table of the k+1 output of the circuit (if available)

A.3 Randomly Generated Circuits

There are 20 randomly generated circuits used in the experiments. These circuits are listed below.

circuit	input(s)	output(s)	circuit	input(s)	output(s)
circuit1.pla	4	1	circuit11.pla	5	1
circuit2.pla	4	1	circuit12.pla	6	1
circuit3.pla	4	1	circuit13.pla	5	1
circuit4.pla	2	1	circuit14.pla	6	1
circuit5.pla	4	1	circuit15.pla	6	1
circuit6.pla	4	1	circuit16.pla	6	1
circuit7.pla	4	1	circuit17.pla	5	1
circuit8.pla	4	1	circuit18.pla	6	1
circuit9.pla	6	1	circuit19.pla	6	1
circuit10.pla	6	1	circuit20.pla	6	1

A.4 Benchmark Circuits

There are 14 benchmark circuits used in the experiments. These circuits are listed below.

circuit	input	output	circuit	input	output
majority.pla	5	1	b1.pla	3	4
xor8.pla	8	1	C17.pla	5	2
xor9.pla	9	1	cm138a.pla	6	8
add2.pla	5	3	cm42a.pla	4	10
add3.pla	7	4	cm82a.pla	5	3
mul2.pla	4	4	con1.pla	7	2
mul3.pla	6	6	rd53.pla	5	3

Bibliography

- [1] J. F. Miller, D. Job, and Vassilev V. K. Principles in the Evolutionary Design of Digital Circuits - Part I. *Journal of Genetic Programming and Evolvable Machines*, 1(1):8–35, 2000.
- [2] J. F. Miller, T. Fogarty, and P Thomson. Designing Electronic Circuits Using Evolutionary Algorithms. Arithmetic Circuits: A Case Study. *Genetic Algorithms and Evolution Strategy in Engineering and Computer Science*, John Wiley and Sons, Chichester, pages 105–131, 1998.
- [3] J. F. Miller and P. Thomson. Aspects of Digital Evolution: Geometry and Learning. *Proceedings of Second International Conference on Evolvable Systems (ICES'98) Lecture Notes in Computer Science*, 1478:25–35, Springer-Verlag, Heidelberg, 1998.
- [4] J. F. Miller and P. Thomson. Discovering Novel Digital Circuits Using Evolutionary Techniques. *IEE Colloquium on Evolvable Systems, Savoy Place, London*, March 1998.

- [5] J. F. Miller and P. Thomson. Aspects of Digital Evolution: Evolvability and Architecture. *Proceedings of Fifth International Conference on Parallel Problem Solving From Nature (PPSN'98) Lecture Notes in Computer Science*, 1498:927–936, Springer-Verlag, Heidelberg, 1998.
- [6] C. A. Coello, A. D. Christiansen, and A. H. Aguirre. Ant Colony System for the Design of Combinational Logic Circuits. *Evolvable Systems: From Biology to Hardware, Edinburgh, Scotland*, pages 21–30, April Springer Verlag, 2000.
- [7] C. A. Coello, A. D. Christiansen, and A. H. Aguirre. Use of Evolutionary Techniques to Automate the Design of Combinational Circuits. *International Journal of Smart Engineering System Design, Elsevier Science*, 2(4):299–314, June 2000.
- [8] Giovanni De Micheli. *Synthesis and Optimization of Digital Circuits*. McGraw-Hill, New York, 1994.
- [9] M. Dorigo, Gianni Di Caro, and Luca M. Gambardella. Ant Algorithms for Discrete Optimization. Technical Report Tech. Rep. IRIDIA/98-10, IRIDIA, Universite Libre de Bruxelles, Brussels, Belgium, 1998.
- [10] Sushil J. Louis. *Genetic Algorithms as a Computational Tool for Design*. PhD thesis, Department of Computer Science, Indiana University, Aug 1993.

- [11] C. A. Coello, A. D. Christiansen, and A. H. Aguirre. Towards Automated Evolutionary Design of Combinational Circuits. *Computers and Electrical Engineering*, Pergamon Press, 27(1):1–28, Jan. 2001.
- [12] B. Hounsell and T. Arslan. A Novel Genetic Algorithm for the Automated Design of Performance Driven Digital Circuits. *CEC-2000*, pages 601–608, 2000.
- [13] B. Hounsell and T. Arslan. A Novel Evolvable Hardware Framework for the Evolution of High Performance Digital Circuits. *GECCO-2000*, pages 525 – 532, July 2000.
- [14] M. Dorigo and M. Maniezzo and A. Colorni. The Ant Systems: An Autocatalytic Optimizing Process. Revised 91-016, Dept. of Electronica, Milan Polytechnic, 1991.
- [15] Sadiq M. Sait and H. Youssef. *Iterative Computer Algorithms with Applications in Engineering: Solving Combinatorial Optimization Problems*. IEEE Computer Society Press, 1999.
- [16] W. Quine. The Problem of Simplifying Truth Functions. *American Mathematical Monthly*, 59:521–531, 1952.
- [17] E. McCluskey. Minimisation of Boolean Function. *Bell System Technical Journal*, 38:1417–1444, 1956.

- [18] R. Brayton, G. D. Hachtel, C. T. McMullen, and A.L. Sangiovanni-Vincentelli. *Logic Minimisation Algorithms for VLSI Synthesis*. Kluwer Academic Publisher, 1984.
- [19] R. Brayton, R. Rudell, A. L. Sangiovanni-Vincentelli, and A. Wang. MIS: A Multiple-Level Logic Optimisation System. *IEEE Trans. on Computer-Aided Design*, CAD-6:1062–1081, Nov. 1987.
- [20] R. Brayton, G. D. Hachtel, and A. L. Sangiovanni-Vincentelli. Multilevel Logic Synthesis. *Proceeding of the IEEE*, 78:264–300, Feb. 1990.
- [21] E. M. Sentovic, K. J. Singh, L. Lavagno, C. Moon, R. Murgai, A. Saldanha, H. Savoj, P. R. Stephan, R. K. Brayton, and A. L. Sangiovanni-Vincentelli. SIS: A System for Sequential Circuit Synthesis. Technical Report UCB/ERL M92/41, University of California, Berkeley, May 1992.
- [22] D. Bostick et al. The Boulder Optimal Logic Design System. *Proceeding of the International Conference on CAD*, pages 62–65, Nov. 1987.
- [23] Hugo de Garis. Evolvable Hardware: Genetic Programming of a Darwin Machine. *Proceedings of the International Conference in Innsbruck, Austria*, pages 441–449, Springer-Verlag, 1993.
- [24] R. S. Zebulum, M. A. Pacheco, and Marley Vellasco. Evolvable Systems in Hardware Design: Taxonomy, Survey and Applications. *Evolvable System:*

- From Biology to Hardware. Proceeding of the First International Conference, ICES 96 Tsukuba, Japan, Lecture Notes in Computer Science*, 1259:344–358, Oct. 1997.
- [25] R. S. Zebulum and M. A. Pacheco and Maria Vellasco. *Evolutionary Electronics: Automatic Design of Electronic Circuits and Systems by Genetic Algorithms*. CRC Press, 2002.
- [26] T. Higuchi, T. Niwa, T. Tanaka, H. Iba, H. de Garis, and T. Furuya. Evolving Hardware with Genetic Learning: A First Step Towards Building a Darwin Machine. *Proceeding of the 2nd Int. Conf. on The Simulation of Adaptive Behavior (SAB92)*, pages 417–427, MIT Press, Aug. 1993.
- [27] J. R. Koza. *Genetic Programming: On the Programming of Computers by Means of Natural Selection*. MIT Press, 1992.
- [28] Adrian Thompson. Silicon Evolution. *Proceedings of the First Annual Conference on Genetic Programming*, pages 444–452, MIT Press, 1996.
- [29] J. R. Koza, F. H. Bennett, D. Andre, and M. A. Keane. Automated Design of Both the Topology and Sizing of Analogue Electrical Circuits Using Genetic Programming. *Artificial Intelligent in Design*, pages 151–170, Kluwer Academic Publishers, 1996.

- [30] J. R. Koza, F. H. Bennett, D. Andre, and M. A. Keane. *Genetic Programming III: Darwinian Invention and Problem Solving*. Morgan Kaufmann, San Francisco, CA, 1999.
- [31] T. Higuchi, M. Iwata, I. Kajitani, M. Murakawa, S. Yoshizawa, and T. Furuya. Hardware Evolution at Gate and Functional Level. *Proceeding of the International Conference on Biologically Inspired Autonomous Systems: Computation, Cognition and Action*, March Durham, USA, 1996.
- [32] Moshe Sipper et. al. A Phylogenetic, Ontogenetic, and Epigenetic View of Bio-Inspired Hardware Systems. *IEEE Trans. on Evolutionary Computation*, 1(1):83–97, 1997.
- [33] Xin Yao and Tetsuya Higuchi. Promises and Challenges of Evolvable Hardware. *IEEE Trans. on Systems, Man, and Cybernetics - Part C: Applications and Reviews*, 29(1):87–97, 1999.
- [34] J. F. Miller and P. Thomson. A Developmental Method for Growing Graphs and Circuits. *Fifth International Conference on Evolvable Systems: From Biology to Hardware*, 2606:93–104, Mar 2003.
- [35] T. Fogarty, J. F. Miller, and P. Thomson. Evolving Digital Logic Circuits on Xilinx 6000 Family FPGAs. *The 2nd Online Conference on Soft Computing in*

- Engineering Design and Manufacturing*, pages 299–305, Springer-Verlag, London, 1998.
- [36] C. A. Coello and Hernandez Aguirre, Arturo,. Evolutionary Multiobjective Design of Combinational Logic Circuits. *Proceedings of the Second NASA/DoD Workshop on Evolvable Hardware*, pages 161–170, Jul 2000.
- [37] C. A. Coello, and Hernandez Luna, Erika and Hernandez Aguirre, Arturo,. Use of Particle Swarm Optimization to Design Combinational Logic Circuits. *Evolvable Systems: From Biology to Hardware. 5th International Conference, ICES 2003*, 2606:398–409, Mar 2003.
- [38] C. Y. Lee. Representation of Switching Circuit by Binary Decision Programs. *Bell Systems Technical Journal*, 38:985–999, 1959.
- [39] S. J. Hong, R. G. Cain, and D. L. Ostapko. MINI: A Heuristic Approach for Logic Minimization. *IBM Journal of Research and Development*, 18:443–458, Sept. 1974.
- [40] L. Berman and L. Trevillyan. A Global Approach to Circuit Size Reduction. *Advance Research in VLSI, 5th MIT Conference*, pages 203 – 214, 1988.
- [41] Shih-Chieh Chang and malgorzata Marek-Sadowska and Kwang-Ting Cheng. Perturb and Simplify: Multilevel Boolean Network Optimizer. *IEEE Trans.*

- Computer Aided Design of Integrated Circuits and Systems*, 15(12):1494 – 1504, Dec 1996.
- [42] Shih-Chieh Chang and David Ihsin Cheng. Efficient Boolean Division and Substitution Using Redundancy Addition and Removing. *IEEE Trans. Computer Aided Design of Integrated Circuits and Systems*, 18(8):1096 – 1106, Aug 1999.
- [43] S. Muroga and Y. Kambayashi and H. C. Lai and J.N. Culliney. The Transduction Method – Design of Logic Networks Based on Permissible Functions. *IEEE Trans. Computer*, 38(10):1404–1424, 1989.
- [44] S. B. Akers. Binary decision diagrams. *IEEE Trans. on Computers*, 27:509–516, 1978.
- [45] R. Bryant. Graph-based Algorithms for Boolean Function Manipulation. *IEEE Trans. on Computers*, 35:677–691, 1986.
- [46] Soha Hassoun and Tsutomu Sasao. *Logic Synthesis and Verification*. Kluwer Academic Publisher, Massachusetts, USA, 2002.
- [47] D. Green. *Modern Logic Design*. Addison-Wesley, Reading, MA, 1986.
- [48] T. Sasao. *Logic Synthesis and Optimisation*. Kluwer Academic Publisher, 1993.

- [49] Deo Singh, J.M. Rabaey, Massoud Pedram, Francky Catthoor, Suresh Rajgopal, Naresh Sehgal, and T.J. Mozdzen. Power Conscious CAD Tools and Methodologies: A Perspective. *IEEE Proceeding*, 83(4):570 – 594, April 1995.
- [50] Massoud Pedram. Power Minimization in IC Design: Principles and Applications. *ACM Trans. Design Automation of Electronic Systems*, 1(1):3 – 56, Jan. 1996.
- [51] Massoud Pedram. Logical-Physical Co-design for Deep Submicron Circuits: Challenges and Solutions. *Proceedings of Design Automation Conference, the ASP-DAC'98. Asia and South Pacific.*, pages 137 – 142, Feb. 1998.
- [52] Sasan Iman and Massoud Pedram. POSE: Power Optimization and Synthesis Environment. *ACM 33rd Design Automation Conference, DAC'96*, pages 21 – 26, Jan. 1996.
- [53] S. Goss, S. Aron, J. L. Deneubourg, and J. M. Pasteels. Self-organized Shortcuts in the Argentine Ant. *Naturwissenschaften*, 76:579–581, 1989.
- [54] M. Dorigo and G. Di Caro. *New Ideas in Optimisation*. McGraw Hill, London, UK, 1999.
- [55] M. Dorigo and T. Stutzle. *The ant colony optimization metaheuristic: Algorithms, applications, and advances*, 2002.

- [56] Carlos M. Fonseca and Peter J. Fleming. Multiobjective Optimization and Multiple Constraint Handling with Evolutionary Algorithms I: A Unified Formulation. Technical report, Dept. of Automatic Control and System Eng., University of Sheffield, Sheffield, U.K., Jan. 1995.
- [57] L.A. Zadeh. Fuzzy sets. *Information and Control*, 8(3):338–353, June 1965.
- [58] L. A. Zadeh. Outline of a new approach to the analysis of complex systems and decision processes. *IEEE Transaction Systems Man. Cybern*, SMC-3(1):28–44, 1973.
- [59] J. M. Mendel. Fuzzy logic systems for engineering: A tutorial. *IEEE Proceeding*, 83(3):345–377, Mar. 1995.
- [60] E. Q. Kang, Rung-Bin Lin, and E. Shragowitz. Fuzzy logic approach to vlsi placement. *IEEE Trans. on Very Large Scale Integration (VLSI) Systems*, 2(4):489–501, Dec. 1994.
- [61] E. Shragowitz, Jun-Yong Lee, and E. Q. Kang. Application of fuzzy logic in computer aided design. *IEEE Trans. on Fuzzy Systems*, 6(1):163–172, Feb. 1998.
- [62] Sadiq M. Sait and Youssef, H. and J. A. Khan and El-Maleh, A. Fuzzy simulated evolution for power and performance optimization of VLSI placement.

- Proceedings of International Joint Conference on Neural Networks, IJCNN '01.*, 1:738–743, July 2001.
- [63] H. J. Zimmerman. *Fuzzy Set Theory and Its Applications*. Kluwer Academic Publishers, 3rd edition, 1996.
- [64] L. A. Zadeh. The concept of linguistic variable and its application to approximate reasoning. *Information Science*, 8:199–249, 1975.
- [65] Ronald R. Yager. On Ordered Weighted Averaging Aggregation Operators in Multicriteria Decision Making. *IEEE Transaction on Systems, MAN, and Cybernetics*, 18(1):183–190, Jan 1988.
- [66] R. Yager. Multiple objective decision-making using fuzzy sets. *International Journal of Man-Machine Studies*, pages 9:375–382, 1977.
- [67] R. Yager. Second Order Structures in multi-criteria decision making. *International Journal of Man-Machine Studies*, pages 36:553–570, 1992.
- [68] Hernandez Aguirre, Arturo, and Buckles, Bill P. and C. A. Coello. Gate-level Synthesis of Boolean Functions using Binary Multiplexers and Genetic Programming. *Congress on Evolutionary Computation.*, pages 675–682, Jul 2000.
- [69] J. F. Miller and P. Thomson. Cartesian genetic programming. *Third European Conference on Genetic Programming Edinburgh*, 1802:121–132, Apr 2000.

- [70] D. Montana and R. Popp, and G. Vidaver and S. Iyer. EvolWare: Genetic Programming for Optimal Design of Hardware Based Algorithm. *Third Annual Conference on Genetic Programming*, pages 869–874, July 1998.
- [71] J. M. Sanchez and J. Lanchares. Multilevel Logic Synthesis Using Algorithm Based on Natural Processes. *Proceeding of the 20th International Conference on Microelectronics*, 2:823–828, Sep 1995.
- [72] J. Miller and P Thomson. Combinational and Sequential Logic Optimisation using Genetic Algorithms. *GALESIA: 1st IEEE/IEE Joint International Conference on GA Applications*, pages 34–38, Sep 1995.
- [73] J. Miller and P. Thomson. Restricted Evaluation Genetic Algorithms with Tabu Search for Optimising Boolean Functions as Multi-level AND-EXOR Networks. *AISB Workshop on Genetic Algorithms and Evolutionary Techniques*, 1143:85–101, Apr 1996.
- [74] Rolf Dreschsler. *Evolutionary Algorithms for VLSI CAD*. Kluwer Academic Publisher, Boston, 1998.
- [75] Sasan Iman and Massoud Pedram. Two-level Logic Minimization for Low Power. *IEEE/ACM International Conference on Computer-Aided Design, ICCAD-95*, pages 433 – 438, Nov 1995.

- [76] Sasan Iman and Massoud Pedram. An Approach for Multilevel Logic OPTimization Targetting Low Power. *IEEE Trans. Computer Aided Design of Integrated Circuits and Systems*, 15(8):889 – 901, Aug. 1996.
- [77] Priya Patil, Tan-Li Chou, Kaushik Roy, and Rabindra Roy. Low-Power Driven Logic Synthesis Using Accurate Power Estimation Techniques. *10th International Conference on VLSI Design*, pages 179 – 184, Jan. 1997.
- [78] Chih-Shun Ding, Chi-Ying Tsui, and Masoud Pedram. Gate Level Power Estimation Using Tagged Probabilistic Simulation. *IEEE Trans. Computer Aided of Integrated Circuit and Systems*, 17(11):1099 – 1107, Nov. 1998.
- [79] Srinivas Devadas and Sharad Malik. A Survey of Optimization Techniques Targeting Low Power VLSI Circuits. *32nd ACM/IEEE Design Automation Conference*, pages 242–247, 1995.
- [80] Standard Cell Library for MOSIS CMOS, <http://www.mosis.org/Technical/Designsupport/std-cell-library-scmos.html>.
- [81] Uthman Al-Saiari. Combinational logic circuits design through simulated evolution. Master’s thesis, King Fahd University of Petroleum and Minerals, Dhahran, KSA, November 2003.

VITA

- **Bambang Ali Basyah Sarif**
- Born in Jakarta, Indonesia, 14 March 1977.
- Received Bachelor Degree in Electrical Engineering from Bandung Institute of Technology, Bandung, Indonesia in February 2000.
- Joined Computer Engineering Department, KFUPM, as a Research Assistant in January 2001.
- Received Master of Science Degree in Computer Engineering from KFUPM, Dhahran, Saudi Arabia in November 2003.